CHARACTERIZATION OF RPE65 AND RDH12, TWO ENZYMES ASSOCIATED WITH RETINAL DYSTROPHY AND RETINOID PROCESSING

by

Jared D. Chrispell

A dissertation submitted in partial fulfillment
of the requirements for the degree of
Doctor of Philosophy
(Biological Chemistry)
in The University of Michigan
2010

Doctoral Committee:

Professor Debra A. Thompson, Chair
Professor Jairam Menon
Professor Anand Swaroop
Associate Professor Raymond C. Trievel
Associate Professor Anne Vojtek

To my mother, father and sister
for all of your love and support over the years

ACKNOWLEDGEMENTS

I would like to thank first and foremost my mentor, Debra Thompson for all of her guidance and assistance throughout my tenure in the lab. Her tireless efforts have without a doubt helped me to become a better scientist and only served to increase my love for research. I would also be remiss if I did not thank the influence and encouragement of my high school chemistry teacher Mr. Doug Getman, my undergraduate teaching advisor Dr. Clyde Herreid, and my undergraduate research advisors Drs. Christine Campbell and Richard Gronostajski.

I would also like to thank my committee members Drs. Anand Swaroop, Jairam Menon, Ray Trievel and Ann Vojtek for their invaluable input and criticisms over the course of my research. This research would not have been possible without the aid of those who laid the groundwork and contributed as co-authors. Dr. Andreas Janecke group at the University of Innsbruck, Austria performed the initial patient screening and Dr. Peter Nurnberg's group at the Max Delbrück Center in Berlin, Germany performed the linkage analysis. Drs. Ingo Kurth, Christian Hübner and Andreas Gal of the Institut für Humangenetik in Hamburg, Germany created of the *Rdh12*-knockout mouse and anti-mouse Rdh12 antibodies and Klaus Ruther of Augenklinik Campus Virchow-Klinikum Charité in Berlin, Germany performed the ERG analysis. Dr. Alan Mears generated the *Nrl*-knockout mouse and performed the subsequent microarray analysis, the results of which were analyzed by Ritu Khanna of the Swaroop lab. Drs. Maureen Kane and

Jospeh Napoli of the University of California, Berkeley performed the retinal retinoic acid analysis and Dr. Janet Sparrow performed the lipofuscin analysis for our studies. Matt Brooks of the Swaroop lab performed the microarray analysis on the *Rdh12*-knockout mouse and whose knowledge was invaluable assistance in several other aspects of our research. I would also like to thank Drs. Hemant Khanna and Carlos Murga for their constructive criticism of my presentations and work in general. I must also thank members of the Thompson lab, past and present. Thanks go to Nahid Hemati for her help in teaching me many immunohistochemical techniques as well as helping to generate a number of RDH constructs. Dr. Christina McHenry's expertise was invaluable in helping me to perform organic extractions and showing me the use of the HPLC machine. Shameka Shelby was of great assistance when performing early protein purification assays. I must also thank Kecia Feathers for her exceeding helpfulness in almost every aspect of my research, and for being such a great lab buddy over the last few years.

I must also thank my many friends, bother here and afar, for their years of constant support and camaraderie, all of which helped to make the low points of the research experience bearable and the high points memorable. And finally I must thank my family, whose unending support and encouragement has allowed me excel at whatever it is I attempt, and are the best role models I could ever hope to have.

TABLE OF CONTENTS

LIST OF FIGURES

LIST OF ABBREVIATIONS

A2E	*N*-retinylidene-*N*-retinylethanolamine
ATP	Adenosine Triphosphate
cDNA	complementary Deoxyribonucleic Acid
CHAPS	3-[(3-Cholamidopropyl)dimethylammonio]-1-propanesulfonate
COS-7	CV-1 (simian) in Origin, SV40 promoter line 7
DHRS3	Dehydrogenase/Reductase (SDR family) member 3
ERG	Electroretinogram
HPLC	High Performance Liquid Chromatography
Hprt	Hypoxanthine guanine phosphoribosyl transferase
IS	Inner Segments(s)
LCA	Leber Congenital Amaurosis
LRAT	Lecithin Retinol Acyltransferase
NADPH	Nicotinamide Adenine Dinucleotide Phosphate, reduced
NRL	Neural Retina Leucine zipper
ONL	Outer Nuclear Layer
OS	Outer Segment(s)
PBS	Phosphate Buffer Saline
PDE	Phosphodiesterase
PNA	Peanut Agglutinin
prRDH (RDH8)	Photoreceptor-specific Retinol Dehydrogenase
RDH	Retinol Dehydrogenase/reductase
RDH10	Retinol Dehydrogenase 10
RDH11	Retinol Dehydrogenase 11
RDH12	Retinol Dehydrogenase 12
RDH13	Retinol Dehydrogenase 13
RDH14	Retinol Dehydrogenase 14
RDH5	Retinol Dehydrogenase 5
RGR	RPE-retinal G-protein coupled Receptor
RPE	Retinal Pigment Epithelium
RPE65	Retinal Pigment Epithelium-specific protein 65-kDa
SDR	Short-chain acyl Dehydrogenase/Reductase
Sod2	Superoxide Dismutase 2

ABSTRACT

Phototransduction in vertebrate vision is mediated by visual pigments composed of opsin apoproteins covalently attached to a light-sensitive chromophore, 11-*cis* retinal. Absorption of light isomerizes 11-*cis* retinal to all-*trans* retinal, initiating a signal transduction cascade. A complex set of enzyme reactions occurring in the retinal pigment epithelium and the retina is responsible for the synthesis and regeneration of the chromophore and is termed the visual cycle. Several forms of inherited retinal degeneration and dysfunction manifest as a result of mutations in the genes associated with visual cycle function, such as *RPE65* and *RDH12*.

RPE65 is essential for the synthesis of 11-*cis* retinal and was recently confirmed to function as the visual cycle isomerase. Cone photoreceptors have been proposed to possess an exclusive chromophore regenerative pathway. Using a monoclonal antibody approach, we have now mapped antigenic determinants of the protein surface, shown that RPE65 is not expressed in cone cells, and confirmed that RPE65 is associated with the visual cycle enzyme RDH5.

Rdh12 has an *in vitro* activity and localization profile that made it an excellent candidate to serve as the all-*trans* retinal reductase of the visual cycle. Immunochemical analysis localized RDH12 protein to the photoreceptor inner segments and outer nuclear layer in both humans and mice, suggesting an equivalent physiological role for RDH12 in both species. However, analysis of the phenotype of Rdh12-deficient mice revealed no

differences in histology, retinoid processing or electroretinogram response compared to wild-type. Rdh12-deficient mice did show a decreased ability to reduce all-*trans* retinal and 11-*cis* retinal as measured by *in vitro* activity assays of retinal homogenates.

These findings suggest that RDH12 function in mice does not directly contribute to visual cycle function. Instead, a critical function of RDH12 is likely the reduction of retinaldehydes that exceed the reductive capacity of the photoreceptor outer segment and gain access to the inner segments in conditions of high illumination. The study of these genes is important not only to gain a better understanding of visual cycle mechanism, but also to elucidate mechanisms of pathogenesis and to develop targeted forms of therapeutic intervention.

CHAPTER 1

INTRODUCTION

The sage wisdom of one's mother to 'eat your carrots' insomuch as to improve your vision is not entirely accurate. The consumption of foods high in beta carotene, the precursor of vitamin A, has not been shown to improve visual acuity. However, it is true that vitamin A and its analogues are extremely important for the proper functioning of the eye. The visual pigments of the eye, such as rhodopsin, are all bound to a chromophore that is required for sensing light and is derived metabolically from vitamin A. The human eye contains some 105 million rods, each of those contains approximately 800 stacked disc membranes, and each of these are studded with rhodopsin molecules at a density of approximately 25000 μm^{-2} (reviewed in [1]). Each rhodopsin molecule is activated by a single photon of light and can react in as fast as 200 femtoseconds [2]. With billions of photons being present even in the dimmest environs, a constant supply of chromophore is critical for sustaining the visual response. Fortunately, evolution has equipped vertebrate retinas with a metabolic pathway that serves to recycle the vitamin A necessary for chromophore production such that continuous dietary uptake is not required for sustained vision, and this pathway is termed the visual cycle.

Several forms of inherited retinal degeneration and dysfunction are caused by mutations in the genes encoding the enzymes and proteins necessary for visual cycle function. The study of these genes is important not only to gain a better understanding of

the visual cycle mechanism, but also to elucidate mechanisms of pathogenesis and to identify potential targets for rational therapies.

Structure of the Retinal Pigment Epithelium and Neural Retina

The retina is an extension of the central nervous system that detects, assimilates and transmits visual input to the brain. In vertebrates, it has a highly organized structure composed of several distinct layers. These layers are, from outside to inside: the retinal pigment epithelium (RPE); the photoreceptor outer segments (OS); the photoreceptor inner segments (IS); the external limiting membrane (EML); the photoreceptor outer nuclear layer (ONL); the outer plexiform layer (OPL), where photoreceptor cells synapse with interneurons; the inner nuclear layer (INL), containing the bipolar, amacrine and horizontal cells; the inner plexiform layer (IPL), where interneurons synapse with the ganglion cell layer; the nerve fiber layer (NFL); and the inner limiting membrane (ILM). Adjacent to the RPE lays the Bruch's membrane, the choriocapillaris and the sclera. The inner layers of the retina, from the OS to the ILM, are often referred to as the neural retina and consist of 6 main types of neurons in mammals - rod and cone photoreceptors, bipolar cells, horizontal cells, retinal ganglion cells and Müller cells (Figure 1-1).

The RPE comprises a single layer of pigmented cells packed in a regular array with each cell having an approximately hexagonal shape. The RPE represents a part of the blood-brain barrier, in this case referred to as the blood-retinal barrier. The cells are sealed together by intracellular tight junctions resulting in this permeability barrier [3]. These junctions also form a barrier between the apical and basolateral surfaces of the RPE cells [4]. The apical surface faces the retina and possesses microvilli that project into the interphotoreceptor matrix (IPM), surrounding the rod and cone photoreceptor

OS, while the basolateral surface faces Bruch's membrane and contains smaller processes [5-7]. The RPE performs a number of specialized functions in the retina (reviewed in [8]). In its role as the outer blood-retinal barrier, it is responsible for the active transport of essential metabolites, such as glucose and vitamin A, from the choroidal blood supply to the photoreceptors that lie too far from the retinal vasculature for passive diffusion [7]. Differential expression of ion channels on the apical and basolateral membranes allow for the active transport of ions and water from the subretinal space, preventing retinal detachment [9]. Another critical function of the RPE is the phagocytosis, ingestion and breakdown of shed membranes from the photoreceptor OS. The phototransductive elements of the photoreceptors are continuously renewed at the base of the OS, followed by shedding of the disc membranes from the tips. Lastly, the RPE serves a critical function in vitamin A metabolism, also referred to as retinoid processing, a point that will be covered extensively in the coming paragraphs.

The photoreceptor cells are highly specialized neurons that transduce light stimuli into nerve signals, and have four distinct parts: An outer segment that houses the bulk of the phototransductive machinery and is composed of stacks of bimembranous discs; an inner segment that contains the typical organelles necessary for cellular metabolism; a perikaryal zone that contains the cell nucleus and comprises the ONL; and a synaptic terminal that terminates at the OPL. Protein synthesis in photoreceptors takes place in the IS, and a slender connecting cilium joins the IS with the OS. All newly synthesized OS resident proteins must be transported within the IS and across the cilium to reach their destination. These phototransduction proteins are constantly turned over through

phagocytosis of the OS tips by RPE cells and the addition of the newly synthesized components at the base of the OS [10] (Figure 1-2).

The two types of photoreceptor cells in the vertebrate retina are the rods and cones. Rods mediate vision in dim light and are more light-sensitive than cones, while cones are responsible for color and high acuity vision. In most vertebrates, rods outnumber cones by as much as 20:1 and the retinas of these animals are dubbed 'rod dominant'. There are some exceptions to this, with species such as chickens and ground squirrels being 'cone-dominant'. The rod and cone cells can be distinguished from one another by a number of morphological and biochemical characteristics. Most notably in regards to ultrastructure, the OS of rods is cylindrical, while cone OS taper in width from the inner segment to the outer. Additionally, the OS of both rods and cones contain stacks of membranous discs. In rods, these discs become separated from the outer membrane, while in cones they maintain a connection to the surface membrane [11]. The photoreceptors can also be characterized by the expression of the visual pigments, with rhodopsin in rods and the cone opsins in cones. Rhodopsin consists of an opsin apoprotein bound to a light sensitive chromophore, and has an absorption peak at ~498 nm. Trichromacy prevails in most primates (including humans) resulting in three cone subtypes, each expressing one of three forms of cone opsin: short wavelength (blue) with an absorption peak ~420 nm (S-); medium wavelength (green) with an absorption peak ~530 nm (M-); and long wavelength (red) with an absorption peak ~564 nm. Most other animals are dichromatic and thus have only two subtypes of cones, and in the mouse retina these are the S- and M- cones. Rods are typically found throughout the retina, while cones are found at the highest density in the macula of primates, appearing as oval-

shaped yellow spot near the center of the retina. In mice, the cone photoreceptors are spatially distributed the dorsal to ventral direction.

In the mouse, the different types of retinal neurons all develop from a pool of multipotent cells called retinal progenitor cells (RPCs). The retinal neurons are formed in a sequential order, albeit with significant overlap. The first cell types to arise are the retinal ganglion cells, the cones, the horizontal cells and the amacrine cells. Rod cells are the next to begin developing in the late prenatal period, and continue to be formed into the postnatal period. The Müller cells and bipolar cells begin to form in the early postnatal period. By the end of the first postnatal week the retina has a clearly laminar structure, and connections between the various retinal neurons are formed during the second postnatal week [12]. The differentiation of RPCs into retinal neurons is influenced by a variety of external growth factors, and a number of transcription factors play important roles in determining the post-mitotic fate of the RPC. One such transcription factor important to our studies was neural retina leucine zipper (NRL) protein. A member of the musculoaponeurotic fibrosarcoma (Maf)-subfamily, NRL is expressed in the rod photoreceptors and regulates the expression of rhodopsin, rod phosphodiesterase (PDE6) and other rod-specific genes [13-16]. Targeted disruption of the *Nrl* gene in mice led to the hypothesis that Nrl plays a critical role in the differentiation of rod photoreceptors, as *Nrl*-knockout *(Nrl–/–)* mice possess a retina composed entirely of cones with S-cone-like characteristics [17]. This mouse model has been especially advantageous when looking at differences in expression and activity between rod and cone photoreceptors.

The Phototransduction Cascade

The visual process in the retina begins when light is absorbed by visual pigments in the photoreceptor cells. These visual pigments, rhodopsin and cone opsins, are integral membrane proteins located in the discs of the OS of the rods and cones, respectively [18]. The light-sensitive chromophore, 11-*cis* retinal, is covalently attached to the opsin proteins via a protonated Schiff base linkage to a specific lysine residue (K296 in human rhodopsin) located in one of seven transmembrane alpha helical segments [19]. Capture of a single photon results in the isomerization of 11-*cis* retinal to all-*trans* retinal. The markedly altered geometry of the retinal moves the Schiff base linkage approximately 5 Å in relation to the ring portion of the chromophore [20]. Converting the photon into atomic motion, the conformational change results in the formation of the photoactive visual pigment (R*) that decays through a number of conformational intermediates [18]. One of these intermediates, meta II (MII), activates transducin, a heterotrimeric G-protein specific to photoreceptor cells. Activation occurs by catalyzing guanosine diphosphate (GDP)–guanosine triphosphate (GTP) exchange on the α subunit of transducin (Tα), which is followed by dissociation of the active form of Tα from the Tβ and Tγ subunits. The Tα subunit in turn activates a photoreceptor-specific cyclic guanosine monophosphate (cGMP) phosphodiesterase (PDE), a multimeric enzyme of four subunits [21]. Upon activation, the two inhibitory γ subunits are released permitting the PDE α and β subunits to hydrolyze cGMP to 5'-GMP. The resulting decrease in intracellular cGMP reduces the permeability of plasma membrane cGMP-gated cation channels, leading to hyperpolarization of the photoreceptor cell membrane and decreased neurotransmitter release at synapses with second-order retinal neurons [22, 23]. This

final step results in the propagation of the visual signal and the completion of the activation phase.

Termination of the light response involves a number of steps which inactivate the transduction cascade and reset the sensitivity of the photoreceptor cells. Recoverin, when bound to Ca^{2+}, interacts with rhodopsin kinase and inhibits its ability to phosphorylate rhodopsin. The decrease in intracellular Ca^{2+} that occurs during the photoresponse releases recoverin from rhodopsin kinase, which then phosphorylates R* at C-terminal serine and threonine residues [24, 25]. Arrestin binds to the phosphorylated opsins, preventing continued activation of transducin [26, 27]. Further decay of the active state results in hydrolysis of the Schiff base linkage and release of all-*trans* retinal from the opsin apoprotein. A GTPase activating protein (GAP) complex, composed of Regulator of G-protein signaling 9, G protein β subunit, and RGS9-1-Anchor Protein (RGS9-1/Gβ5/R9AP), stimulates the intrinsic GTPase activity of transducin and allows the inactive complexes of both transducin and cGMP phosphodiesterase to reform [28]. Cytoplasmic levels of cGMP are restored by activation of photoreceptor-specific guanylate cyclases (GC1 and GC2) that are regulated by calcium-binding to guanylyl cyclase activating proteins [29-32]. (Figure 1-3)

Light-Driven Translocation of Retinal Proteins

An interesting phenomenon observed in the rod photoreceptors is the massive light-driven translocation of transducin, arrestin and recoverin between the major subcellular compartments of the photoreceptors. Most photoexcitation and recovery components, such as rhodopsin, PDE, the cGMP-gated channel, the RGS9-1/Gβ5/R9AP complex, and the retinal guanylyl cyclases are integral or peripheral membrane proteins

that reside in the OS regardless of illumination conditions. In contrast transducin, arrestin, and recoverin have been shown to undergo bidirectional translocations between the OS and IS in a light-dependent manner. In dark-adapted photoreceptors, transducin and arrestin are concentrated in the OS and IS, respectively. Sufficiently bright light induces extensive and relatively rapid movement in rods, with transducin moving from the OS into the IS and the synaptic terminal, and arrestin moving from the IS into the OS. Recoverin translocates from the OS towards the synapse [33-39]. In cones, arrestin translocates to the OS in light, but only partial translocation of transducin is observed and this only under high intensity light [40-43]. Recoverin translocation has not yet been observed in cones. This light-dependent translocation of proteins may contribute to light/dark adaptation and could potentially protect the photoreceptor cell from light- and phototransduction-associated retinal degeneration [32, 36, 44]. (Figure 1-4)

The Visual Cycle

In order to sustain phototransduction, 11-*cis* retinal consumed as a result of the light activation of the visual pigments must be regenerated. The aggregate reactions responsible for this recycling are termed the visual cycle, and the conventional view is that vitamin A analogs cycle between the photoreceptor cells and the RPE, the major site of 11-*cis* retinal synthesis [45]. The chemical structures of the major vitamin A intermediates involved in RPE synthesis of 11-*cis* retinal and the cellular locations of the proteins and enzymes involved in this pathway are shown in (Figure 1-5).

The visual cycle begins with the dissociation of all-*trans* retinal from the bleached visual pigments. Some of the free all-*trans* retinal reacts with phosphatidylethanolamine (PE) in disc membranes to form the Schiff base product N-retinylidene-

phosphatidylethanolamine (NR-PE) until an equilibrium between the two forms is reached [46, 47]. The mechanism of all-*trans* retinal transport across the disc membrane to the photoreceptor cytoplasm and eventually the RPE has yet to be determined, but evidence points to a role for the retina-specific adenosine triphosphate (ATP)-binding cassette transporter (ABCR) [48-51]. Biochemical studies are consistent with an ATP-switch model in which NR-PE binds to a high-affinity site on ABCR in the absence of ATP [52, 53]. This binding causes a conformational change that alters the affinity of the nucleotide binding domains (NBDs) for ATP [46, 48]. Binding of ATP to one or both NBDs causes dimerization of the NBDs and a conformational change in the protein. This converts the high-affinity NR-PE substrate binding site to a low-affinity site with access to the cytoplasmic side of the disc membrane, and is followed by dissociation of NR-PE from ABCR on the cytoplasmic side of the lipid bilayer [53].

In the photoreceptor OS, free all-*trans* retinal is reduced to all-*trans* retinol, most likely by photoreceptor-specific retinol dehydrogenase (prRDH, or RDH8). Retinol dehydrogenase/reductases, also referred to as RDHs, belong to the family of short chain acyl-CoA dehydrogenase/reductases (SDRs) [54-56].The resulting all-*trans* retinol is transported across the IPM to the RPE via a poorly defined process, potentially involving the interphotoreceptor/interstitial retinoid-binding protein (IRBP) present in the IPM, as well as passive diffusion [57]. All-*trans* retinol (vitamin A) is also supplied to the RPE from the blood supply *via* the choriocapillaris. Uptake is a receptor-mediated process involving recognition of a serum retinol-binding protein/transthyretin (RBP/TTR) complex that is essential for sufficient uptake of retinol to support vision in the neonate [58-60]. Within the RPE, all-*trans* retinol is bound to cellular RBP (CRBP) [61].

Three enzymes associated with the smooth endoplasmic reticulum of the RPE are required to convert vitamin A to 11-*cis* retinal. The first enzyme, lecithin retinol acyltransferase (LRAT), esterifies all-*trans* retinol to phosphatidlycholine in the lipid bilayer to form all-*trans* retinyl esters [62-65]. These esters are then bound by the second enzyme, RPE-specific protein 65-kDa (RPE65), an abundant protein in the RPE that has a high affinity for all-*trans* retinyl esters [66]. In early studies, RPE65 was shown to be necessary for the isomerization reaction, but intrinsic isomerase activity was not detected [67]. However, recent studies have demonstrated that RPE65 is the retinoid isomerohydrolase of the visual cycle that converts all-*trans* retinyl esters to 11-*cis* retinol. [68, 69]. A third enzyme, 11-*cis* retinol dehydrogenase (11*cis*RDH), converts 11-*cis* retinol to the final aldehyde product in a reaction that is accelerated by the presence of cellular retinaldehyde-binding protein (CRALBP) [70-72]. Genetic studies have demonstrated that retinol dehydrogenase 5 (*RDH5*)- and retinol dehydrogenase 11 (*RDH11*)-knockout mice have minor modifications in dark adaptation that are consistent with a role as the 11*cis*RDH in the visual cycle, and human mutations in *RDH5* result in fundus albipunctatus [73-75]. Excess 11-*cis* retinol can also be esterified by LRAT and stored in the RPE as 11-*cis* retinyl esters when the cycle slows in the absence of light [76, 77]. Finally, 11-*cis* retinal moves back to the rod photoreceptors, either in IRBP-dependent or -independent fashion, where it joins with opsin to regenerate visual pigment [78-82].

Alternative mechanisms for the production of 11-*cis* retinal have been proposed. The RPE-retinal G-protein coupled receptor (RGR), expressed in the RPE and Müller cells, was initially proposed to function in a light-dependent pathway that regenerates 11-

cis retinal [83-85]. The ligand for RGR is all-*trans* retinal, and was observed to isomerize to 11-*cis* retinal in response to illumination of the protein [86, 87]. RGR also associates with other visual cycle proteins, such as RDH5, and analysis of single *RGR*- and double *RGR/RDH5*-knockout mouse models suggest a nonessential role for RGR in the production of 11-*cis* retinal [88]. More recent studies have shown that RGR in fact modulates isomerohydrolase activity independent of light exposure, with the mode of this modulation still being researched [89-91].

Proposed Cone Visual Cycle

While the rod photoreceptors have been shown to require the RPE to recycle 11-*cis* retinal for rhodopsin regeneration, evidence has been presented that cones are distinct from rods in regard to retinoid processing [92, 93]. Cones have been suggested to have an alternative retinoid–metabolic pathway which functions independently of the RPE. RPE65 was proposed to directly participate in this cone visual cycle based on reported expression of *RPE65* mRNA in salamander cones and protein expression in mammalian cones, but not in rod photoreceptors [94, 95]. This stood in conflict to data generated by our group, and will be further discussed in Chapter 2.

Direct evidence of a light-driven cone cycle was obtained in the cone-rich chicken retina. Subsequent to dark adaptation, light exposure resulted in the accumulation of 11-*cis* retinyl esters in the retina and all-*trans* retinyl esters in the RPE [96, 97]. The involvement of Müller cells in this pathway has been proposed, and a recent study has shown that cultured Müller cells from chickens can synthesize 11-*cis* retinyl esters from 11-*cis* retinol, an activity enhanced by the presence of CRALBP [98, 99]. Other evidence came from the characterization of three novel enzyme activities in retina membrane

fractions from cone-dominated retinas (chicken and ground squirrel): First, an 11-*cis*-retinyl-ester synthase activity indicating that LRAT is not required for the synthesis of retinal esters in cones as it is in the RPE visual cycle; second, an 11cisRDH activity in the retina that was found to prefer nicotinamide adenine dinucleotide phosphate (NADP+) as a cofactor rather than the NAD+ cofactor of the RPE visual cycle; and third, an all-*trans*-retinol isomerase activity displaying the ability to convert all-*trans* retinol to 11-*cis* retinol without the synthesis of retinyl esters in the presence of CRBP [100, 101].

Inherited Forms of Retinal Degeneration

Various forms of inherited retinal dysfunction result from mutations in the genes necessary for visual cycle function and other aspects of retinoid processing, and exhibit a range of diverse phenotypes including retinitis pigmentosa, Stargardt disease and Leber congenital amaurosis (LCA). The identification of these genes is an important aspect in furthering our understanding of the pathology of these diseases, as well as in designing effective therapies and treatments.

LCA is the most early-onset and severe of all of the inherited retinal dystrophies. Accounting for approximately 5% of all retinal dystrophies, it is characterized by four clinical features: severe and early visual loss, sensory nystagmus (involuntary eye movement), amaurotic pupils (no light perception, but papillary contraction when opposite eye receives light stimuli), and absent electrical signals on an electroretinogram (ERG) [102]. Inheritance can be autosomal recessive or autosomal dominant, and is caused by defects in a number of genes. To date, 14 genes have been found mutated in patients, estimated to account for 70% of all LCA cases. (reviewed in [103]). While

these genes affect a number of aspects critical to the proper functioning of the retina, mutations were found in three genes encoding proteins associated with vitamin A metabolism: *LRAT*, *RPE65* and *RDH12 [104-106]*. The latter two have been the primary focus of my research endeavors, and will be further detailed in the following sections.

Retinal Pigment Epithelium-specific Protein 65-kDa (RPE65)

The *RPE65* gene, located on chromosome 1p31 in humans and distal chromosome 3 in mice, encodes a 533-amino acid protein that is evolutionarily conserved and is expressed in the RPE [107-109]. It is a marker gene for RPE differentiation, and its expression during development begins as the photoreceptors are formed in the retina [110, 111]. Mutations in *RPE65* are associated with LCA, and targeted disruption of *Rpe65* in mouse has shown that RPE65 is essential for synthesis of 11-*cis* retinal by the RPE [67, 104, 112, 113]. Additionally, the phenotype of the *Rpe65*-knockout (*Rpe65–/–*) mouse displays a mild disorganization of the rod photoreceptor OS, a lack of 11-*cis* retinoids and rhodopsin, and a lack of rod visual function as measured by ERG. The *Rpe65–/–* mouse phenotype is similar to that present in Swedish briard dogs that experience progressive vision loss as a result of carrying a null functional allele of canine *Rpe65* [114]. Rpe65-deficient mice are extremely insensitive to light, which protects them from light damage and establishes rhodopsin as the mediator of light-induced retinal damage [116, 117].

While RPE65 was found to be required for 11-*cis* retinal synthesis, no intrinsic isomerase activity was initially observed in assays of the recombinant protein. However, addition of recombinant RPE65 to RPE microsomal membranes prepared from *Rpe65–/–* mice was found to restore retinoid isomerase activity [115]. It was proposed that, due to

its ability to bind to all-*trans* retinyl esters, RPE65 serves to present the ester substrate to the retinoid isomerase [118, 119]. Subsequently, during the time our work was ongoing, RPE65 was shown to possess isomerase activity in cell culture experiments in which LRAT was coexpressed [68, 69, 120]. Further studies showed that LRAT was not required for isomerization beyond the synthesis of the all-*trans* retinal ester substrate, and that RPE65 is an iron(II) dependent isomerohydrolase [121, 122]. In addition, *RPE65* missense variants present in individuals with LCA displayed loss-of-function when assayed for isomerase activity *in vitro* [120].

Formation of Dead-end Retinoid Products

Excess retinaldehydes can form lipofuscin dead-end products that accumulate with aging. Lipofuscin are fine, yellow-brown pigment granules that accumulate within the RPE as a result of aging [123]. The major fluorophore of lipofuscin has been identified as *N*-retinylidene-*N*-retinylethanolamine (A2E) and its isomers that form as a result of dephosphorylation of A2-PE [47]. A2-PE most likely forms infrequently during situations of increased intradiscal levels of all-*trans* retinal, which allow a second molecule of all-*trans* retinal to react with NRPE [124, 125]. These fluorophores then accumulate in the RPE when the shed OS are phagocytosed. Stargardt's disease is an early-onset form of macular dystrophy that is also characterized by increased levels of fluorescent lipofuscin deposits in the RPE, which are considered to result in atrophy of the RPE [126, 127]. Mutations in the *ABCA4* gene encoding ABCR, whose proposed role was earlier described as trafficking NRPE to the cytoplasm of the rod photoreceptors, are a cause of autosomal recessive Stargardt disease. Areas of intense fundus autofluorescence in patients with age-related macular degeneration have been

shown to correspond to sites prone to atrophy, suggesting a link in the etiology of these diseases [128-130].

Studies of susceptibility to light damage in various mouse strains identified a hypomorphic variant of mouse *Rpe65*. These studies linked light-damage resistance in C57BL/6 albino mice with the chromosome 3 locus for *Rpe65*, identifying the Met450 variant of Rpe65 in light-resistant mice and the Leu450 variant in light-sensitive mice of the albino BALB/c strain [131]. Resistance to light damage in C57BL/6 mice was directly associated with the Met450 variant, and correlated with lowered expression and lower overall activity of Rpe65 protein in all mice of the C57BL/6 strain [132, 133]. Additionally, mice possessing the Met450 variant displayed decreased levels of A2E and A2E isomers in retina and RPE compared to those with the Leu450 variant. As RPE65 has a rate-determining role in the visual cycle, reduced production of all-*trans* retinal that accompanies slowing of the regenerative pathway in the presence of the Met450 variant of RPE65 is likely responsible for the decreased formation of A2E [134].

Retinol Dehydrogenase 12 (RDH12) and Isoforms

Retinoids comprise a family of isoprenoid lipids including vitamin A (all *trans*-retinol) and its natural and synthetic derivatives. Retinoids regulate a wide variety of essential biological processes, including development, cell growth arrest, differentiation and apoptosis, and homeostasis. The oxidation and reduction of retinoids is critical to each of their explicit purposes, and this is particularly evident where the retinoids of the visual cycle are concerned. These reactions are carried out by RDHs that belong to the SDR superfamily.

RDH12 is a 316 amino acid, 35 kDa protein with transcript expression localized by *in situ* hybridization to the photoreceptor layer of the retina. *In vitro* analyses show it can metabolize both all-*trans* and 11-*cis* retinoids, and that it is an NADP(+)-dependent oxidoreductase capable of reducing retinal to retinol or oxidizing retinol to retinal, depending on substrate and cofactor availability [135, 136]. Mutations in *RDH12* are linked to LCA, with most patient missense mutations causing profound loss of catalytic activity due to decreased protein stability [106, 137, 138]. In addition, RDH12 exhibits reductive capacity towards several other metabolic substrates *in vitro*, including C9 aldehydes resulting from lipid photo-oxidation, as well as certain steroid substrates like dihydrotestosterone [136, 139, 140].

Additional RDH isoforms that possess substrate specificity and activity comparable to RDH12 are also present in the retina and RPE. (Figure 1-6) One of the earliest detected and most studied is RDH5, an 11-*cis*-retinol dehydrogenase expressed in the RPE [70, 71]. RDH5 has been shown to oxidize 11-*cis* retinol to 11-*cis* retinal in an NAD+ dependent manner, and has a very low activity toward all-*trans* retinol [141]. Mutations in the human *RDH5* gene were identified in individuals with delayed dark adaptation, and further analysis showed decreased activity of RDH5 mutant proteins to oxidize 11-*cis*-retinol [75]. Targeted disruption of *Rdh5* in mice was shown to cause a large increase in the concentration of 11-*cis* retinol and 11-*cis* retinyl esters, but not to result in retinal degeneration nor affect normal dark adaptation [101, 142, 143]. These findings suggest that while RDH5 is a strong candidate for the 11-*cis* retinol dehydrogenase, other RDHs may participate in retinol oxidation in the RPE.

RDH8 (prRDH) is the only member of the RDH family so far found expressed in the rod photoreceptor OS. RDH8 utilizes NADPH as a cofactor to reduce both all-*trans* retinal and 11-*cis* retinal, although activity towards the latter is far lower [55]. While no mutations linked to human disease have been reported, an *Rdh8*-knockout (*Rdh8–/–*) mouse has been generated. The *Rdh8–/–* mouse phenotype displayed no signs of degeneration or alteration in visual cycle throughput following brief light exposure. However, Rdh8-deficiency caused accumulation of all-*trans* retinal following exposure to bright light, delayed recovery of rod function as measured by ERG, and accumulation of A2E [56]. So while RDH8 can reduce all-*trans* retinal, it is not rate limiting for visual cycle function.

RDH11 was first identified as an SDR expressed in pancreas, and expression was later found in the RPE and the photoreceptor IS [135, 144]. Human RDH11 has been purified and kinetically characterized in a manner similar to human RDH12, and has been found to act on all-*trans* and 11-*cis* retinoids in both an oxidative and reductive capacity, depending on the cofactor available (NADP+ or NADPH, respectively) [135, 145]. However, with regards to the reduction of all-*trans* retinal, RDH12 has a greater V_{max} value than RDH11 [136, 145]. Disruption of the *Rdh11* gene in mice resulted in a phenotype with no obvious retinal defects, although a delay in dark adaptation was observed [73, 74]. *RDH11* and *RDH12* are highly related evolutionarily and are located in head-to-head orientation on the same chromosome in human and mouse [106, 146].

Other RDHs expressed in the retina include DHRS3 (retSDR1), RDH10, RDH13 and RDH14. DHRS3 was reported to utilize NADPH as cofactor to catalyze the reduction of all-*trans* retinal to all-*trans* retinol [54]. No human *DHRS3* mutations linked

to disease have been reported, nor has a knockout mouse been generated. RDH10 was found expressed in RPE and Müller cells, and was reported to utilize NADP+ as a cofactor to oxidize all-*trans* retinol *in vitro* [147, 148]. Mice deficient in Rdh10 exhibited drastic limb, craniofacial, and organ defects. This was found to be the result of abrogated Rdh10 oxidative activity needed to convert all-*trans* retinol to all-*trans* retinal, leading to insufficient retinoic acid signaling during embryogenesis [149]. RDH13 and RDH14 were initially identified based on sequence homology to RDH12 and RDH11. RDH13 is the mitochondrial form found expressed in the photoreceptor IS, and exhibited oxidoreductive activity towards retinoids, preferring NADPH as a cofactor, with a much greater catalytic efficiency as a reductase [135, 150]. RDH14 transcripts were localized to the photoreceptor IS. RDH14 activity was found to be similar to that of RDH11 and RDH12, acting in an oxidative and reductive capacity, depending on the cofactor available (NADP+ or NADPH, respectively) [135].

Synopsis of Dissertation

RPE65 and *RDH12* are disease genes associated with severe forms of retinal dystrophy. RPE65 has been shown to be critical for visual cycle function, and better understanding of its structure and function will be critical to the improvement of current therapeutic measures. The severity of the phenotype caused by *RDH12* mutations is consistent with a nonredundant role in photoreceptor physiology. When *in vitro* activity toward retinoids is considered, RDH12 has the potential to play a unique role in the visual cycle mechanism as an all-*trans* retinol dehydrogenase. The role of RDH12 in retinoid processing in the retina and disease pathogenesis is a major focus of our research

endeavors as outlined in this dissertation. I have evaluated these issues and documented my findings in the following chapters:

1. To further define the role of RPE65 in the visual cycle through the characterization of RPE65 expression, surface epitopes and protein-protein interactions, I employed a monoclonal antibody approach. Immunohistochemical analysis showed that RPE65 is not expressed in cone cells, thus excluding a proposed direct role of RPE65 in a cone regenerative pathway of 11-*cis* retinal synthesis. Immunoaffinity studies mapped antigenic determinants of the protein surface and found that RPE65 is associated with the visual cycle enzyme RDH5. (Chapter 2)

2. To evaluate RDH12 protein expression and determine whether subcellular localization supports its proposed role as a visual cycle retinoid reductase, I generated an anti-RDH12 antibody. When used for western and immunohistochemical analysis, this antibody showed that RDH12 expression is confined to the photoreceptor IS in both human and mouse. This suggests an equivalent physiological role for RDH12 in both species, but at the same time places it away from the phototransduction reactions occurring in the OS. Additionally, functional characterization of a *RDH12* knockout mouse revealed no differences in histology, retinoid processing or ERG response compared to wild-type, suggesting that Rdh12 function in mice does not directly contribute to visual cycle function. (Chapter 3)

3. To determine the effects of Rdh12 deficiency on the retinoid reductase activity of the retina as well as retinoid processing, I performed *in vitro* reductase assays of *Rdh12*-knockout and wild-type mouse retinal homogenates towards retinaldehydes substrates. This showed that the reductive capacity of the Rdh12-deficient mouse is greatly

decreased compared to the wild-type. In addition, transcript levels of *Rdh12* correlated with visual cycle activity as determined by the genetic background of the mouse. These findings suggest that one role of RDH12 is likely the reduction of retinaldehydes that exceed the reductive capacity of the photoreceptor OS.

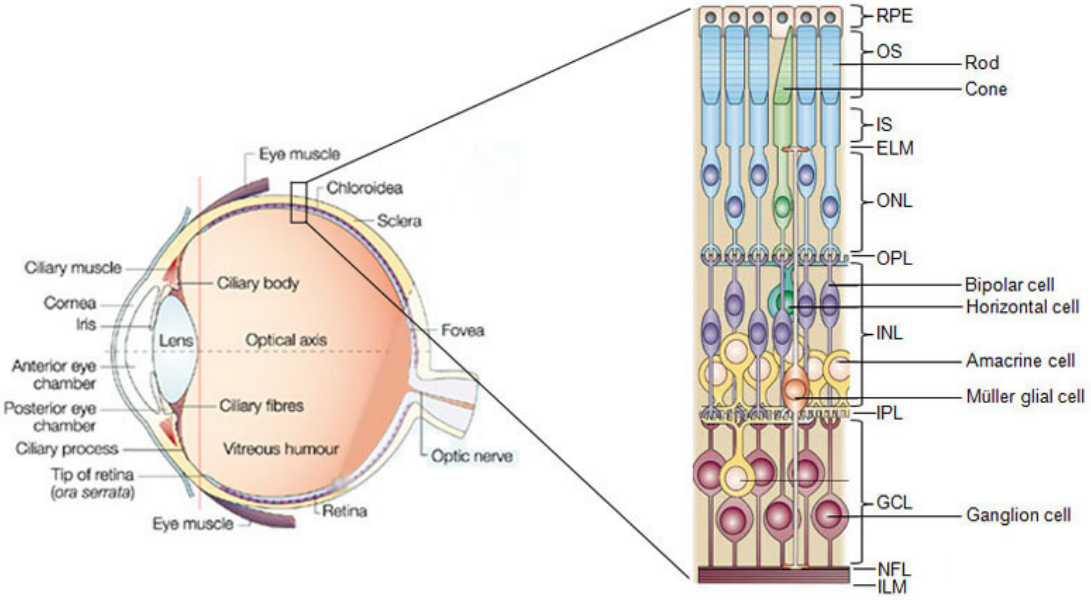

Figure 1-1. Structure of the human eye and the layers of the retina. This illustration points out the major anatomical features of the human eye. Light enters the eye through the cornea, passing through the lens and the anterior chamber (delineated by the red vertical dashed line) which is composed mostly of the vitreous humor before striking the retina. The blown-up section of the eye shows the layers of the retina, with the major cell types of the retina labeled. The layers of the retina, from outside to inside (and viewed here top to bottom) they are: retinal pigment epithelium (RPE), outer segments (OS), inner segments (IS), external limiting membrane (ELM), outer nuclear layer (ONL), outer plexiform layer (OPL), inner nuclear layer (INL), inner plexiform layer (IPL), ganglion cell layer (GCL), inner limiting membrane (ILM) and nerve fiber layer (NFL). This figure is printed with permission from [151, 152].

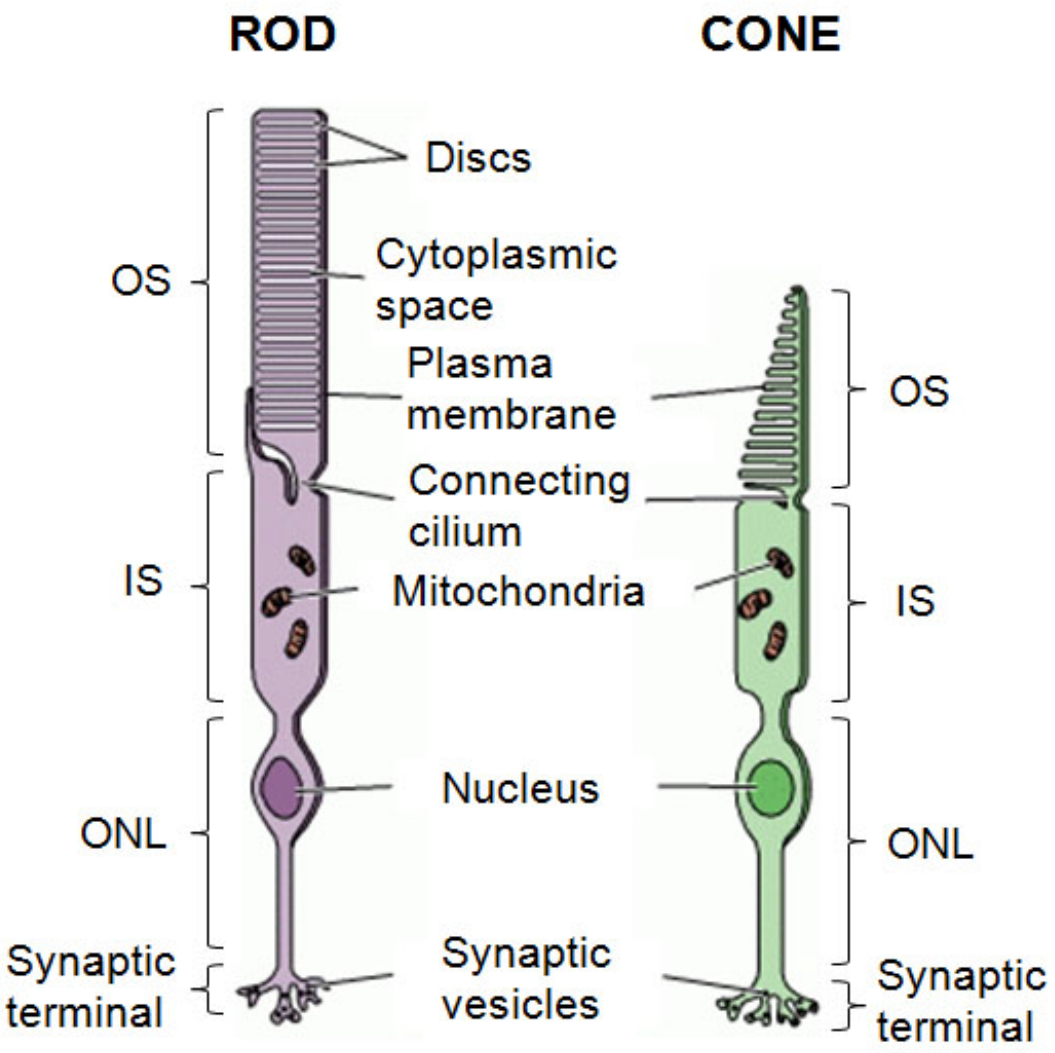

Figure 1-2. Structure of the rod and cone photoreceptors. This schematic depicts the major divisions of the photoreceptors, which are: the outer segment composed of stacks of bimembranous discs which contain the phototransductive machinery, the inner segment that contains the mitochondria and other cellular metabolism organelles; the outer nuclear layer which contains the cell nucleus; and the synaptic terminal where neurotransmitter release is facilitated. This figure is printed with permission from [153], and http://www.ncbi.nlm.nih.gov/bookshelf/br.fcgi?book=neurosci&part=A751

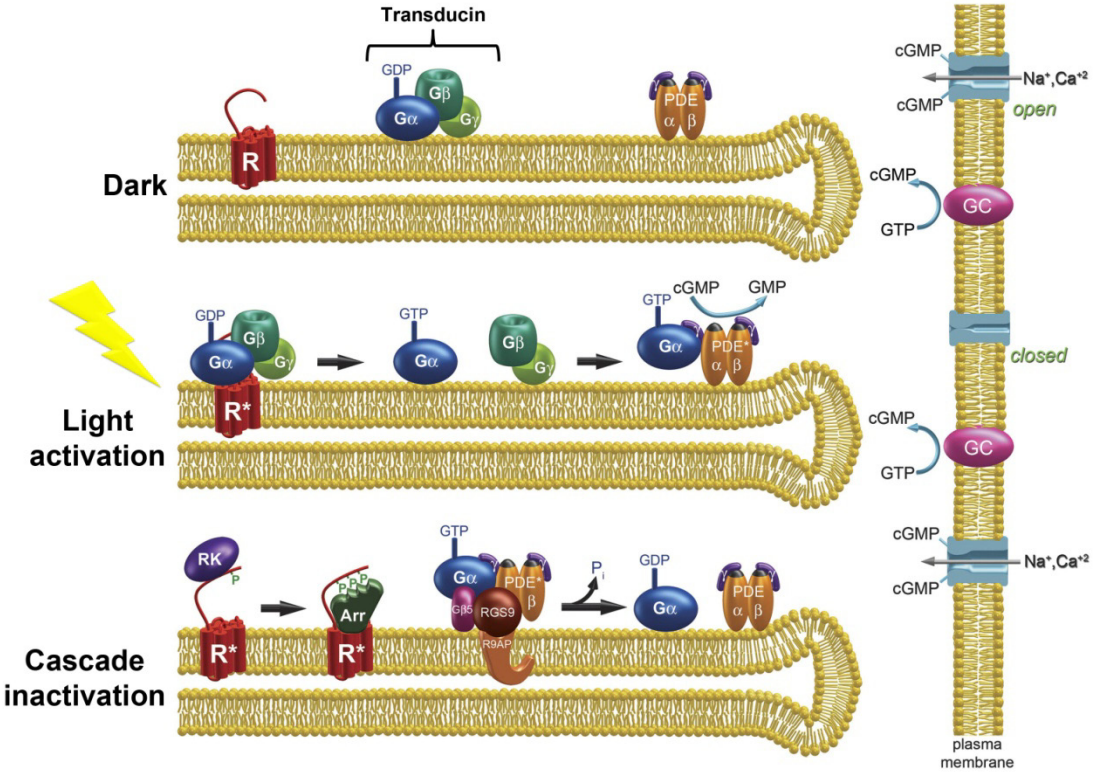

Figure 1-3. Phototransduction cascade activation and inactivation. This illustration depicts three rod discs, and to the right a representation of the plasma membrane. The top disc illustrates inactive rhodopsin (R), transducin (Gα, Gβ, and Gγ subunits), and PDE (α, β, and γ subunits) in the dark. Adjacent to the right, calcium and sodium channels in the plasma membrane as open in response to guanylate cyclase (GC), shown converting GTP to cGMP. The middle disc shows the activation of transducin and PDE in response to light stimuli, while the adjacent plasma membrane shows the ion channels as having shut due to decreased cellular levels of cGMP- a result of PDE activation. The reactions in the bottom disc represent inactivation of active rhodopsin via phosphorylation by rhodopsin kinase (RK) followed by arrestin (Arr) binding and transducin/PDE inactivation by the RGS9-1/Gβ5/R9AP complex. Cytoplasmic levels of cGMP are restored by GC. This figure is printed with permission from [32].

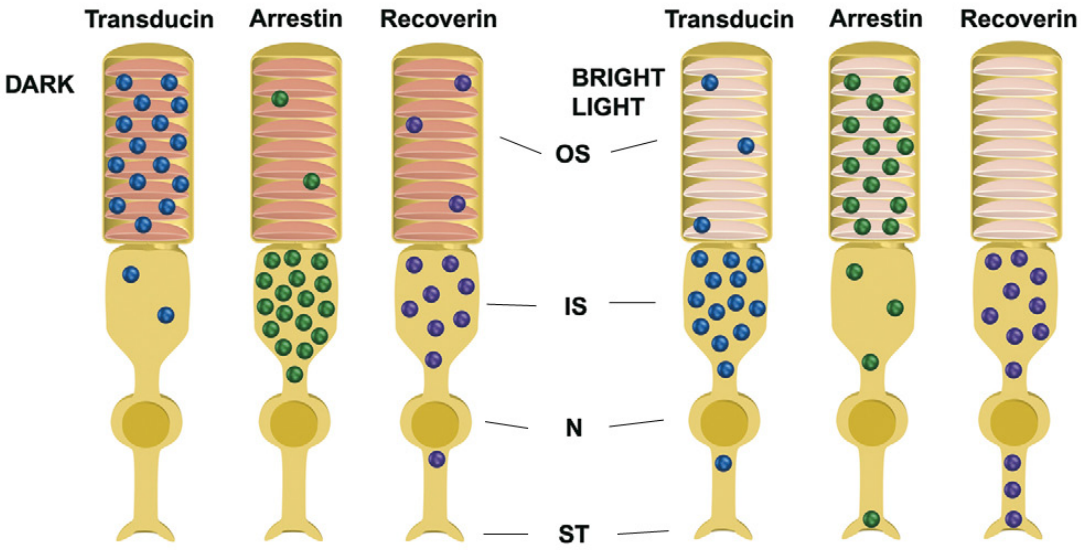

Figure 1-4. Translocating proteins in visual signal transduction. Schematic illustration of transducin, arrestin and recoverin distribution in dark-adapted and light-adapted rods. In rods, transducin moves out of the outer segment and accumulates primarily in a region known as the inner segment, arrestin moves in the opposite direction, and recoverin shifts from the outer segment towards the synapse. In cones, arrestin but not transducin moves in light; recoverin translocation has not yet been analyzed in cones The subcellular rod compartments are abbreviated on the right: OS, outer segment; IS, inner segment; N, nucleus; ST, synaptic terminal. This figure is printed with permission from [38].

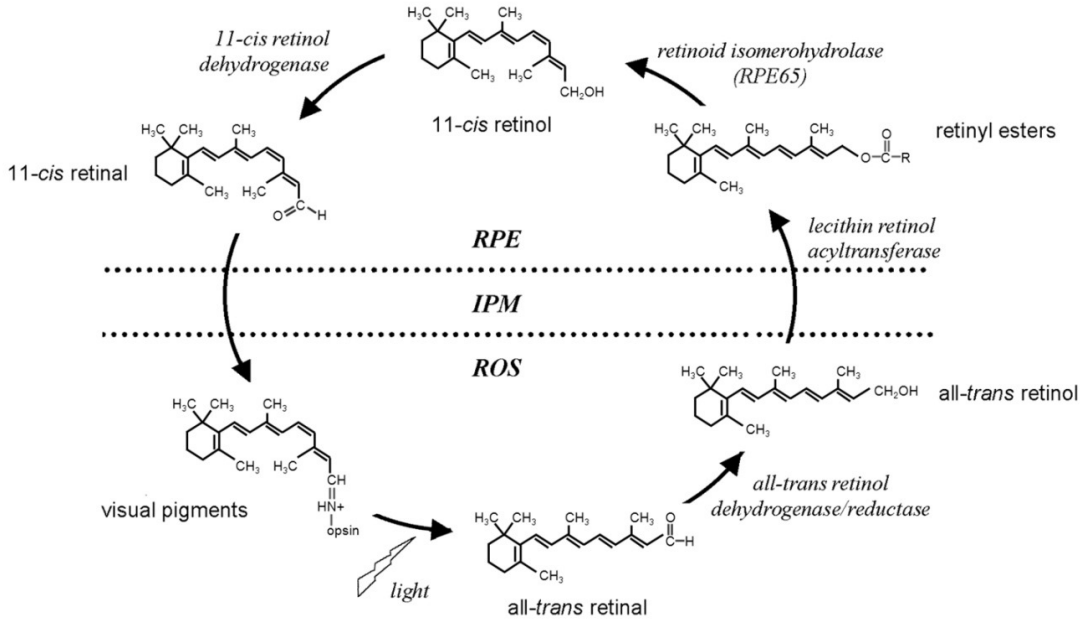

Figure 1-5. The visual cycle. Schematic of the visual cycle mechanism showing the interconversion of vitamin A analogs and necessary enzyme activities. RPE, retinal pigment epithelium; IPM, interphotoreceptor matrix; ROS, rod outer segments.

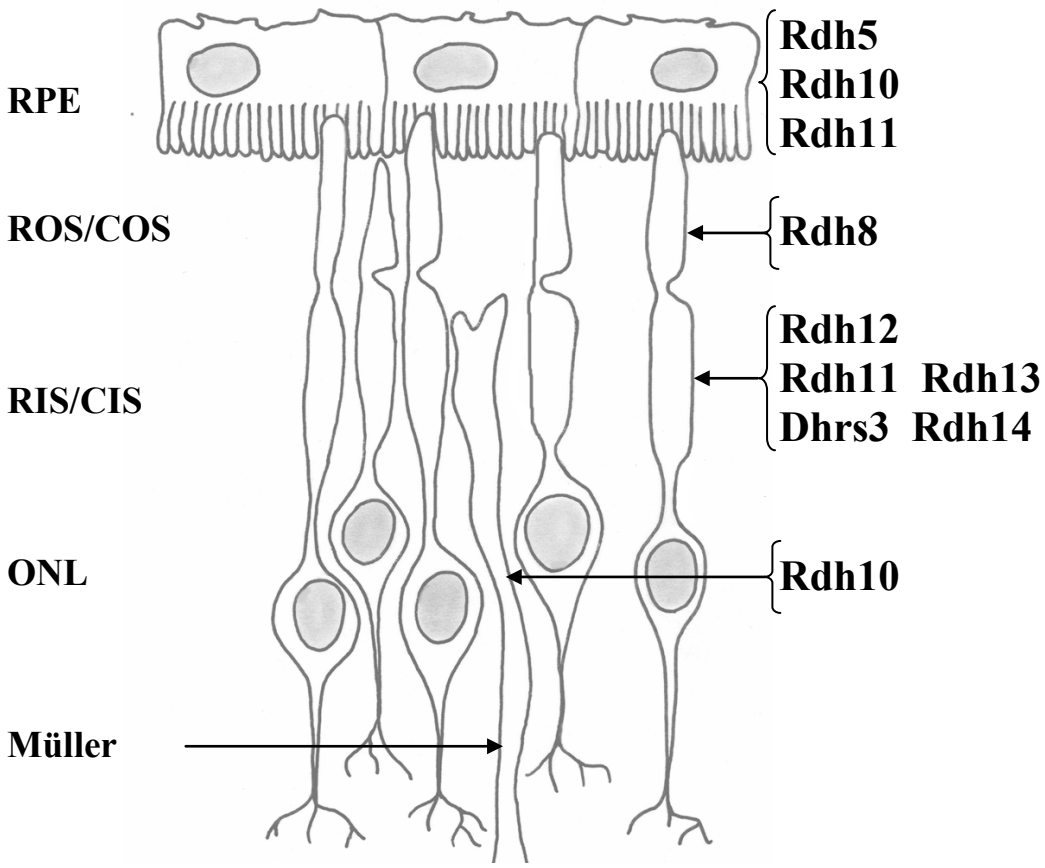

Figure 1-6. RDH Isoforms in the retina. This schematic shows the localization of the major RDH isoforms present in the retina, as based on the current data. RPE, Retinal pigment epithelium; ROS/COS, rod or cone outer segment; RIS/CIS, rod or cone inner segment; ONL, outer nuclear layer; Müller, Müller cell.

CHAPTER 2

RPE65 SURFACE EPITOPES, PROTEIN INTERACTIONS, AND EXPRESSION IN ROD- AND CONE-DOMINANT SPECIES*

Introduction

RPE65 is an abundant protein expressed in the RPE where its function in the visual cycle is necessary for the synthesis of 11-*cis* retinal, the chromophore of the visual pigments [67, 109]. Developmentally, RPE65 is an important marker for the differentiated phenotype of the RPE [111]. Mutations in the gene encoding *RPE65* are associated with early-onset forms of autosomal recessive severe retinal dystrophy, including Leber congenital amaurosis in an estimated 5% of cases. [103, 104, 112, 113, 154]. A number of research groups over the years have been involved in efforts to develop therapeutic methods specific for RPE65 loss-of-function [155-158]. These efforts have culminated in recent clinical trials of gene replacement therapy, in which patients suffering from advanced stages of LCA displayed improvement in visual function [159-162].

Studies have shown that RPE65 functions as the retinoid isomerohydrolase in the RPE that converts all-*trans* retinyl esters to 11-*cis* retinol by coupling the free energy of ester hydrolysis to the *trans* to *cis* isomerization reaction [68, 69, 120, 163]. This role is in agreement with earlier studies, the results of which show that RPE65 is a retinoid-

* Portions of this chapter were published in:
Hemati N, Feathers KL, **Chrispell JD**, Reed DM, Carlson TJ, Thompson DA. RPE65 surface epitopes, protein interactions, and expression in rod- and cone-dominant species. Mol Vis. 2005 Dec 21;11:1151-65.

binding protein [66, 118, 164]. A molecular switch mechanism whereby RPE65 binds all-*trans* retinyl esters when palmitoylated on Cys231, Cys329, and Cys330 by LRAT, but binds all-*trans* retinol when depalmitoylated, was proposed [165]. However, further studies showed that LRAT activity was not required beyond the synthesis of the all-*trans* retinyl ester substrate [122]. Pathogenesis associated with RPE65 loss-of-function has been proposed to result from constitutive opsin activity due to loss of chromophore [117, 166, 167], although alternative interpretations have also been put forward [168].

The relatively high incidence of *RPE65* mutations in patients with early-onset retinal dystrophy, as well as its central role in current therapeutic efforts, created a strong incentive to garner a mechanistic understanding of RPE65 in the context of visual cycle function. Among the many critical issues to resolve include elucidating the mechanism by which missense mutations disrupt RPE65 function, and establishing the role of RPE65 in rod- and cone-associated visual cycles. Cones have been proposed to have a private pathway of visual pigment regeneration that may involve their ability to oxidize 11-*cis* retinol to 11-*cis* retinal [96-98, 100]. RPE65 has been proposed to directly participate in the cone visual cycle based on its reported expression in cones [94, 95].

For studies of RPE65 expression, function, and structure, our lab developed monoclonal antibodies specific for RPE65. One of these, mAb 8B11, elicited using RPE membranes as immunogen, has been widely distributed and used in various applications [107, 169-172]. A second antibody, mAb 1F9, was elicited using an RPE65 synthetic peptide. Studies outlined in this chapter report on the generation and utility of this second antibody to corroborate standing evidence regarding aspects of RPE65 structure,

interactions with other proteins of the visual cycle, and pattern of immunoreactivity in eyes from rod- and cone-dominated species.

Materials and Methods

Synthesis of RPE65 synthetic peptides

The antigenic index for RPE65 was calculated using the Jameson-Wolf prediction of the Protean module in Lasergene suite of software (DNA STAR, Inc., Madison, WI). Peptides of interest were synthesized by the University of Michigan Protein Facility. For use as immunogen, peptide 1 (50-FHHINTYEDNGFLIV-64), peptide 2 (312-FHHINTYEDNGFLIV-326) and peptide 3 (444-PDRLCKLNVKTETWV-459) corresponding to the human RPE65 protein were synthesized with an added carboxy-terminal cysteine residue and conjugated to keyhole limpet cyanin (KLH) using Imject Maleimide Activated Immunogen Conjugation Kit (Pierce Chemical Co., Rockford, IL) according to manufacturer's instructions. Peptides were similarly conjugated to ovalbumin for use as substrates in enzyme-linked immunosorbent assays (ELISAs). A peptide of the 8B11 epitope (154- KVNPETLETI-163) was generated for use in immunoaffinity assays, as was RPE65 peptide 93-MTEKRIVITE-102 (peptide 18), for the assessment of nonspecific effects.

mAb production and screening

The protocol used for mAb production adhered to the Association for Research in Vision and Ophthalmology (ARVO) Statement for the Use of Animals in Ophthalmic and Vision Research and was performed by the University of Michigan Diabetes Research and Training Center hybridoma facility. Six-week-old BALB/c female mice were

immunized by intraperitoneal injection with 40 μg of KLH-conjugated peptide FHHINTYEDNGFLIV. mAb 8B11 was previously generated by immunization bovine RPE microsomal membranes and the corresponding antigenic determinant was mapped to the sequence 154- KVNPETLETI-163 by ELISA) [107, 173-175]. A minimum of three immunizations in adjuvant were given at three week intervals, and fusions were performed using standard procedures [176, 177] and the AGA-X63.653 cell line [178]. Hybridoma supernates were screened by ELISA using bovine RPE membranes or peptide FHHINTYEDNGFLIV conjugated to ovalbumin as substrates, and subsequently screened by western and immunohistochemical analysis, as described below. For western analysis, bovine RPE and mouse RPE/choroid membrane proteins were separated by sodium dodecyl sulfate-polycrylamide gel electrophoresis (SDS-PAGE), transferred to nitrocellulose, and incubated with primary and secondary antibody (alkaline phosphatase-conjugated) using standard methods [179]. Typing of antibody class and subclass was performed using ImmunoPure Monoclonal Antibody Isotyping Kit (Pierce Chemical Co.) according to manufacturer's instructions. Hybridomas producing RPE65 antibodies were expanded and grown in culture for six weeks prior to harvest. Immunoglobulin G (IgG) was isolated from ascites fluid obtained from *in vivo* hybridoma cultures using chromatography on diethylaminoethyl-Sepharose in high salt [180] or protein-A Sepharose (Prosep A kit, Millipore Corp., Billerica, MA).

Immunohistochemical analysis

For cryosections, eyes were fixed in cold 4% paraformaldehyde (mice and rats were first perfused with PBS, then 4% paraformaldehyde), washed in PBS, transitioned to sucrose/Optimal Cutting Temperature compound (OCT), frozen in dry-ice cooled

hexanes, and 10 μm sections cut through the retina/choroid/RPE (for large eyes) or whole globes (for small eyes). For mAb 8B11, sections (except mouse) were blocked with 20% sheep serum and 0.2% Triton X-100 (Sigma-Aldrich, St. Louis, MO) in PBS, incubated with mAb 8B11 (2 μg/ml) for 2 h, then with Alexa Fluor 555-conjugated anti-mouse IgG (1:500; Molecular Probes, Inc., Eugene, OR) for 1 h. For mouse sections with mAb 8B11, and all sections with mAb 1F9 (30 μg/ml), the Mouse on Mouse (M.O.M.) Peroxidase kit (Vector Laboratories, Burlington, CA) was used for blocking and antibody incubation (1 h at RT), and the tyramide signal amplification (TSA)-Alexa Fluor 568 kit (Molecular Probes, Inc.) was used for visualization.

For retina flatmounts, mouse eyes were enucleated and the retinas dissected and fixed in cold 4% paraformaldehyde for 1 h. Immunohistochemistry and lectin labeling was performed essentially as in [94]. In brief, retinas were washed in PBS, blocked with 20% sheep serum and 0.2% Triton X-100 in PBS, incubated with mAb 8B11 or mAb 1F9 and fluorescein isothiocyanate (FITC)-conjugated peanut agglutinin (PNA)-lectin (0.05 mg/ml; Molecular Probes, Inc.) in 2% sheep serum and 0.2% Triton X-100 in PBS for 12 h, washed and incubated in the same buffer with Alexa Fluor 555-conjugated anti-mouse IgG (1:500) for 12 h. Alternatively, retinas were incubated with mAb 8B11 (2 μg/ml) and rabbit anti-S-opsin (1:500) or anti-M/L-opsin (1:500, Chemicon International, Inc., Temecula, CA) for 12 h, then with Alexa Fluor 555-conjugated anti-mouse IgG (1:500) and Alexa Fluor 488-conjugated anti-rabbit IgG (1:400) for 12 h.

Specimens were viewed and photographed on a Nikon Eclipse E800 microscope with a Nikon DMX1200 digital camera using the manufacturer's data acquisition software. Phase contrast and fluorescence images were obtained (FITC-PNA lectin, 488

nm; Alexa Fluor, 555 and 568 nm). The approximate ages of the eyes used for immunohistochemical analysis were: human, 49 years; bovine, 4 months; wild-type (B6/129) mouse, 40 days; *Rpe65*-knockout (*Rpe65–/–*) mouse, 50 days; *Nrl*-knockout (*Nrl–/–*) mouse, 42 days; rat, 6 months; *Xenopus laevis*, 4 week; and chicken, 4 months.

Immunoadsorption and peptide elution

Affinity matrices were generated by crosslinking mAb 8B11 or mAb 1F9 to cyanogen bromide-activated Sepharose 4B (Amersham Biosciences, Piscataway, NJ) according to manufacturer's instructions. Bovine RPE membranes (200 μg) were solubilized in 10 mM sodium phosphate, 150 mM NaCl, pH 7.0, and Complete protease inhibitors (Roche Diagnostics Corp., Indianapolis, IN) containing either 0.8% CHAPS, 0.8% octylglucoside, 0.5% laurylmaltoside, or 0.5% Genapol. The solubilized membranes were incubated with affinity matrix (50 μl) overnight at 4 °C, then washed and eluted by incubation with 500 μM peptide (100 μl) for 1 h at RT in the same detergent solution used for solubilization, but at lower concentrations (0.7% CHAPS, 0.7% octylglucoside, 0.2% laurylmaltoside, or 0.2% Genapol). The eluted proteins were analyzed by SDS-PAGE, coomassie blue staining, and western analysis using mAb 8B11 or mAb 1F9, and antibodies against 11-*cis* retinal dehydrogenase (RDH5) [135], the retinal G protein-coupled receptor (RGR) [85], and lecithin retinol acyl transferase (LRAT) [181].

Generation of predicted RPE65 tertiary structures

A low-resolution model of the tertiary structure of the RPE65 protein was derived, *ab initio*, by submitting the human RPE65 amino acid sequence (GenBank AAA99012) to the automated I-sites/HMMSTR/Rosetta server [182]. The server

automates a process of modeling tertiary structure from amino acid sequence using HMMSTR, a hidden Markov model based on protein structures in the invariant or initiation folding sites (I-sites) library of nonredundant short sequence motifs (supersecondary structures) that correlate with local structures [183], coupled with the Rosetta program to build structures from protein fragments [184]. The resulting tertiary structure with predicted coordinates was visualized and displayed with Discover Studio ViewerPro 5.0 (Accelrys, San Diego, CA).

A second model of RPE65 tertiary structure was generated using the recently solved structure of the apocarotenoid-cleaving oxygenase from *Synechocystis* sp. PCC 6803 (PDB 2biw:a) as a template; a member of the retinal-forming carotenoid oxygenases protein family of which RPE65 and β-carotene-15, 15'-oxygenase are members [185]. Using the functions for matching and aligning available in Swiss-PDBViewer/DeepView (version 3.71b1), the human RPE65 amino acid sequence was placed into the structure of PDB 2biw and the resulting file was submitted to the SWISS-MODEL server [186]. The resulting tertiary structure with coordinates was displayed and annotated with DS ViewerPro.

Results

Antibody development

In screens of hybridomas generated from mice immunized with bovine RPE membranes, clone 8B11 (IgG1 kappa) was found to produce a high-affinity monoclonal antibody specific for RPE65 in western analysis of bovine RPE membranes (Figure 2-2). Specificity for RPE65 was further demonstrated by comparison of immunoreactivity in

mouse eye sections from wild-type and *Rpe65–/–* mice that showed reactivity only in the RPE of the wild-type animals (Figure 2-3).

The production of the novel anti-RPE65 antibody began with the creation of three synthetic peptides selected based upon the antigenic profile of human RPE65 (Figure 2-1). Mice were immunized with one of these peptides, with the most robust anti-sera derived from the mouse treated with peptide 2 (312-FHHINTYEDNGFLIV-326). This resulted in the identification of a hybridoma producing a monoclonal antibody, 1F9 (IgG1 kappa), specific for RPE65 in westerns of bovine RPE membranes (Figure 2-2) and in immunohistochemical analysis of wild-type and *Rpe65–/–* mice (Figure 2-3). However, the working concentrations of mAb 1F9 needed were at least 10 fold greater than those for mAb 8B11 (Figure 2-2). This is indicative of the relatively lower affinity of mAb 1F9 for the bovine and mouse proteins compared to mAb 8B11.

RPE65 immunoaffinity purification

To determine whether the epitopes recognized by mAb 8B11 and mAb 1F9 are accessible on the surface of RPE65, and to establish a mechanism for purifying the native protein, bovine RPE membranes solubilized in non-ionic detergents were incubated with immunoaffinity matrices, followed by elution with various RPE65 peptides.

When RPE membrane proteins were incubated with a mAb 8B11 affinity matrix, RPE65 could be bound and specifically eluted by incubation with peptides containing the KVNPETLETI sequence, appearing as a 61 kDa band on coomassie blue stained gels. Results obtained using CHAPS and elution with the KVNPETLETI peptide corresponding to the 8B11 epitope are shown in Figure 2-4. Peptide 18, another peptide from RPE65, was used a control for nonspecific elution. Comparable results were

obtained using laurylmaltoside, octylglucoside, or Genapol, with the identity of RPE65 confirmed by western analysis (Figure 2-4). The amount of RPE65 recovered by peptide elution was somewhat less than when the affinity matrix was eluted by stripping with SDS sample buffer. However, elution with SDS sample buffer also resulted in the release of small amounts of IgG light chain (MW about 25 kDa) from the matrix (presumably due to reduction of intramolecular disulfide linkages), as well as trace amounts of nonspecifically bound protein. Residual RPE65 remaining on the matrix following elution with KVNPETLETI-containing peptides was also released by SDS stripping, suggesting that RPE65 undergoes significant hydrophobic interaction with the solid support, a situation also observed using a non-immune mouse IgG affinity matrix.

Similar results were obtained for purification of RPE65 from bovine RPE membranes using the mAb 1F9 affinity matrix eluted with the FHHINTYEDNGFLIV peptide, with some differences (Figure 2-4). The mAb 1F9 matrix was effective at binding RPE65, however incubation with nonspecific peptides resulted in leaching of RPE65 from the matrix, and total yields of purified protein were significantly less than obtained with mAb 8B11; both effects are presumably due to the lower apparent affinity of mAb 1F9 for bovine RPE65. In addition, purification trials using the non-ionic detergent Genapol were not successful.

The finding that affinity matrices made using either mAb 8B11 or mAb 1F9 are effective for immunoadsorption of RPE65 solubilized in non-ionic detergent is consistent with the interpretation that the corresponding antigenic amino acid sequences are located on the surface of the native protein.

Visual cycle protein co-purifies with RPE65

Although RPE65 preparations obtained by affinity purification appeared to be relatively pure on coomassie blue-stained gels, western analysis was used to assess whether visual cycle proteins that potentially associate with RPE65 *in vivo* were co-eluted in our protocols. Immunoblots of the proteins eluted from the mAb 8B11 matrix with KVNPETLETI and probed with an antibody against the 11-*cis* retinol dehydrogenase RDH5 (approximately 35 kDa) showed that small amounts of RDH5 co-eluted with RPE65 in all four detergents tested (Figure 2-4) [135]. Trace amounts of RDH5 were also seen on blots of the proteins eluted from the mAb 1F9 matrix using FHHINTYEDNGFLIV in laurylmaltoside (Figure 2-4). For both mAb 8B11 and mAb 1F9 matrices, as well as non-immune IgG matrix, RDH5 in significant amounts was seen in SDS-sample buffer eluates, consistent with nonspecific interactions of RDH5 with the solid support. In contrast, western analysis using antibodies against RGR and LRAT did not detect these RPE proteins in peptide eluates of either mAb 8B11 or mAb 1F9 matrices (data not shown) [85, 181].

Predicted tertiary structure and epitope placement

Two approaches were used to generate structural models of RPE65 useful for experimental interpretation and design. First, a low-resolution tertiary structure for RPE65 was predicted from the primary sequence using the I-sites/HMMSTR/Rosetta server that automates the use of protein folding rules to predict local, secondary, and supersecondary structures using a Markov state to represent a position in an I-site motif, coupled with the Rosetta program to build structures from protein fragments using a Monte Carlo simulated annealing algorithm [182-184] (Figure 2-5). A second model was

generated based on the recently solved structure of the apocarotenoid-cleaving oxygenase from *Synechocystis* sp. PCC 6803 [PDB 2biw:a], a member of the retinal-forming carotenoid oxygenase family that contains RPE65 and β-carotene-15, 15'-oxygenase [185]. In DeepView, the RPE65 sequence was aligned and fit to the PDB 2biw sequence, the resulting structure was further modeled by the SWISS-MODEL server, and the coordinates annotated in DS ViewerPro [186] (Figure 2-5). The resulting RPE65 structures with predicted coordinates were displayed and annotated to highlight the epitope recognized by mAb 8B11 and mAb 1F9, and the locations of the amino acid substitutions resulting from patient missense mutations. The KVNPETLETI sequence recognized by mAb 8B11 and the FHHINTYEDNGFLIV sequence used to elicit mAb 1F9 both localize to surface exposed loops that are relatively unstructured. No predicted sites of posttranslational modifications or patient mutations are present within the mAb 8B11 antigenic determinant. However, the mAb 1F9 peptide contains both sites of patient mutations (N321K, 962-963 ins A) and potential interaction with metal ions (His313).

Immunohistochemical analysis of species and tissue specificity

To establish the specificity of RPE65 expression in eyes with rod- and cone-dominant retinas, mAb 8B11 and mAb 1F9 reactivity was assessed using immunohistochemical analysis of retina/RPE/choroid or whole globe cryosections from various species. With mAb 8B11, intense reactivity restricted to the RPE layer was seen in human, bovine, and rat; all species having rod dominant retinas (Figure 2-6). mAb 8B11 reactivity was also seen only in the RPE in chicken and *Xenopus laevis* whose retinas contain a high ratio of cone to rod cells, as well as in *Nrl–/–* mice whose retinas contain exclusively cone-like photoreceptor cells [17, 187-189]. With mAb 1F9,

immunoreactivity confined to the RPE layer was seen in human, bovine, and the *Nrl–/–* mouse (Figure 2-7). However, mAb 1F9 reactivity was completely absent in chicken and *Xenopus*, apparently due to lack of crossreactivity with RPE65 protein from these species as a result of sequence differences.

The reactivity of mAb 8B11 and mAb 1F9 was also evaluated in retina flatmounts and compared to the pattern of cone labeling using PNA-lectin, as well as to the reactivity of antibodies against S-opsin and M/L-opsin present in the cone photoreceptor outer segments (OS) (Figure 2-8). Retinas were from wild-type mice (C57BL/6/Sv129), *Rpe65–/–* mice in which no protein is detected, and *Nrl–/–* mice [67]. In all three mouse genotypes, no RPE65 immunoreactivity could be seen in cones or any other cells of the retina using either antibody, establishing that the absence of signal in retina/RPE/choroid sections was not due to masking by the intense signal from the RPE.

Discussion

A new monoclonal antibody against RPE65 has been developed and reactivity compared to that of the well studied anti-RPE65 antibody mAb 8B11. We have shown that a second human RPE65 sequence, FHHINTYEDNGFLIV, is also antigenic. The corresponding mAb 1F9 exhibits specificity similar to mAb 8B11 that is specific for KVNPETLETI, but has a lower affinity and a lower degree of reactivity across species, most likely due to differences in amino acid sequence between species. The KVNPETLETI sequence is conserved among bovine, newt, and frog RPE65 orthologs, and differs only at the second position (Ile vs. Val) in human, monkey, rat, mouse, dog, chicken, and salamander. It is interesting to note that, in studies by others in which

RPE65 antibodies were developed by immunization with synthetic peptides, the most effective antibodies obtained were elicited by 150-NFITKVNPETLETIK-164 containing the epitope recognized by mAb 8B11 [190]. The convergence of these two different approaches to RPE65 antibody production on the same amino acid sequence suggests that this region possesses high antigenicity.

The antigenic determinants recognized by mAb 8B11 and mAb 1F9 are amino acid sequences likely to be present on the RPE65 protein surface. The ability of each antibody to recognize native RPE65 solubilized in non-ionic detergents made it possible to develop immunoaffinity purification protocols effective in purifying RPE65 from bovine RPE membranes, and from transfected COS-7 cells expressing the recombinant protein (data not shown). Establishing the surface accessibility of the KVNPETLETI and FHHINTYEDNGFLIV epitopes represented a first step toward validating predicted models of RPE65 tertiary structure derived using *ab initio* and comparative methods, confirming the potential utility of such models in future experimental design.

Preparations of RPE65 purified from bovine RPE membranes using mAb 1F9 or mAb 8B11 immunoaffinity chromatography were found to contain co-eluted RDH5 that was observable by western analysis. Only small amounts of RDH5 were detected, even when washes were performed in the cold using minimum times and volumes, and various detergents. RDH5 is an abundant protein in the RPE that appears to undergo significant nonspecific interaction with the affinity matrix solid support. However, two other visual processing proteins, RGR and LRAT, that are relatively abundant in the RPE and likely to interact with RPE65, were not detected in immunoaffinity purified material. It is therefore likely that the co-purification of RDH5 with RPE65 reflects a high affinity

association of these proteins *in vivo*, rather than a nonspecific effect. This is in agreement with previous studies reporting that RDH5 co-purifies with RPE65 when nonspecific methods of elution (e.g. high pH) are used [70]. Studies to determine whether RPE65 and RDH5 exist in a stable retinoid processing complex *in vivo* have to date been inconclusive.

Analysis of immunoreactivity in eye cross-sections and retina flatmounts using mAb 8B11 detected RPE65 expression only in the RPE in a number of species that have rod- or cone-dominant retinas, including *Xenopus laevis* (~40% cones), chicken (~ 60% cones), and the *Nrl–/–* mouse in which the cone-like phenotype of the photoreceptor cells has been established on the basis of a number of morphological, molecular, and electrophysiological criteria that distinguish the photoreceptors from rods [17, 187-189, 191, 192]. Corroborating data were obtained using mAb 1F9 to assess immunoreactivity in mouse, human, and *Nrl–/–* mouse. Our finding of RPE65 expression only in the RPE and not in retina is in agreement with an earlier study where this issue was addressed in the mouse [193]. In contrast, studies by Ma and coworkers reported RPE65 expression in cones, first detecting *RPE65* mRNA in salamander cones using reverse transcriptase-coupled polymerase chain reaction and then finding RPE65 immunoreactivity in mouse, bovine, rabbit, and *Xenopus laevis* retina flatmounts using a polyclonal antibody elicited against 150-NFITKVNPETLETIK-164 [94, 95]. Curiously, in the second study a higher density of labeled cells was seen in rod-dominant mouse, bovine, and rabbit retinas than in *Xenopus laevis* retinas comprised of 30% cones, an incongruity not discussed by the authors. Also of note, the reactivity of preimmune serum on the retina flatmounts was not shown. Our studies do not exclude the possibility that extremely low level expression of

RPE65 exists outside the RPE. In fact, in a recent study, low level *RPE65* expression in the ciliary body was detected using RT-PCR and western analysis, but not by immunohistochemistry [194]. It remains to be seen whether reported cone expression is genuine or a result of contamination of retina preparations with small amounts of RPE, a valid concern considering the close physical association between the two tissues.

We conclude that the primary site of RPE65 function is in the RPE-based visual cycle, as we find no physical evidence to suggest a direct role of RPE65 in an alternate visual cycle involving cone cells. The identification of two distinct RPE65 surface epitopes represented a first step toward developing a structural understanding of this important disease gene product.

Outside Contributions: Nahid Hemati performed the epitope mapping for mAb 8B11 as well as immunoaffinity experiments with that antibody, and assisted with the mAb 1F9 immunoaffinity experiments. Kecia Feathers performed the mAb 8B11 and flatmounted retina immunohistochemistry, and assisted with the mAb 1F9 immunohistochemistry. David Reed generated the models of RPE65 tertiary structure.

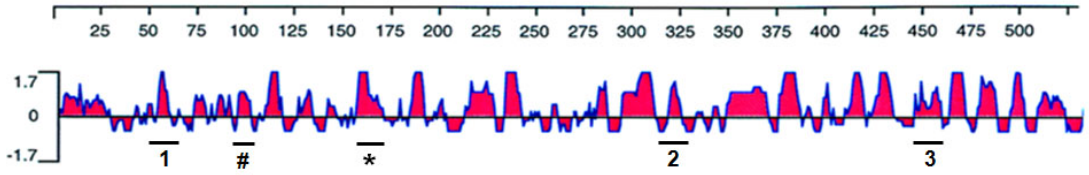

peptide 1. 50-FEVGSEPFYHLFDGQ-64

peptide 2. 312-FHHINTYEDNGFLIV-326 ← mAb 1F9

peptide 3. 444-PDRLCKLNVKTETWV-459

* mAb 8B11. 154-KVNPETLETI-163

peptide 18. 93-MTEKRIVITE-102

Figure 2-1. Schematic of RPE65 amino acid sequence. RPE65 antigenic index calculated using the Jameson-Wolf prediction in the DNASTAR program Protean. Positions of synthetic peptides 1-3 corresponding to the 3 sequences of highest predicted antigenicity (excluding the 8B11 epitope) are shown underlined in the enlarged section. Amino acid sequences of the 8B11 epitope and the non-specific synthetic peptide used in this study are also shown underlined.

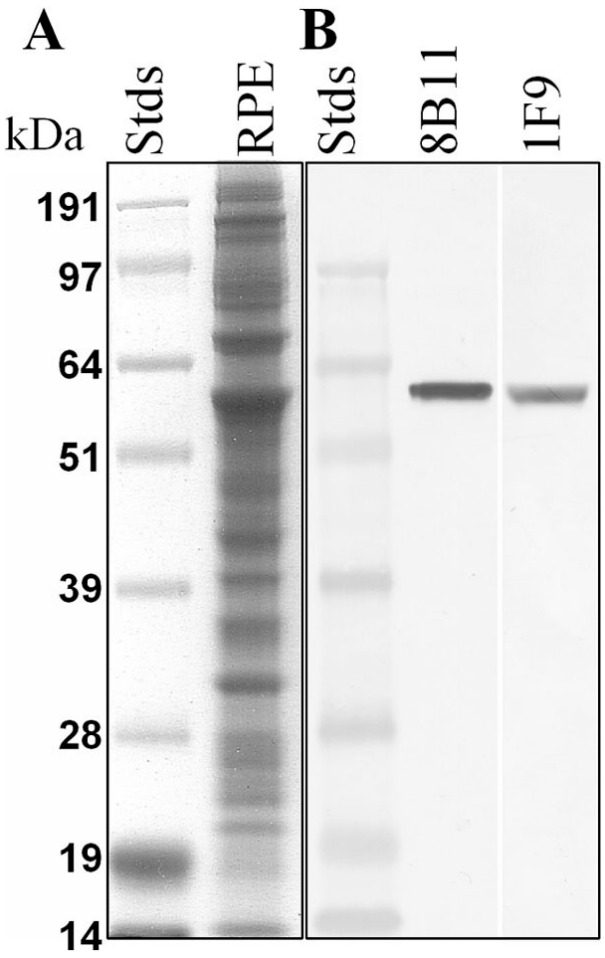

Figure 2-2. Immunoreactivity of mAb 8B11 and mAb 1F9 with bovine RPE membranes. A: Coomassie blue staining of proteins separated by SDS-PAGE (20 μg protein). B: Western analysis (1 μg protein) of proteins separated by SDS-PAGE, transferred to nitrocellulose, incubated with mAb 811 (0.2 μg/ml), or mAb 1F9 (3 μg/ml), and immunoreactivity visualized using alkaline phosphatase coupled anti-mouse IgG. RPE65 migrates at about 61 kDa.

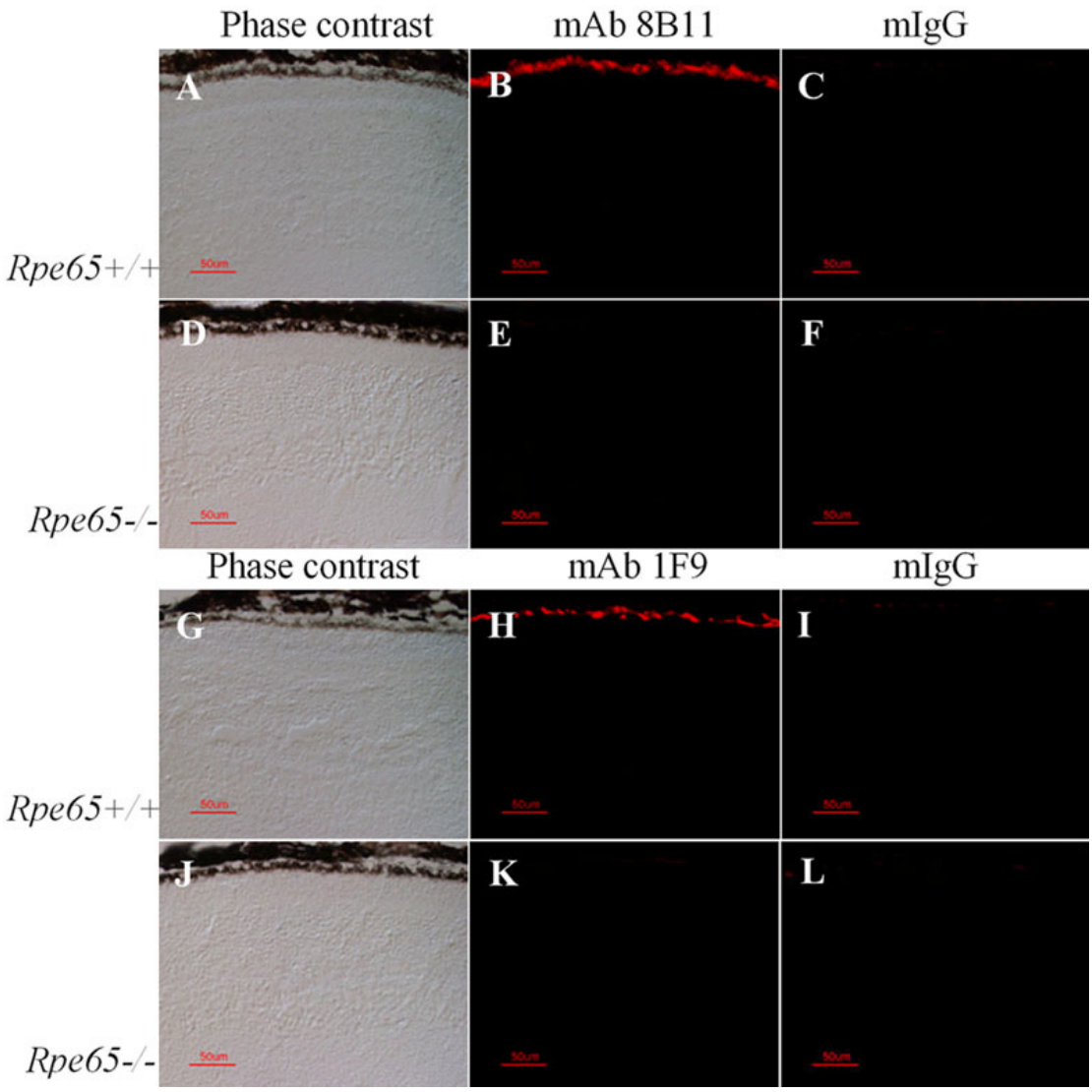

Figure 2-3. Immunohistochemical analysis of mAb 8B11 and mAb 1F9 reactivity in wild-type and *Rpe65*–/– mice. Cryosections were incubated with mAb 8B11 (2 µg/ml) or mAb 1F9 (30 µg/ml) using M.O.M. Peroxidase reagents, with visualization using TSA-Alexa Fluor 568 reagents and using fluorescence imaging (1/30 s). Phase contrast images (A,D,G,J); mAb reactivity (B,E,H,K); non-immune mIgG reactivity (C,F,I,L).

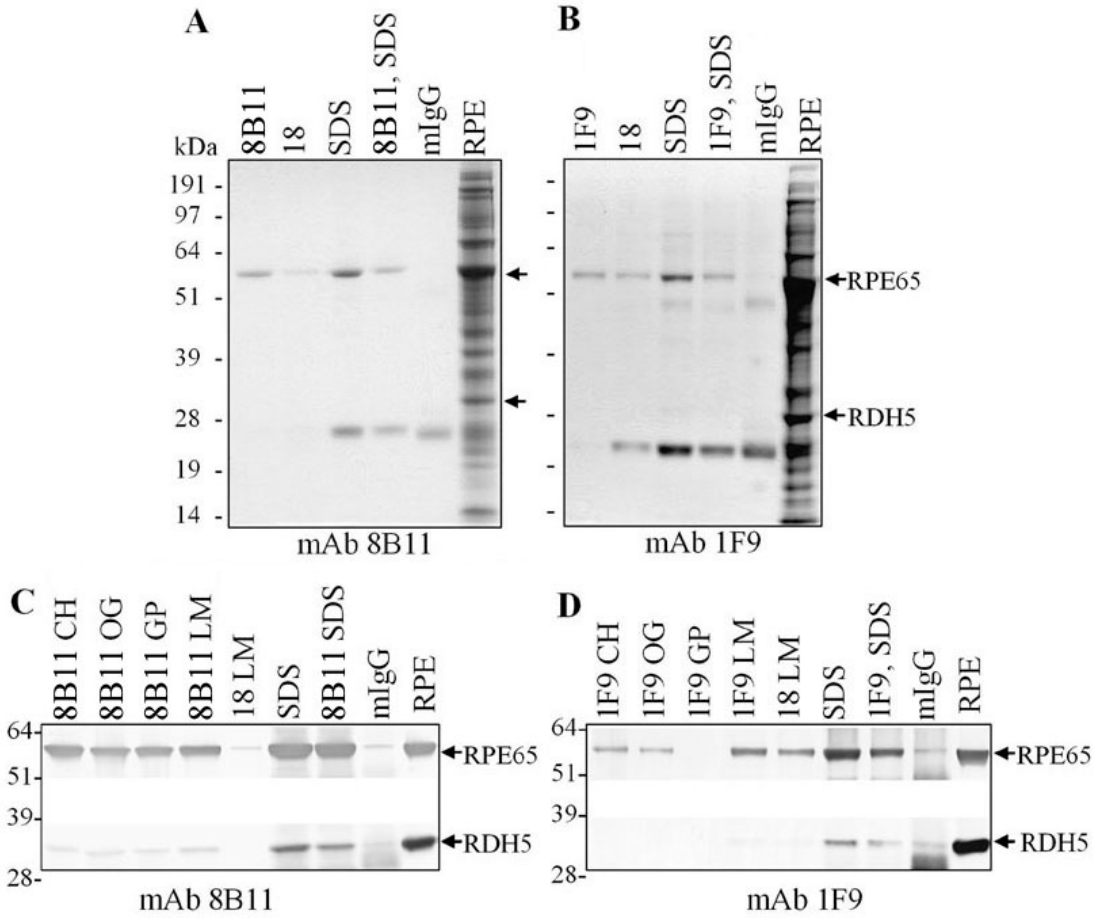

Figure 2-4. RPE65 immunoadsorption and peptide elution. A, C: Bovine RPE membranes in CHAPS (A) or bovine RPE membranes in laurylmaltoside (B) were incubated with mAb 8B11-Sepharose (A) or with mAb 1F9-Sepharose (B). Coomassie blue stained gels of proteins eluted with the KVNPETLETI peptide corresponding to the mAb 8B11 epitope (A), with the FHHINTYEDNGFLIV peptide used to generate mAb 1F9 (B), with peptide 18 corresponding to an RPE65 sequence that did not compete in ELISA's, or with SDS-sample buffer. C, D: Western analysis of bovine RPE membranes in various detergents immunoabsorbed on mAb 8B11-Sepharose (C), or on mAb 1F9-Sepharose (D), and eluted with peptides or SDS-sample buffer, as shown. Proteins were transferred to nitrocellulose and probed with mAb 8B11 (C), mAb 1F9 (E), or an antibody against RDH5 (C, D), and reactivity visualized using alkaline phosphatase coupled anti-mouse IgG. Arrows indicate the positions of RPE65 and RDH5. CH represents CHAPS; OC represents octylglucoside; GP represents Genapol; LM represents laurylmaltoside; mIgG represents nonspecific mIgG-Sepharose matrix; 8B11 represents KVNPETLETI; 1F9 represents FHHINTYEDNGFLIV; 8B11, SDS represents peptide KVNPETLETI eluted matrix subsequently eluted by SDS; 1F9, SDS represents peptide FHHINTYEDNGFLIV eluted matrix subsequently eluted with SDS.

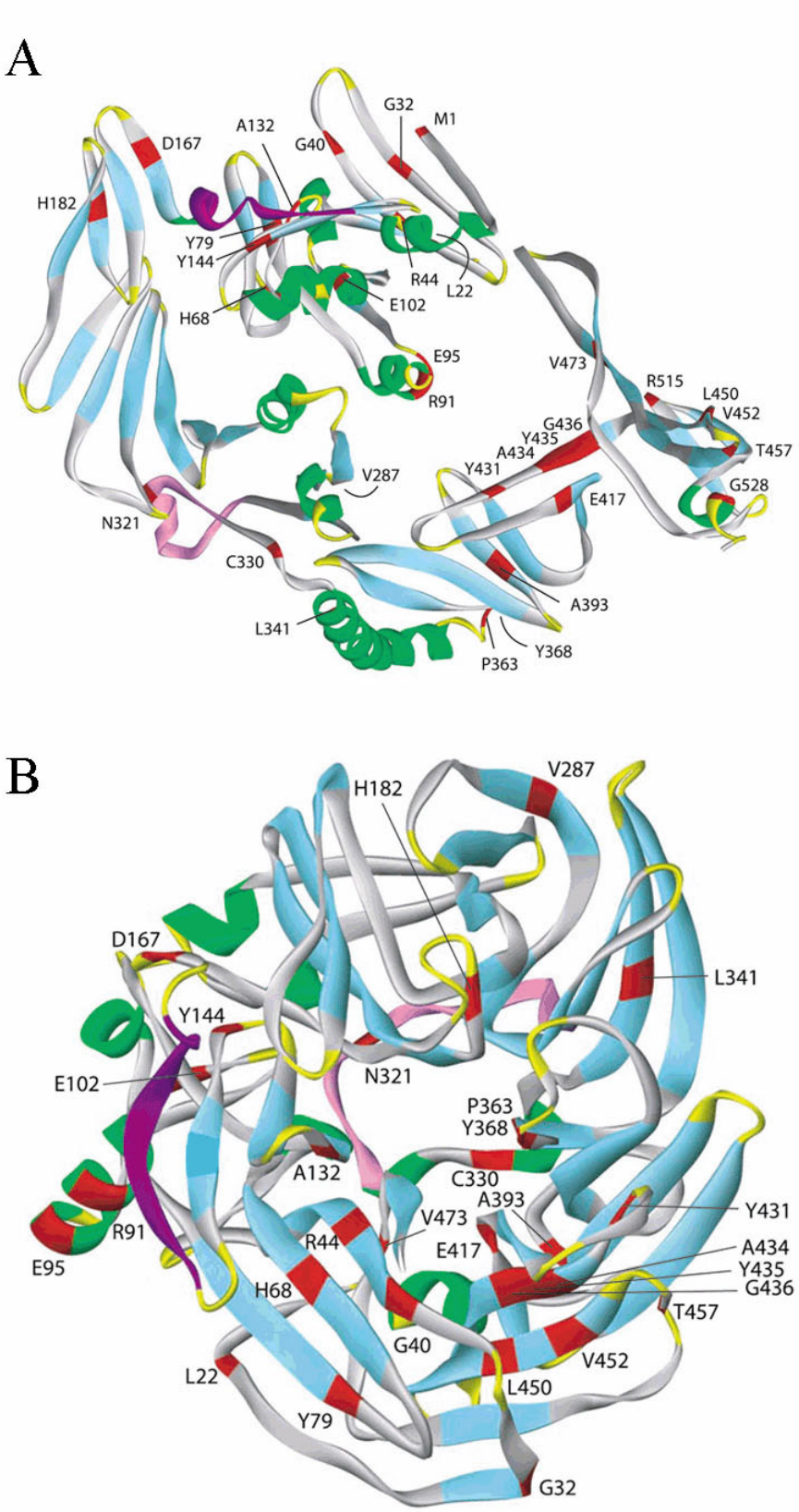
A
G32
M1
A132
G40
D167
H182
Y79
Y144
R44
L22
E102
H68
E95
R91
V473
R515
L450
V452
G436
Y435
A434
T457
Y431
G528
V287
E417
N321
C330
A393
L341
P363
Y368
B
V287
H182
D167
L341
Y144
E102
N321
P363
Y368
A132
C330
A393
Y431
V473
R91
R44
E417
A434
Y435
G436
E95
H68
T457
G40
V452
L22
L450
Y79
G32

Figure 2-5. Models of RPE65 tertiary structure. A: An *ab initio* model of the three-dimensional structure for the RPE65 protein was predicted using the method of Bystroff and Shao [182]. B: A correlative model of the three-dimensional structure for the RPE65 protein was predicted by comparison to the apocarotenoid-cleaving oxygenase from Synechocystis and modeled by the SWISS-MODEL server [186]. The ribbon representing the peptide backbone is color coded according to structural components: α-helices are green; β-pleated sheets are blue; and random coil is gray. The linear sequence corresponding to the epitope recognized by mAb 8B11 is shown in purple and for mAb 1F9 is shown in pink. Sites of amino acid substitutions resulting from patient missense mutations associated with inherited retinal degeneration in patients are shown in red.

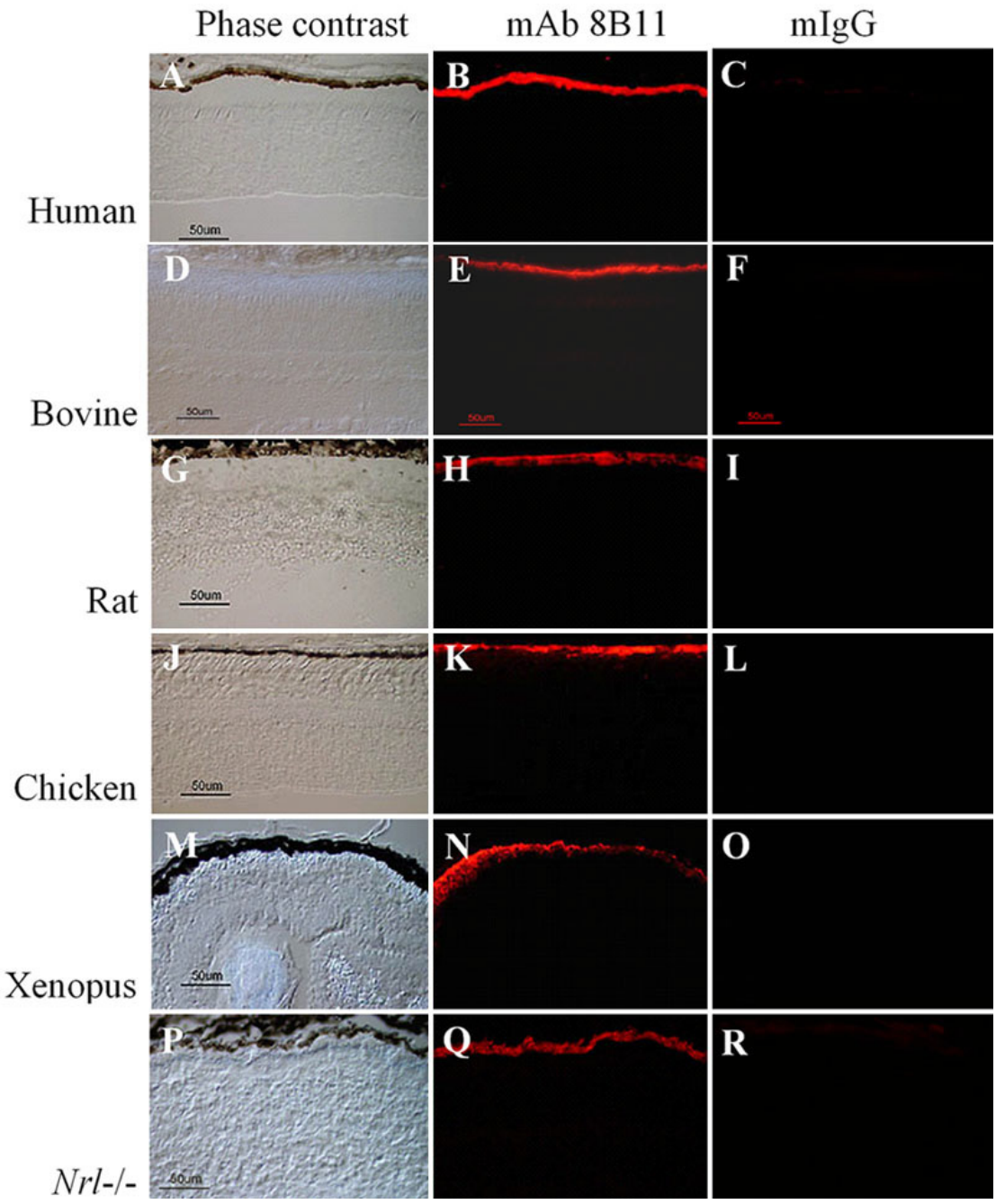
Phase contrast
mAb 8B11
mIgG
Human
Bovine
Rat
Chicken
Xenopus
Nrl-/-
A
B
C
D
E
F
G
H
I
J
K
L
M
N
O
P
Q
R
50um

Figure 2-6. Immunohistochemical analysis of mAb 8B11 reactivity in rod- and cone-dominant retinas. Retina/choroid/RPE cryosections of paraformaldehyde-fixed eyes from bovine, human, rat (rod-dominant), and from *Xenopus laevis*, chicken, *Nrl–/–* mouse (cone-dominant) were incubated with mAb 8B11 or mouse non-immune IgG, and immunoreactivity was visualized with Alexa Fluor 555-conjugated anti-mouse IgG using fluorescence imaging. Retina/choroid/RPE cryosections from paraformaldehyde eyes were incubated with mAb 8B11 or mouse non-immune IgG, and reactivity was visualized with Alexa Fluor 555-conjugated anti-mouse IgG using fluorescence imaging. Phase contrast (A,D,G,J,M,P), mAb 8B11 reactivity (B,E,H,K,N,Q), non-immune mouse IgG reactivity (C,F,I,L,O,R). Bovine sections are from an amelanotic region of the RPE. The scale bars represent 50 μm.

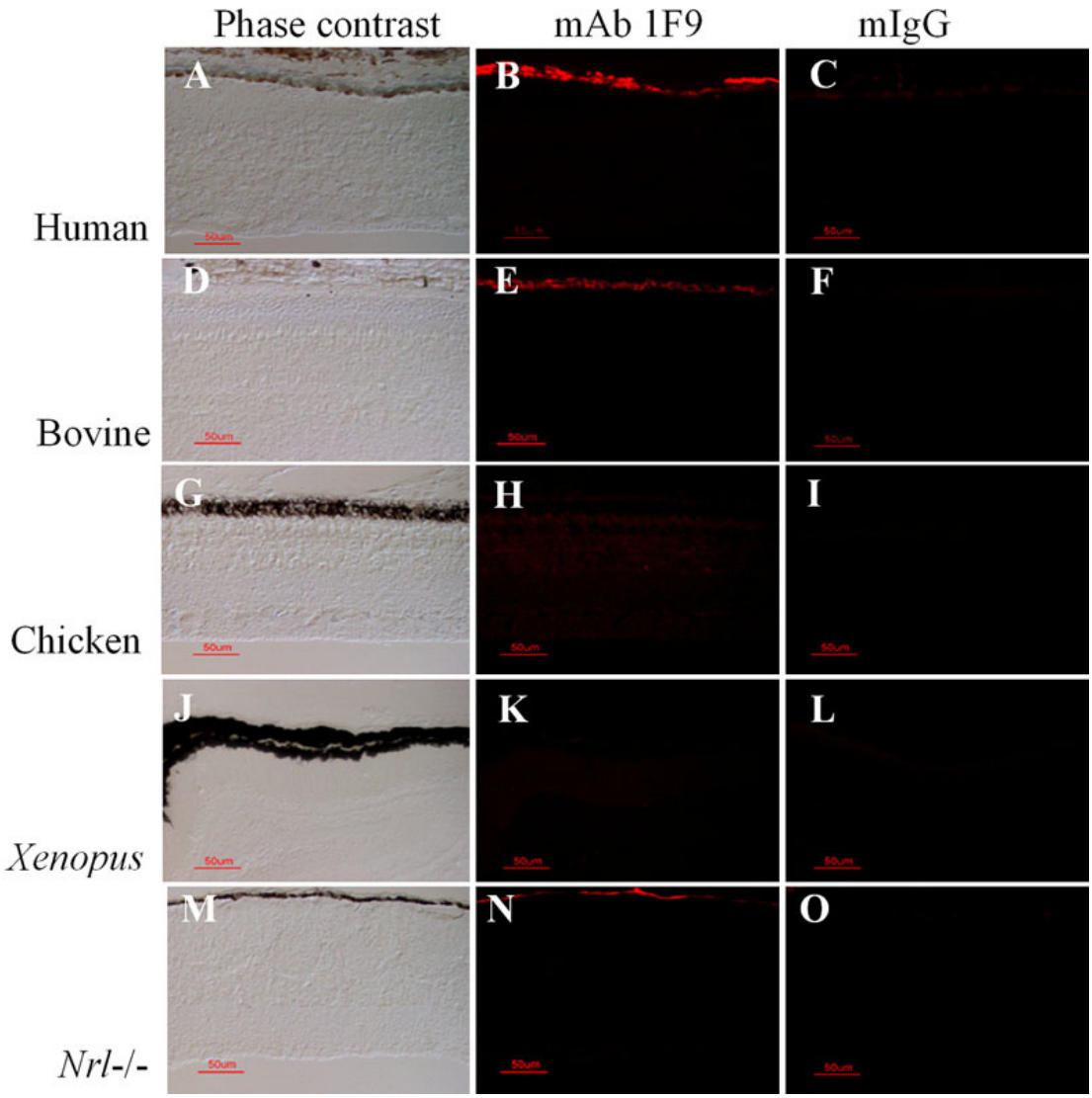

Figure 2-7. Immunohistochemical analysis of mAb 1F9 reactivity in rod- and cone-dominant retinas. Retina/choroid/RPE cryosections of paraformaldehyde-fixed eyes from bovine, human (rod-dominant), and from *Xenopus laevis*, chicken, *Nrl–/–* mouse (cone-dominant) were incubated with mAb 1F9 or mouse non-immune IgG using M.O.M. Peroxidase reagents, and visualized using TSA-Alexa Fluor 568 reagents using fluorescence imaging (1/50 s human, all others 1/30 s). Phase contrast (A,D,G,J,M), mAb 1F9 reactivity (B,E,H,K,N), non-immune mouse IgG reactivity (C,F,I,L,O). Bovine sections are from an amelanotic region of the RPE. The scale bars represent 50 μm.

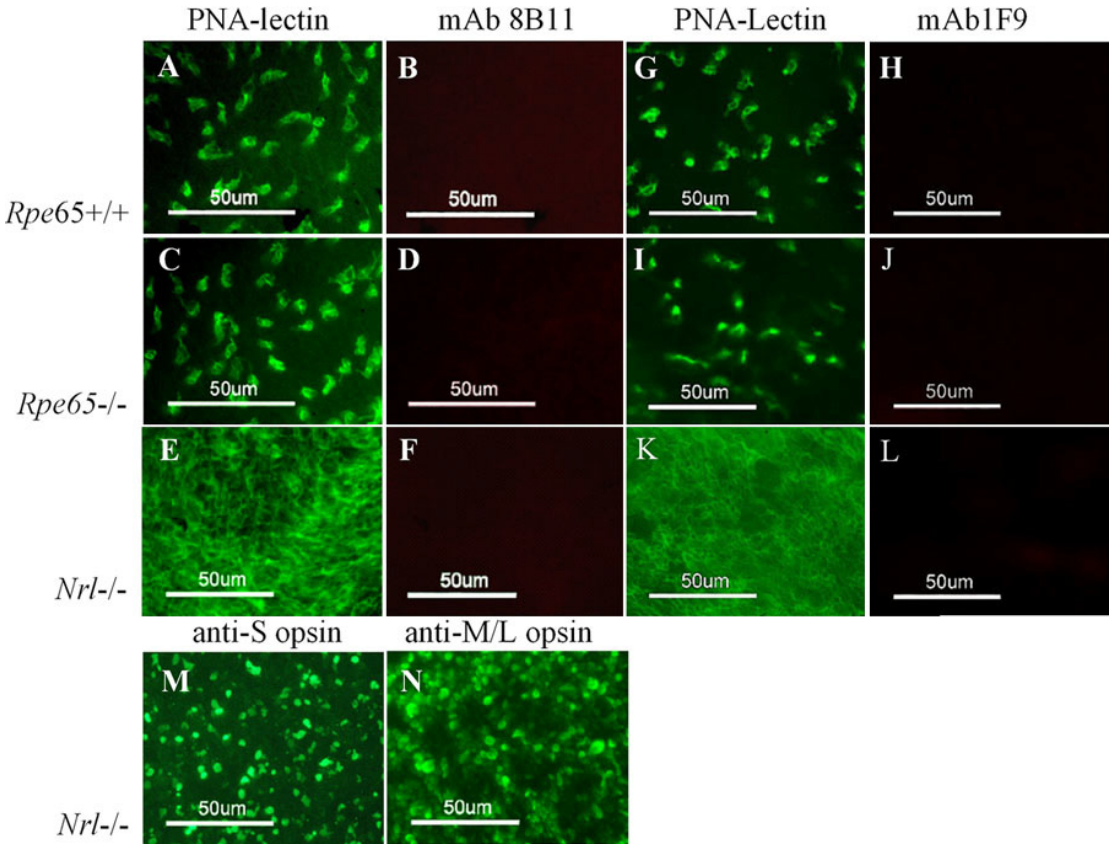

Figure 2-8. Immunohistochemical analysis of retina flatmounts. Retinas from wild-type (A,B,G,H), *Rpe65–/–* (C,D,I,J), and *Nrl–/–* mouse (E,F,K-N) were fixed on coverslips and incubated with PNA-lectin (FITC-conjugated), mAb 8B11, mAb 1F9, or antibodies against S-opsin and M/L-opsin. Alexa Fluor 555-conjugated anti-mouse IgG was used as secondary antibody. PNA labeling (A,C,E,G,I,K), mAb 8B11 labeling (B,D,F), mAb 1F9 labeling (H,J,L), S-opsin labeling (M), M/L-opsin labeling, (N). Fluorescence imaging: PNA-lectin, opsin antibodies 1/60 s; mAb 8B11 1/12 s; mAb 1F9, 1/20 s. The scale bars represent 50 μm.

CHAPTER 3

LOCALIZATION OF RDH12 AND EVALUATION OF THE RDH12-DEFICIENT MOUSE[†]

Introduction

Retinoid dehydrogenases/reductases (RDHs) perform critical oxidation-reduction reactions in the visual cycle mechanism that converts vitamin A (all-*trans* retinol) to 11-*cis* retinal, the light-absorbing chromophore of the visual pigments in photoreceptor cells [195]. One of these reactions involves the oxidation of 11-*cis* retinol produced by retinoid isomerohydrolase activity in the retinal pigment epithelium (RPE), resulting in formation of 11-*cis* retinal that is delivered to the photoreceptor cell outer segments (OS). The second reaction involves reduction of all-*trans* retinal released from rhodopsin and cone opsins upon bleaching, resulting in formation of all-*trans* retinol that is returned to the RPE for *trans*-to-*cis* isomerization. A number of RDH isoforms are expressed in the RPE and/or the neural retina that differ in terms of substrate specificity and sites of expression.

Within the RPE, RDH5 is thought to be the key enzyme involved in converting 11-*cis* retinol to 11-*cis* retinal [70]. Mutations in *RDH5* in humans result in fundus

---

[†] Portions of this chapter were published in:
Kurth I, Thompson DA, Rüther K, Feathers KL, **Chrispell JD**, Schroth J, McHenry CL, Schweizer M, Skosyrski S, Gal A, Hübner CA. Targeted disruption of the murine retinal dehydrogenase gene *Rdh12* does not limit visual cycle function. Mol Cell Biol. 2007 Feb;27(4):1370-9.; Copyright © American Society for Microbiology;
And
Chrispell JD, Feathers KL, Kane MA, Kim CY, Brooks M, Khanna R, Kurth I, Hübner CA, Gal A, Mears AJ, Swaroop A, Napoli JL, Sparrow JR, Thompson DA. Rdh12 activity and effects on retinoid processing in the murine retina. J Biol Chem. 2009 Aug 7;284(32):21468-77.

albipunctatus, a form of congenital stationary night blindness [75]. Since *Rdh5*-knockout mice exhibit very mild visual disturbances, it has been suggested that RDH5 activity may be redundant with that of other isoforms [142]. Consistent with this notion, mice deficient for Rdh11 and for Rdh8, two isoforms expressed in the photoreceptors, exhibit a mild phenotype without signs of retinal degeneration [73, 74]. Functional interaction of RDH5 with RDH11 has been proposed, but studies showing that RDH11 is expressed in the photoreceptor cell inner segment (IS) complicate this interpretation [73, 74]. RDH10 is expressed in both the RPE and Müller cells and is specific for the oxidation of all-*trans* retinol [147]. At least five RDH isoforms, including RDH8, RDH11, RDH12, RDH14, and DHRS3, have been reported to be expressed in the photoreceptor cells [55, 135, 196]. *In vitro*, each exhibits substrate specificity compatible with a role in converting all-*trans* retinal to all-*trans* retinol in the recovery phase of the visual cycle.

Mutations in *RDH12* cause a severe form of autosomal-recessive retinal dystrophy (arRD) with childhood onset that is often diagnosed as Leber congenital amaurosis [106, 137, 138]. The severe phenotype associated with *RDH12* mutations is consistent with a nonredundant role of RDH12 in photoreceptor physiology, leading to the notion that it may play a unique role in the visual cycle mechanism. RDH12 has also been proposed to detoxify medium-chain aldehydes potentially present in the photoreceptors as a result of lipid peroxidation [136].

In order to better understand the potential role of RDH isoforms in the visual cycle and other critical functions of the photoreceptors, we have characterized the spatio-temporal expression of members of this family within the retina. In addition, a collaboration was established with Ingo Kurth and Christian Hübner of the Institut für

Humangenetik (Hamburg, Germany) in which these researchers generated an *Rdh12*-knockout (*Rdh12–/–*) mouse. The gene targeting strategy used resulted in deletion of *Rdh12* exons 1 to 3, encoding the N-terminal one-third of the protein (Figure 3-1). To exclude side effects from the neomycin selection cassette, the *neo* gene was removed from the targeted allele by Cre-mediated excision in the embryonic stem cells used to generate the engineered mice. We characterized the retinal phenotype of this *Rdh12–/–* mouse using functional assays. Our findings suggest that the phenotype associated with RDH12 deficiency does not result from disruption of visual cycle function, and leave open the possibility that multiple RDH isoforms may contribute to the regulation of the oxidation state of retinoids in the outer retina.

Materials and Methods

All experimental procedures complied with the regulations of the University of Michigan Committee on Use and Care of Animals and the ARVO Statement for the Use of Animals in Ophthalmic and Vision Research. *Rdh12–/–* mice were obtained from Institut für Humangenetik, Universitätsklinikum Hamburg-Eppendorf, Hamburg, Germany, reared in a 12h-12h light-dark cycle (~800-lux room light, as indicated below) and euthanized by CO_2 inhalation.

Analysis of *Rpe65* genotypes

Mice were genotyped for an Rpe65 polymorphism, p.Leu450Met, which affects the efficiency of 11-*cis* retinal synthesis [126]. PCR products (~300 bp) were obtained (sense primer, 5'-GCATACGGACTTGGGTTGAATCAC-3'; antisense primer, 5'-GGTTGAGAAACAAAGATGGGTTCAG-3') and digested with the restriction enzyme

MwoI, which recognizes the Leu450 allele, and the pattern of cutting was evaluated on agarose gels. Studies were performed in a mixed 129Sv;C57BL/6 background, using the F3 and F4 generations. Littermates matched for *Rpe65* genotype, as indicated, served as controls.

Antibody development

Antibodies specific for human or mouse RDH12 were raised against synthetic peptide sequences chosen on the basis of predicted antigenicity and uniqueness within the family of RDH proteins. Peptides were coupled via an N-terminal cysteine to the keyhole limpet hemocyanin carrier protein. For the generation of an antibody against human RDH12, mice were immunized with one of three peptides: peptide 1, C-PSIRKFFAGGVCRTNVQ (amino acids 20 to 36, with an additional N-terminal cysteine); peptide 2, C-SAASEIRVDTKNSQ (amino acids 78 to 91, with an additional N-terminal cysteine); and peptide 3, C-DCKRTWVSPRARNNKT (amino acids 284 to 299, with an additional N-terminal cysteine; Protein Data Bank accession number gi:19343614). Sera from the mouse immunized with peptide 3 gave the most robust and specific response, and a hybridoma cell line secreting monoclonal antibody (mAb) 2C9 was generated and used to elicit ascites fluid in mice. IgG was purified from ascites on protein A-Sepharose by using standard protocols [180]. For mouse Rdh12, rabbits were immunized against the peptide CKRMWVSSRARNKKT (amino acids 285 to 299; Protein Data Bank accession number gi:58037513) or C-SPFFKSTSQGAQ (amino acids 252 to 263, with an additional N-terminal cysteine), and each resulting antiserum (termed rAb CKR or rAb CSP, respectively) was purified on an affinity matrix made by conjugation with the same peptide.

Western analysis

Mouse eyes were enucleated and homogenized in sodium dodecyl sulfate sample buffer, insoluble material was removed by low-speed centrifugation, and proteins were separated by polyacrylamide gel electrophoresis and blotted onto membranes by using standard protocols. Blots were probed by incubation with the affinity-purified rAb CSP rabbit antiserum diluted 1:500, and reactivity was detected using an alkaline phosphatase-coupled secondary antibody (1:4,000; GE Healthcare). Human retinas were dissected from postmortem donor eyes (Midwest Eye Bank and Transplantation Center), homogenized in sodium dodecyl sulfate sample buffer, electrophoresed, and blotted as described for mouse eyes. Blots were probed by incubation with mAb 2C9 IgG (~0.5 μg/ml), and reactivity was detected using an alkaline phosphatase-conjugated secondary antibody (1:500; Molecular Probes). Western analysis of COS-7 cells transfected with cDNA constructs encoding either mouse or human RDH12 with an amino-terminal His tag (pcDNA3.1/HIS) and probed with anti-Xpress antibody served as a positive control.

Immunohistochemistry

Mouse eyes were enucleated, and corneas were removed. The eye cups were fixed in 4% paraformaldehyde in PBS for 30 min at 4°C, washed three times for 5 min each with PBS, placed in 20% sucrose in PBS at 4°C overnight, and then flash frozen in Tissue-Tek O.C.T. Sections (8 μm) were blocked with 3% normal goat serum and 0.3% Triton X-100 in PBS for 30 min, incubated with primary antibody (rAb CSP [1:500] or anti-rhodopsin) or fluorescein isothiocyanate-conjugated peanut agglutinin (PNA)-lectin (0.05 mg/ml; Molecular Probes) in blocking solution overnight, washed three times for 5

min each with PBS, incubated with Alexa Fluor 488- or 555-conjugated secondary antibody (1:3,000; Molecular Probes) and Toto-3 for counterstaining of nuclei (1:10,000; Molecular Probes) in blocking solution for 2 h, washed, and covered with coverslips.

For images of protein translocation, anesthetized mice (~3 months old) were perfused with 4% paraformaldehyde in 0.1 M sodium phosphate, pH 7.4, the eyes were enucleated and post-fixed (total fixation time ≤ 15 min) and rinsed in phosphate buffer, and the anterior segments and lenses were removed. The posterior eyecups were transitioned through a sucrose series and flash-frozen in sucrose-OCT. Cryosections (18 μm) were permeabilized with 0.125% Triton X-100 in PBS, treated with biotin blocking reagents (Invitrogen), blocked with 1% bovine serum albumin, 10% normal goat serum, and 0.125% Triton X-100 in PBS for 1 h, and then incubated overnight at 4 °C with primary antibody in 1% bovine serum albumin, 1% normal goat serum, and 0.125% Triton X-100 in PBS and washed. Sections were incubated with biotinylated anti-rabbit secondary antibody (1:400; Molecular Probes) for 3 h, washed, and incubated with streptavidin-Alexa Fluor-488 or -555 (Molecular Probes, 1:500). Sections were washed, mounted in ProLong Gold containing 4′, 6-diamidino-2-phenylindole (DAPI) (Molecular Probes) to stain nuclei, and imaged using an Olympus FV500 confocal microscope with FluoView FV500 data acquisition software.

Human eyes were dissected to obtain pieces of retina/RPE/choroid/sclera that were fixed in 4% paraformaldehyde for 15 min, placed in 20% sucrose for 5 min, and then flash frozen in Tissue-Tek O.C.T. Sections (10 μm) were blocked with 20% sheep serum and 0.2% Triton X-100 in PBS, incubated with primary antibody (mAb 2C9, ~1 μg/ml; anti-rhodopsin, 1:1,000; or anti-prRDH, 1:25) or FITC-conjugated PNA-lectin

(0.05 mg/ml; Molecular Probes) in 2% sheep serum and 0.2% Triton X-100 in PBS, washed, and incubated in the same buffer with Alexa Fluor 488- or 555-conjugated secondary antibody. Specimens were viewed and photographed either with a confocal microscope (Leica TCS) or on a Nikon Eclipse E800 microscope with a Nikon DMX1200 digital camera, using the manufacturer's data acquisition software.

Morphological analysis

For high-power micrographs and electron microscopy, mice were perfused with 4% paraformaldehyde and 1% glutaraldehyde in phosphate-buffered saline (PBS). Tissues were postfixed in 1% OsO4, dehydrated, and embedded in Epon. Sections (0.5 μm) were stained with methylene blue. Ultrathin sections (60 nm) were stained with uranyl acetate and lead citrate and viewed and photographed using a Zeiss EM 902 microscope.

Assays of oxidative stress indicators

Mice were subjected to bleaching light (5,000 lux for 30 min) before being sacrificed. Lipid peroxidation products potentially resulting from photooxidation were assayed as thiobarbituric reactive substances (TBARs) in retinal homogenates in RIPA buffer [136, 197]. The transcript abundance of heme oxygenase 1 (HO-1), a marker for oxidative stress, was assayed in retinal total RNA by using quantitative PCR (sense primer, 5'-GCATGCCCCAGGATTTGTC-3'; antisense primer, 5'-CTGGCCCTTCTGAAAGTTCCTCATG-3') and was normalized with respect to *Hprt* expression (sense primer, 5'-GCAAGCTTGCTGGTGAAAGGAC-3'; antisense primer, 5'-CCTGAAGTACTCATTATAGTCAAGGGC-3').

Analysis of retinoid content

Mice were allowed to dark adapt or were exposed to various light regimens and then were euthanized. Eyes were then enucleated and frozen in liquid N_2 in the dark. Retinoids were extracted using a modification of a previously described method [198]. Briefly, under dim red light and on ice, two eyes were homogenized in 1 ml chloroform:methanol:hydroxylamine (2 M) (3:6:1) and incubated at room temperature for 2 min. Next, 200 µl chloroform and 240 µl water were added, and each sample was vortexed and centrifuged at 14,000 rpm for 5 min. The lower phase was collected, the solvent was evaporated under N_2, and the sample was dissolved in hexane. Retinoids in the extracts were identified and quantified by high-performance liquid chromatography (HPLC) analysis, using a Waters Alliance separation module and photodiode array detector with a Supelcosil LC-31 column (25 cm by 4.6 mm by 3 µm) developed with 5% 1,4-dioxane in hexane. For quantification of retinyl esters, the column effluent at 3 to 6 min was collected and saponified by incubation in ethanolic KOH (40 mM) at 55°C for 30 min, and the products were then extracted into hexane and subjected to HPLC analysis as described above. Peak identification was done by comparison to retention times of standard compounds and evaluation of wavelength maxima. Quantitative analysis was done by comparison of peak areas and published extinction coefficients: at 325 nm for all-*trans* retinol (ε_M = 51800 M cm^{-1}); 318 nm for 11-*cis* retinol (ε_M = 34320 M cm^{-1}); 357 nm for syn-all-*trans* retinal oxime (ε_M = 55500 M cm^{-1}); 361 nm for anti-all-*trans* retinal oxime (ε_M = 51700 M cm^{-1}); 347 nm for syn-11-*cis* retinal oxime (ε_M = 35900 M cm^{-1}); 351 nm for anti-11-*cis* retinal oxime (ε_M = 30000 M cm^{-1}); and 325 nm for all-*trans* retinal esters (ε_M = 49256 M cm^{-1}) [199]. Data were analyzed using analysis of

variance (α= 0.05) (Excel software), and statistical differences were designated for P values of <0.05.

Results

RDH12 antibody development and immunoreactivity

Three synthetic peptides were used to illicit anti-RDH12 antibodies in mice, selected based upon the antigenic profile of human RDH12 (Figure 3-2A). The most robust serum was derived from the mouse treated with peptide 3 (284-DCKRTWVSPRARNNKT-299). This resulted in the identification of a hybridoma producing a monoclonal antibody, mAb 2C9. Specificity was established by Western analysis of COS-7 cells transfected with a cDNA encoding Xpress-tagged human RDH12, in which mAb 2C9 was shown to recognize the same bands as those recognized by anti-Xpress antibody that correspond to glycosylated and unglycosylated forms of RDH12 [106]. These immunoreactive bands were not seen in western blots of untransfected cells or COS-7 cells transfected with RDH11- or DHRS3-encoding cDNAs (Figure 3-3B), nor in COS-7 cells transfected with RDH5-encoding cDNA (data not shown). The three bands recognized by mAb 2C9 in cells expressing RDH12 are, from lowest to highest molecular weight: untagged RDH12 at ~33 kDa, a result of translation from the native start (ATG) codon; a His-tagged version at ~36 kDa in which the full-length recombinant protein has been translated; and a band at ~42 kDa corresponding to glycosylated RDH12. mAb 2C9 also recognized RDH12 as an ~33-kDa protein on immunoblots of lysates of human retinas but not RPE/choroid. (Figure 3-2B and 3-3L).

However, mAb 2C9 only recognized the human RDH12, and failed to recognize the mouse ortholog (Figure 3-2C).

Rabbit polyclonal antibodies rAb CSP and rAb CKR were elicited by immunization with synthetic peptides corresponding to 252-SPFFKSTSQGAQ-263 and 285-CKRMWVSSRARNKKT-299 of the mouse Rdh12 sequence, respectively. These antibodies possessed similar affinities for mouse Rdh12, and did not display cross-species reactivity with the human ortholog (Figure 3-2C).

RDH12 immunolocalization in mice and humans

To determine localization of Rdh12 expression in mouse eyes, immunohistochemical analysis was performed with both rAb CSP and rAb CKR. Each antibody showed similar immunoreactivities in wild-type retina/RPE/choroid cryosections that were absent in *Rdh12–/–* mice (shown for rAb CSP antibody in Figure 3-3A to K). The signal in the case of all anti-RDH12 antibodies (anti-mouse or anti-human) was sensitive to paraformaldehyde fixation, with optimal staining achieved with sections fixed for short times (30 min) or without paraformaldehyde (e.g., with cold methanol).

The pattern of Rdh12 immunoreactivity present in mouse retina/RPE/choroid sections was consistent with expression in the photoreceptor IS and outer nuclear layer (ONL), with no apparent expression in the RPE or photoreceptor OS (Figure 3-3A to D). Double-labeling experiments using rhodopsin antibodies specific for the rod OS (Figure 3-3E to G) and PNA-lectin staining of cone sheaths (Figure 3-53 to K) showed no overlap with Rdh12 immunoreactivity.

For localization of RDH12 expression in human eyes, the mouse mAb 2C9 was used. As in the mouse, the pattern of mAb 2C9 immunoreactivity in human eyes was consistent with RDH12 expression in photoreceptor IS and the ONL (Figure 3-3N), with no evidence of overlap with rhodopsin expression in the rod OS (Figure 3-3O), with PNA-lectin labeling of cone sheaths (Figure 3-5P), or with RDH8 expressed in rod and cone OS (Figure 3-3Q) [55].

The similar localization of Rdh12 and RDH12 proteins in mouse and human photoreceptors, respectively, may indicate an analogous physiological role of the enzymes in both species and suggests that the *Rdh12–/–* mouse is likely to recapitulate, at least in part, deficits resulting from RDH12 loss-of-function mutations in humans.

Rdh12 localization in dark- and light-adapted mouse retina

To determine whether RDH12 undergoes light-induced movements similar to the translocation of other photoreceptor proteins (46), we compared the pattern of Rdh12 immunoreactivity in retinas of wild-type albino mice that were dark-adapted or exposed to bleaching light (2000 lux for 2 h) (Figure 3-4). Under conditions resulting in redistribution of transducin from photoreceptor OS in the dark to IS in the light, Rdh12 immunoreactivity remained confined to the IS. Similar results were obtained for wild-type pigmented mice, in which bleaching was less efficient (data not shown).

Retinal histology of *Rdh12–/–* mice

Light micrographs of retina/RPE/choroid sections from *Rdh12–/–* and wild-type mice showed comparable retinal histology at 7 months of age (Figure 3-5A and B), with normal lamination, numbers of cells, and apposition with the RPE. Similarly, transmission electron micrographs at 7 months of age revealed no major differences in

retinal architecture or in the ultrastructure of photoreceptor OS and IS, nor of the ONL (Figure 3-5C and D). There was no evidence of accumulated bone spicule pigment, photoreceptor debris, retinyl ester droplets, retinal detachment, or altered ratios of rods to cones. Although the thickness of the ONL did not appear to be decreased at 10 months of age, morphometric analysis showed slightly decreased OS-plus-IS lengths in the inferior retinas of *Rdh12–/–* animals (Figure 3-5E and F).

Analysis of oxidative stress in *Rdh12–/–* mice

Indicators of oxidative stress were assayed in retinas from *Rdh12–/–*, *Rdh12+/–*, and wild-type mice subjected to bleaching light (5,000 lux for 30 min) before being sacrificed. Levels of lipid peroxidation products present in retinal homogenates, assayed as TBARs, were not significantly increased due to Rdh12 loss-of-function (Figure 3-6A). In addition, transcript levels for HO-1, an enzyme that is upregulated in response to oxidative stress, were not markedly increased (Figure 3-6B) [200]. Thus, despite the ability of RDH12 to recognize C9 aldehydes resulting from lipid photooxidation, our data do not indicate that Rdh12 is unique in counteracting oxidative stress in the retina, at least in the short term [136].

Retinoid analysis with *Rdh12–/–* mice

To assay the steady-state function of the visual cycle, HPLC analysis was used to compare the retinoid content of whole eyes from *Rdh12–/–*, *Rdh12+/–*, and wild-type mice that were dark adapted or light adapted and subjected to intense bleaching light (5,000 lux for 20 min), or subjected to bleaching and allowed to recover in the dark (30 min). Under dark-adapted and light-adapted conditions, the retinoid content of eyes from *Rdh12–/–* and wild-type animals were equivalent and unaffected by the Leu450Met

polymorphism of Rpe65. In all cases, 11-*cis* retinal predominated in the dark-adapted state, and all-*trans* retinal and all-*trans* retinol predominated in the light-adapted state, with no significant differences between genotypes (Figure 3-7A). In addition, there were no significant differences in retinyl ester content between *Rdh12–/–* and wild-type animals, with low levels of all-*trans* retinyl esters present in the dark- and light-adapted states that increased upon bleaching (data not shown). However, the *Rpe65* genotype was a major factor in determining rates of 11-*cis* retinal regeneration during recovery in the dark after bleaching for both *Rdh12–/–* and wild-type mice. In both cases, recovery in Rpe65-Leu450/ Rpe65-Leu450 (L/L) and Rpe65-Leu450/ Rpe65-Met450 (L/M) animals was significantly faster than that in Rpe65-Met450/ Rpe65-Met450 (M/M) animals (data not shown). We therefore excluded the last genotype in such comparisons and found that 11-*cis* retinal, all-*trans* retinal, and all-*trans* retinol contents were equivalent in eyes from *Rdh12–/–* and wild-type animals that were subjected to bleaching and allowed to recover in the dark for 30 min (Figure 3-7).

Discussion

Mutations in human *RDH12* cause a severe form of childhood onset arRD associated with massive accumulation of bone spicule pigment, RPE atrophy, and macular scarring [106, 137, 138]. Young children possess visual function, whereas the condition progresses to legal blindness in early adulthood. RDH12 activity has been proposed to be necessary for the recovery phase of the visual cycle on the basis of *in vitro* studies showing that recombinant RDH12 efficiently converts all-*trans* retinal to all-*trans* retinol and that *RDH12* transcripts are present in the ONL in monkey and mouse retinas

[135, 136] . In this case, it follows that *RDH12* loss-of-function mutations should decrease visual cycle efficiency, potentially resulting in reduced 11-*cis* retinal synthesis and the buildup of potentially toxic aldehyde intermediates in the retina.

Rdh12–/– mice kept in a regular light-dark cycle did not develop any histological signs of retinal degeneration within the first 10 months of life, as assessed at the light microscope or ultrastructural level. Analysis of ocular retinoids showed no significant differences in 11-*cis* retinal content or rates of recovery following exposure to full bleaching light, with no accumulation of all-*trans* retinal or other aldehydes potentially resulting from lipid peroxidation [136]. In addition, an enzyme marker of oxidative stress, heme oxygenase 1, was not upregulated. Electroretinogram (ERG) analysis, performed by Klaus Rüther of Augenklinik Campus Virchow-Klinikum Charité (Berlin, Germany) showed only minor alterations in responses in the dark-adapted state or for recovery after bleaching in both young and old animals [200, 204]. In addition, we found that RDH12 expression localizes to the photoreceptor IS and the ONL in both mouse and human retinas and is not present in OS, where phototransduction takes place. This expression pattern is similar to that reported for RDH11 and contrasts with those reported for DHRS3 and RDH8, as present throughout cone cells and in rod OS, respectively [54, 55]. Further, we found no evidence of light-induced translocation of Rdh12 within the photoreceptors.

Our analysis of the ocular phenotype of *Rdh12–/–* mice showed much less severe consequences than associated with human *RDH12* mutations. The findings that *Rdh12–/–* mice retain nearly normal visual cycle throughput and that expression of the Rdh12 protein is confined to photoreceptor IS are consistent with at least two different

interpretations. The first is that RDH12 activity is not essential for regeneration of the 11-*cis* retinal chromophore in mice or humans and, instead, functions in an unrelated aspect of photoreceptor physiology not addressed by our studies. In this case, the absence of a rapid retinal degeneration phenotype in *Rdh12–/–* mice could be due to species differences related to retinal physiology, compensation of Rdh12 loss-of-function by another RDH isoform, or disease onset linked to time in years rather than relative age, a notion consistent with the mild pathology observed in very young children that progresses to devastating retinal degeneration over the course of approximately 20 years.

A second possibility is that RDH12 activity is normally required for visual cycle function but that another RDH isoform can compensate for loss-of-function in mice, but not in humans. Such a scenario has been proposed for RDH5, as human mutations result in fundus albipunctatus but *Rdh5–/–* mice do not exhibit the flecked retinas or ERG responses characteristic of the disease [75]. Expression of RDH12 in photoreceptor IS, but not OS, would require that reduction of all-*trans* retinal occur at a site distant from its release from bleached photopigments, potentially involving a novel trafficking mechanism. Although it is somewhat counterintuitive, perhaps the dual-substrate specificity of RDH12 necessitates this compartmentalization in order to protect 11-*cis* retinal from reduction in the OS.

Although analysis of the retinal phenotype of the *Rdh12–/–* mouse does not yet permit us to distinguish between these two alternatives, several pieces of evidence support the notion that RDH12 function is analogous in both mouse and human retina. The general pattern of RDH expression in the retina is similar, with Rdh12 localizing to the photoreceptor IS and Rdh8 localizing to the OS. Microarray expression profiling of

photoreceptor cells during development shows that *Rdh12* expression in the mouse is upregulated between postnatal days 6 and 10, corresponding to the time the OS are elaborated, and expression is dramatically downregulated in mice deficient in Nrl, a transcription factor required for the differentiation of rod precursor cells [17, 188, 205, 206].

Additionally, it is clear that the outcomes of RDH12 and RPE65 loss-of-function are fundamentally different, with mutations in the latter resulting in uniformly severe functional deficits in canines, mice, and humans [67, 207, 208]. In addition, the genetic background of *Rdh12–/–* mice with respect to an Rpe65 polymorphism (Leu450Met) that affects rates of 11-*cis* retinal synthesis is a major factor that needs to be controlled for in comparisons of visual performance and visual cycle activity in *Rdh12–/–* versus wild-type mice. In fact, consideration of the *Rpe65* genotype is also likely to be important for studies of other visual cycle genes, especially other RDH isoforms, but has not always been done in previous studies of the effects of Rdh5, Rdh11, and Rdh8 loss-of-function on specific *in vivo* functional roles.

Our understanding of RDH12 *in vivo* function is likely to be improved by developing appropriate challenges of the relevant physiological pathway(s) in knockout mice. This approach has proven successful in eliciting profound phenotypes in a number of strains of knockout mice in which no or mild differences from the wild-type were initially observed [209]. Mice deficient in multiple RDHs may also be useful for identifying a minimal set of isoforms that contribute to visual cycle function. Identifying the functional correlates between the *Rdh12–/–* mouse phenotype and human disease will

be critical for establishing an animal model useful for evaluating potential modes of therapeutic intervention.

Outside Contributions: Ingo Kurth and Christian Hübner generated anti-mouse Rdh12 antibodies and captured preliminary confocal images of immunolocalization in the mouse. Klaus Rüther performed the ERG analysis. Kecia Feathers performed the oxidative stress assays and assisted in the immunoassays. Christina McHenry performed the retinoid content assays.

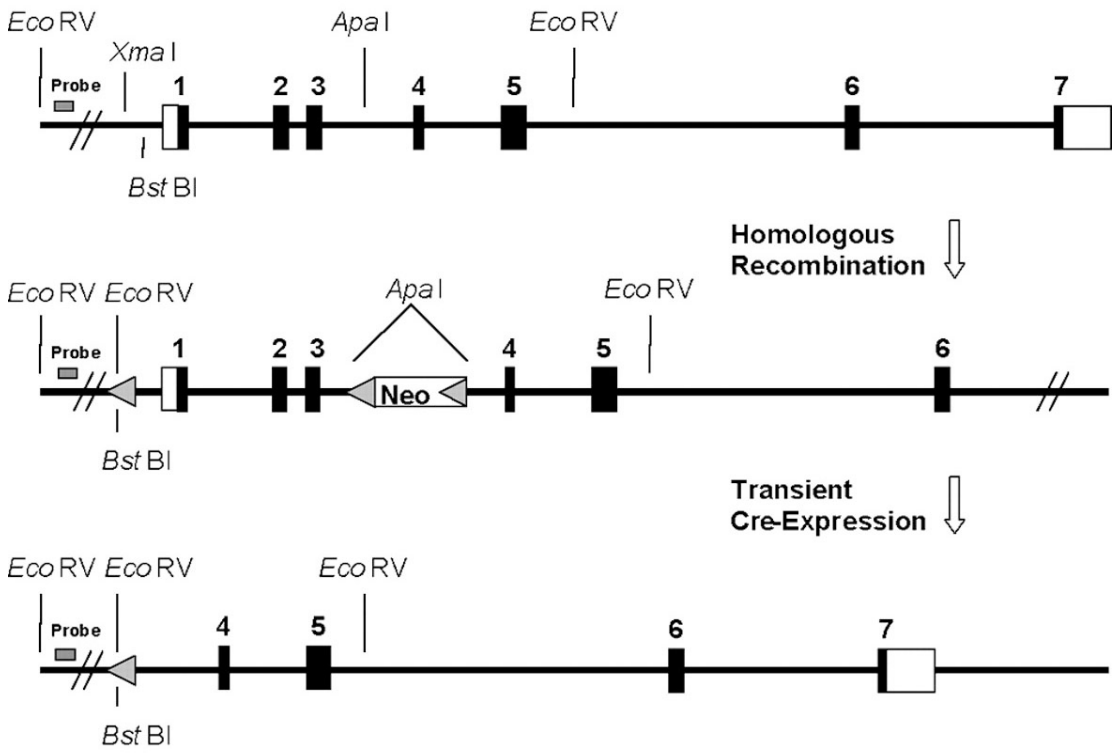

Figure 3-1. Construct design for the generation of *Rdh12–/–* mice. An *Rdh12*-carrying clone isolated from a 129/SvJ mouse genomic λlibrary (Stratagene) was used to construct the targeting vector. A 12.9-kb XmaI/NotI fragment including exons 1 to 5 of the Rdh12 gene was cloned into the pKO-V901 plasmid (Lexicon Genetics) with a phosphoglycerate kinase gene (*pgk*) promoter-driven diphtheria toxin A cassette. A *pgk* promoter-driven neomycin resistance cassette flanked by loxP sites was ligated into the ApaI site in intron 3. A third loxP site and an additional EcoRV site were inserted into the BstBI site in the 5' region of the *Rdh12* gene. The construct was electroporated into R1 mouse embryonic stem (ES) cells. Neomycin-resistant clones were analyzed by Southern analysis, using an external, ~300-bp probe to screen for an additional EcoRV site incorporated into the targeted allele. Correctly targeted ES cells were transfected with a plasmid expressing Cre recombinase to remove the neomycin cassette and exons 1 to 3. Two independent embryonic stem cell clones were injected into C57BL/6 blastocysts to generate chimeras that were backcrossed with C57BL/6 mice.

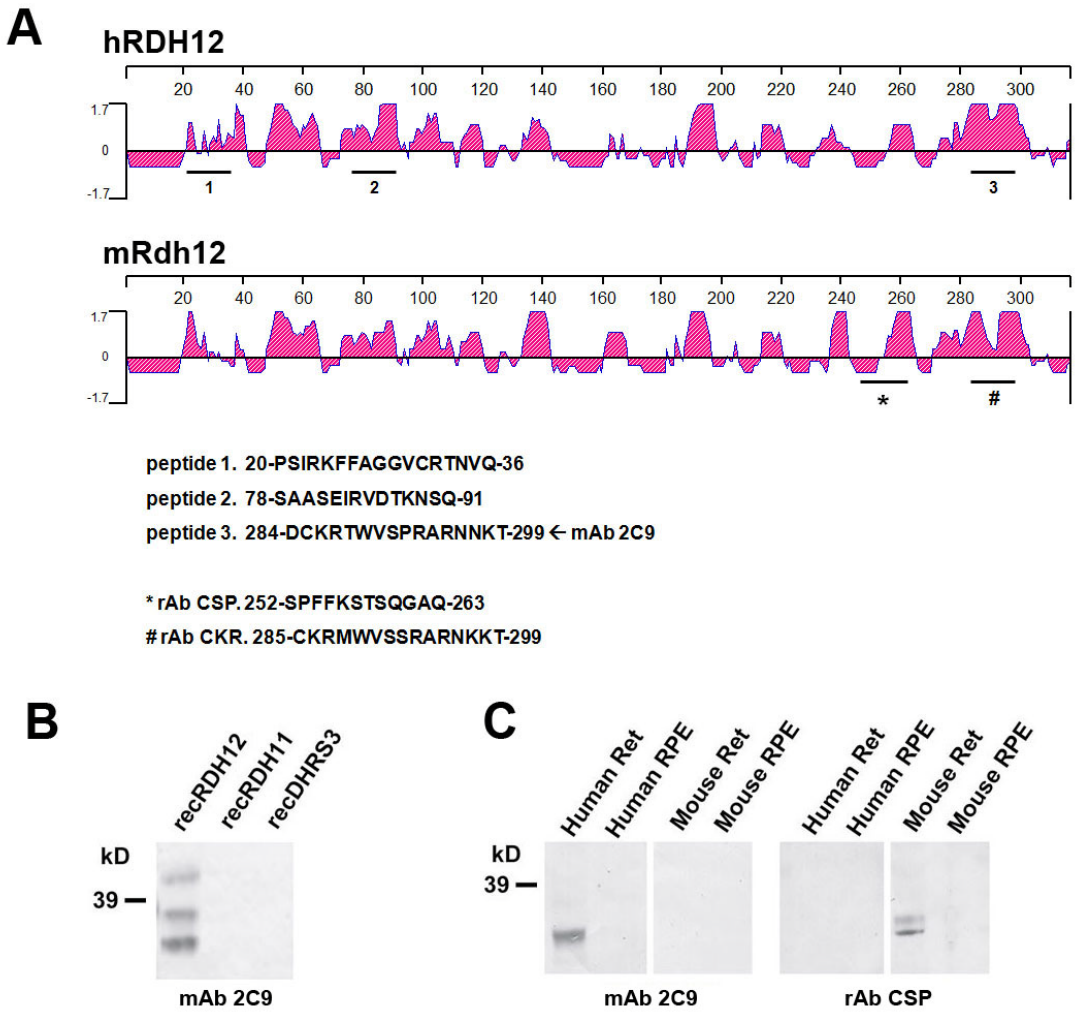

Figure 3-2. Development of anti-RDH12 antibodies. A: Schematic of human and mouse RDH12 amino acid sequence. RDH12 antigenic index calculated using the Jameson-Wolf prediction in the DNASTAR program Protean. Positions of synthetic human RDH12 peptides 1-3 corresponding to the 3 sequences of highest predicted antigenicity are shown underlined in the enlarged section. The synthetic mouse Rdh12 peptides used to generate the rabbit polyclonal antibodies. B, C: Western blot analysis of anti-RDH12 antibodies. mAb 2C9 is specific towards recombinant human RDH12, but not RDH11 or DHRS3. C, mAb 2C9 detects a corresponding band in human retina lysates but not in human RPE or mouse tissue. rAb CSP detects a band in mouse retina lysates but not in mouse RPE or human tissue.

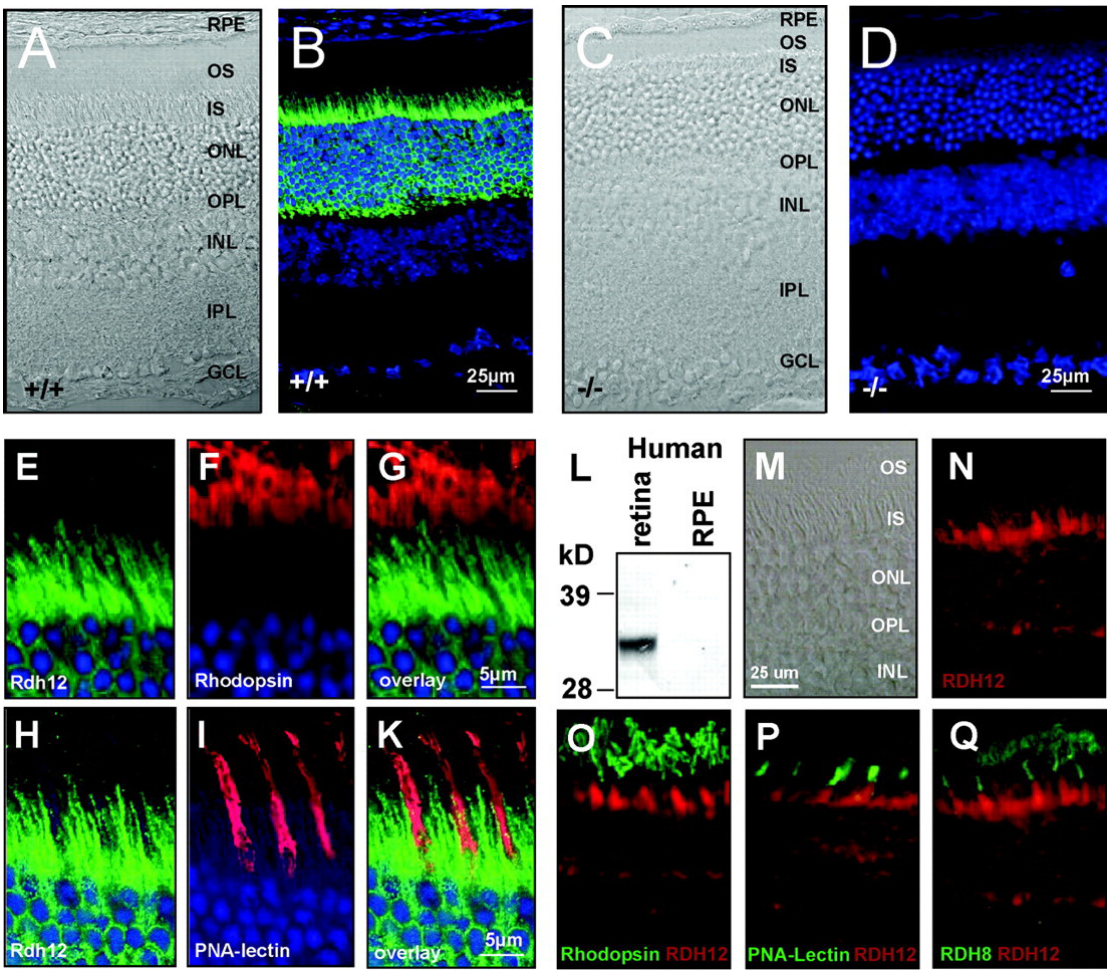

Figure 3-3. RDH12 localizes to photoreceptor inner segments. Cryosections of wild-type (A, B, and E to K) and *Rdh12–/–* (C and D) eyes are shown. (B, D, and E to K) Murine sections were counterstained with TOTO-3 to label cell nuclei, shown in blue. (M to Q) Cryosections of human eyes. (A, C, and M) Phase-contrast microscopy images. (D) Absence of Rdh12 staining in tissue from *Rdh12–/–* mice confirms the specificity of the antibody. Rdh12 labeling (green) did not colocalize with rhodopsin (red) (E to G) or PNA-lectin (red) (H to K). (L) A monoclonal antibody directed against human RDH12 detects a corresponding band in retina lysates but not in RPE. (N) In the human retina, RDH12 localizes to photoreceptor inner segments as well and does not overlap with (O) rhodopsin, (P) PNA-lectin, or (Q) Rdh8. OS, outer segments; ONL, outer nuclear layer; IS, inner segments; INL, inner nuclear layer; IPL, inner plexiform layer; GCL, ganglion cell layer; RPE, retinal pigment epithelium.

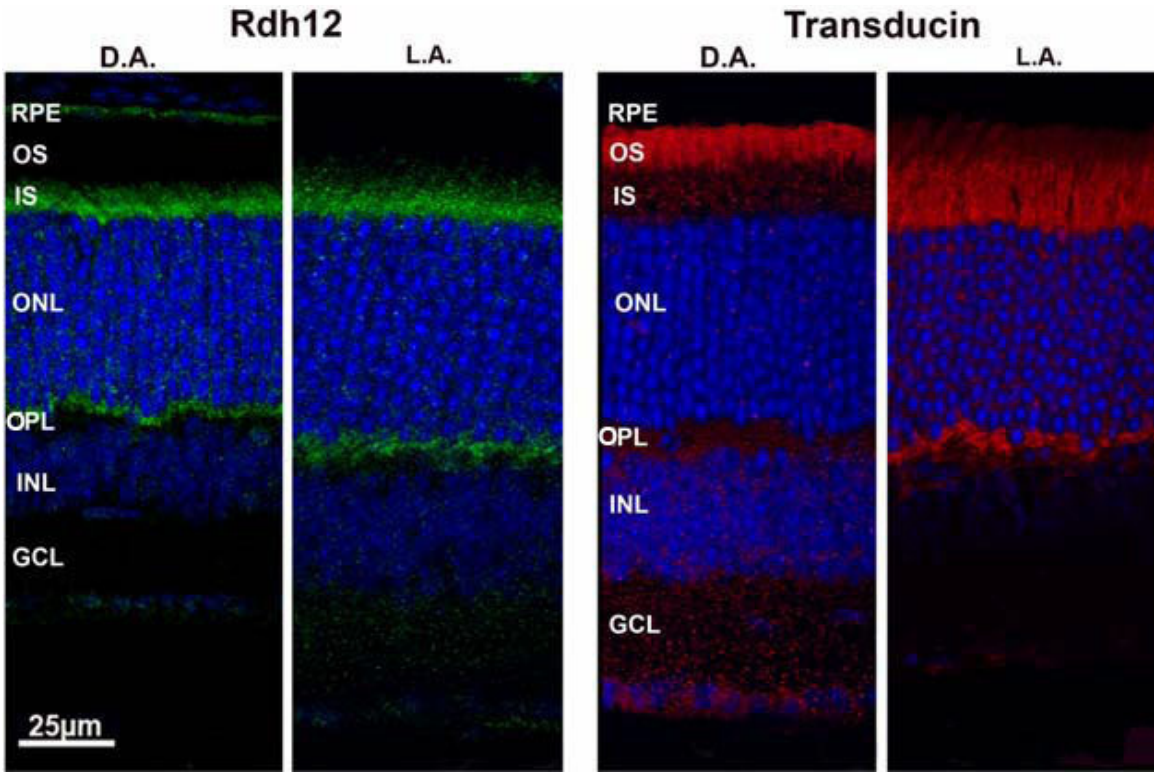

Figure 3-4. Rdh12 immunolocalization dark-adapted and light-adapted mouse retina. Wild-type albino mice were maintained in darkness overnight or exposed to 2000 lux fluorescent white light for 2 h. Retina/RPE/choroid cryosections were incubated with primary antibody specific for mouse Rdh12 or transducin, and then with streptavidin-AlexaFluor-488 (green) and -555 (red), respectively. DAPI (blue) was used to label cell nuclei. Sections were imaged using fluorescence confocal microscopy. D.A., dark-adapted; L.A., light-adapted. OS, outer segments; IS, inner segments; ONL, outer nuclear layer; OPL, outer plexiform layer; INL, inner nuclear layer; IPL, inner plexiform layer; GCL, ganglion cell layer.

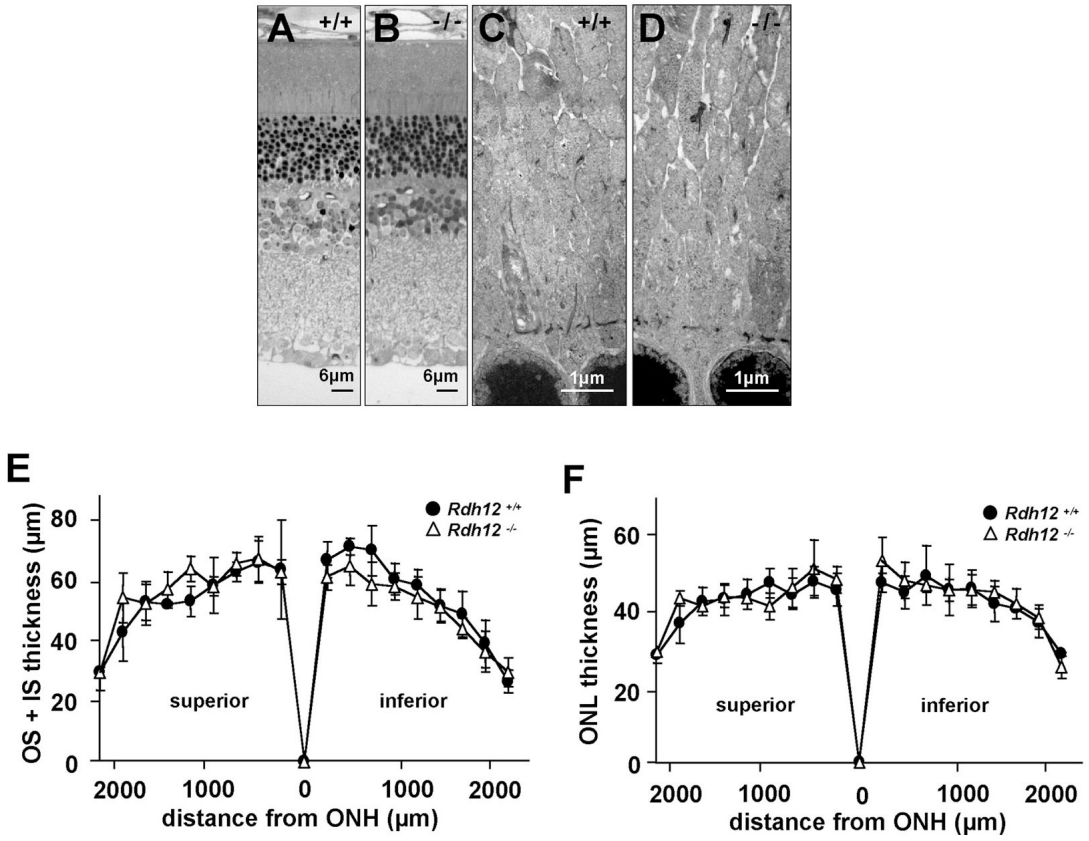

Figure 3-5. Retinal histology and thickness measurements for *Rdh12–/–* versus wild-type mice. (A and B) Semithin sections of *Rdh12–/–* and wild-type retinas/RPE/choroid stained with methylene blue. (C and D) Transmission electron micrographs of photoreceptor inner segments in *Rdh12–/–* and wild-type mice at 7 months of age. (E and F) Plots of photoreceptor layer and total retinal thicknesses for *Rdh12–/–* and wild-type mice, with measurements made on sections parallel to the vertical meridian of the eye and with standard deviations shown. ●, wild-type; △*Rdh12–/–*. OS, outer segment; IS, inner segment; ONL, outer nuclear layer; ONH, optic nerve head.

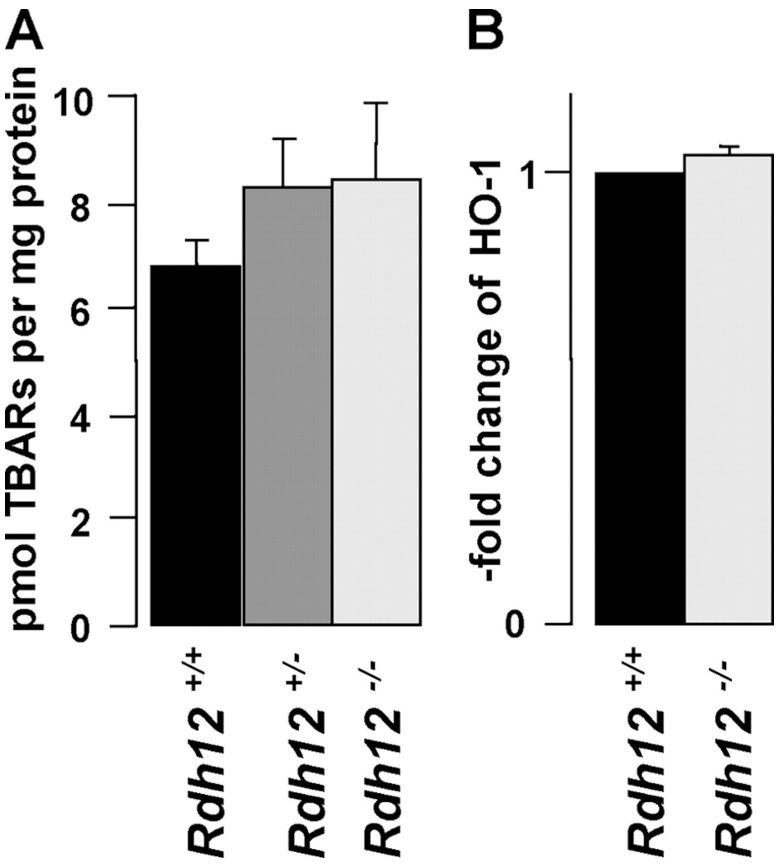

Figure 3-6. Analysis of oxidative stress in *Rdh12*–/– mice. (A) Comparison of TBARs in retinal homogenates as an index of lipid peroxidation and oxidative stress. (B) Assay of HO-1 expression using quantitative real-time PCR with retinal cDNAs, with transcript levels being normalized to Hprt and shown as x-fold increases compared to the wild-type level.

A

	Rdh12	n	11-*cis* retinal	all-*trans* retinal	all-*trans* retinol
			Retinoid content (pmol/eye)		
Dark-adapted	+/+	3	475 ± 17	16 ± 3	n.d.
	+/–	2	480 ± 6	15 ± 1	n.d.
	–/–	4	469 ± 28	21 ± 2	n.d.
Light-adapted	+/+	3	336 ± 55	165 ± 12	72 ± 12
	+/–	2	352 ± 17	183 ± 57	75 ± 14
	–/–	3	360 ± 19	169 ± 5	71 ± 9
Bleached	+/+	7	49 ± 5	216 ± 22	305 ± 30
	+/–	4	55 ± 9	260 ± 61	335 ± 49
	–/–	5	47 ± 7	221 ± 53	311 ± 70
Recovered	+/+	3	266 ± 28	29 ± 10	46 ± 3
	+/–	3	213 ± 22	31 ± 4	48 ± 2
	–/–	4	209 ± 21	33 ± 9	47 ± 7

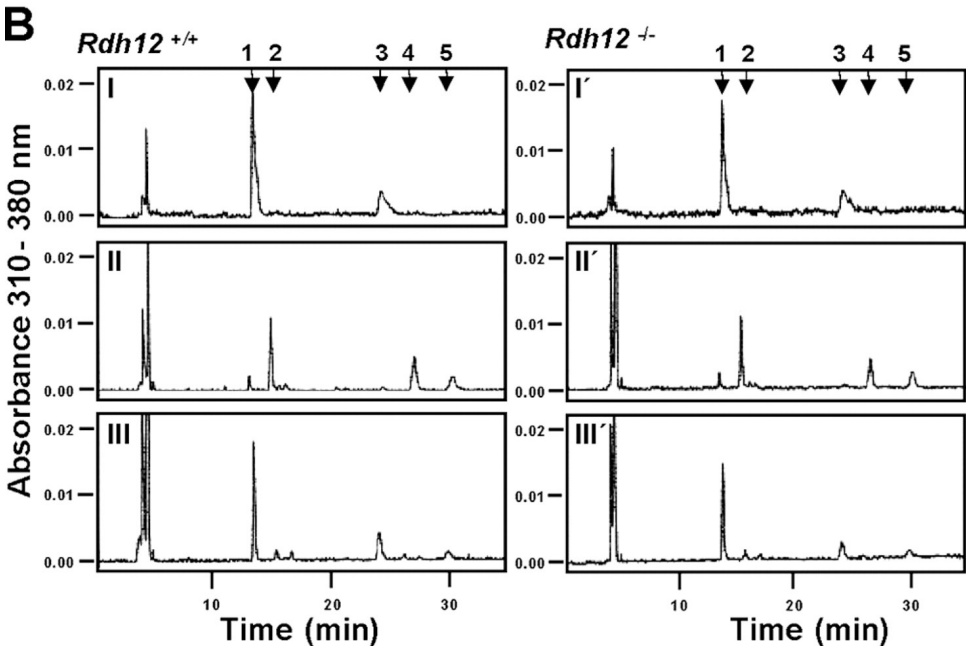

Figure 3-7. Retinoid content of eyes from *Rdh12*–/– mice. (A) Retinoid content given in absolute amounts. (B) HPLC analysis of retinoids extracted from eyes from (I to III) wild-type (*Rdh12*+/+) and (I' to III') *Rdh12*–/– mice that were (I) dark adapted, (II) bleached (5,000 lux for 10 min), or (III) bleached and allowed to recover (5,000 lux for 10 min, dark for 30 min). Retinaldehydes were extracted as syn- and anti-retinal oximes and summed. 1, syn-11-*cis* retinal oxime; 2, syn-all-*trans* retinal oxime; 3, anti-11-*cis* retinal oxime; 4, all-*trans* retinol; 5, anti-all-*trans* retinal oxime. n.d., not detected.

CHAPTER 4

RDH12 ACTIVITY AND EFFECTS ON RETINOID PROCESSING IN THE MURINE RETINA[‡]

Introduction

RDH12 is a major disease gene for Leber congenital amaurosis (LCA), with *RDH12* mutations responsible for ~2% of cases of childhood-onset severe autosomal recessive retinal dystrophy [106, 137, 138, 210]. These individuals experience poor vision in early life that progressively declines with age as a result of both rod and cone degeneration [211]. Analyses of retinal organization and visual function in patients with mutations in *RDH12* or *RPE65*, another LCA gene involved in retinoid metabolism, show distinctly different pathologies associated with defects in each gene that will be important to consider when developing targeted forms of therapy [212].

RDH12 encodes a member of the family of short chain dehydrogenases/reductases (SDRs) that catalyze oxidation and reduction reactions involved in various aspects of metabolism (reviewed in Refs. [213] and [214]). In the photoreceptor cells and retinal pigment epithelium (RPE), the interconversion of oxidized and reduced retinoids by retinol dehydrogenase/reductase (RDH) enzymes is an important feature of the visual cycle, the process responsible for the conversion of vitamin A (all-*trans* retinol) to 11-*cis* retinal, the chromophore of the visual pigments (reviewed in [215]). On the basis of *in*

[‡] Portions of this chapter were published in:
Chrispell JD, Feathers KL, Kane MA, Kim CY, Brooks M, Khanna R, Kurth I, Hübner CA, Gal A, Mears AJ, Swaroop A, Napoli JL, Sparrow JR, Thompson DA. Rdh12 activity and effects on retinoid processing in the murine retina. J Biol Chem. 2009 Aug 7;284(32):21468-77.

vitro assays showing reactivity toward retinaldehyde substrates and expression in photoreceptor cells, RDH12 was initially proposed to function in the reduction of all-*trans* retinal released by bleached visual pigments [135]. Subsequent *in vitro* studies showed that RDH12 also acts upon C9 aldehydes resulting from lipid photo-oxidation, as well as certain steroid substrates, suggesting that it may contribute to additional pathways important for photoreceptor function [136, 139, 140, 216]. In previous studies, we generated Rdh12-deficient mice and evaluated their retinal phenotype, finding grossly normal retinal histology, visual responses, retinoid content, and assays of oxidative stress [204]. We also showed that RDH12 localizes to photoreceptor inner segments (IS) in both humans and mice, distant from the phototransduction reactions occurring in the outer segment (OS) disc membranes. Based on this analysis, we concluded that RDH12 deficiency does not limit chromophore synthesis or visual cycle throughput, in agreement with Maeda et al. [217].

Earlier attempts to identify an RDH isoform essential for chromophore synthesis also failed to do so. These studies included generation and analysis of Rdh5-deficient mice lacking the RDH isoform specific to the RPE, Rdh11-deficient mice lacking the RDH isoform most closely related to Rdh12, and Rdh8-deficient mice lacking the RDH isoform that localizes to photoreceptor OS [56, 73, 74, 142]. In each case, loss-of-function resulted in only minor slowing of dark adaptation without retinal degeneration, raising the possibility of redundancy in RDH function relative to the visual cycle mechanism.

In this chapter, we show that the retinas of Rdh12-deficient mice exhibit a markedly decreased capacity to reduce retinaldehyde substrates *in vitro* but do not exhibit

decreased synthesis of 11-*cis* retinal *in vivo*. Our data are consistent with a mechanism in which RDH12 contributes to the reduction all-*trans* retinal that escapes conversion to all-*trans* retinol by enzyme(s) present in the OS. Although fundamental differences exist between species, our findings in mice point to an important role of RDH12 in retinoid metabolism occurring in photoreceptor cells, and of likely relevance to disease pathology in the human retina, but that does not limit chromophore synthesis *in vivo*.

Materials and Methods

All experimental procedures complied with the regulations of the University of Michigan Committee on Use and Care of Animals and the ARVO Statement for the Use of Animals in Ophthalmic and Vision Research. Mice were reared in a 12 h-12 h light-dark cycle (~800-lux room light, as indicated below) and euthanized by CO_2 inhalation.

Animals and antibodies

Transgenic mice of the following genotypes were used for our studies: *Rdh12−/−* mice homozygous for a Rpe65-Leu450 (L/L) or Rpe65-Met450 (M/M) polymorphism on a mixed Sv129;C57BL/6 (pigmented) background (15); *Rdh12−/−* mice on the BALB/c (albino) background and homozygous for Rpe65-Leu450 (L/L) that were obtained by breeding (generation F6); *Rdh12−/−* mice heterozygous for a *Sod2* null allele (*Sod2+/−*) and homozygous for Rpe65-Met450 (M/M) obtained by breeding with mice from The Jackson Laboratory (Bar Harbor, ME; stock No. 002973, strain B6.129S7-Sod2tm1Leb); *Rdh11−/−* mice homozygous for Rpe65-Leu450 (L/L) (pigmented) characterized by P. Nelson and K. Palczewski [73]; and *Nrl−/−* mice homozygous for Rpe65-Met450 (M/M) that have a model “all-cone” retina [17](21). Primary antibodies used were: a rabbit anti-

Rdh12 polyclonal antibody specific for the mouse protein (rAb CSP) [204]; a rabbit anti-transducin polyclonal antibody (Genetex); and a rabbit anti-arrestin polyclonal antibody (Affinity Bioreagents).

Analysis of visual cycle retinoids

All-*trans* retinal, all-*trans* retinol, and 11-*cis* retinal levels in mouse eyes were determined using normal-phase high performance liquid chromatography (HPLC) as described previously [138]. In brief, dark-adapted mice (~3 months old) were subjected to bleaching light (5000 lux, 15 min), recovered in the dark for 0–60 min, and euthanized. Under dim red light, whole eyes were homogenized in chloroform:methanol: hydroxylamine, the organic phases were collected, and the solvent evaporated. The extracts were dissolved in hexane and chromatographed on a Supelcosil LC-31 analytical column (25 cm × 4.6 mm, 5 μm) developed with 95% hexane, 5% 1,4-dioxane. Absorbance peaks were identified by comparison with external standards, and molar quantities per eye were calculated by comparison with standard concentrations determined spectrophotometrically using extinction coefficients (Chapter 3) and normalizing to total sample volumes [199]. Retinaldehyde content was calculated as the sum of syn- and anti-retinal oximes. Data were analyzed and curves fitted using SigmaPlot (Systat Software Inc.). Standards used were: all-*trans* retinol (Sigma Aldrich), 11-*cis* retinol obtained by NaBH4 reduction of 11-*cis* retinal (R. Crouch), and all-*trans* and 11-*cis* retinal oximes obtained by hydroxylamine reaction of the corresponding aldehydes [218].

Analysis of retinal reductase activity

Mouse retina homogenates were assayed for retinal reductase activity with exogenous substrates. Light-adapted mice (~2–5 months old) were euthanized, and dissected retinas from 4–8 animals were pooled and homogenized in 300 µl of 0.25 M sucrose, 25 mM Tris acetate, pH 7, 1 mM dithiothreitol. The homogenates were centrifuged at 1000 × g for 5 min to remove unbroken cells, and then the supernates were sonicated with a microtip probe (30 times for 1 s) on ice. Protein concentrations were determined by a modification of the Lowry procedure, and levels of Rdh12 and arrestin (a marker for total photoreceptor proteins) were evaluated by densitometric analysis of Western blots [219]. Assay reactions (200 µl) were prepared that contained 20 µg of retinal protein, 200 µM all-*trans* retinal or 11-*cis* retinal, and 200 µM NADPH in HEPES buffer (pH 8); reactions were incubated for 0–60 min at 32 °C (a reaction temperature that minimizes thermal isomerization of the retinoid substrates, as well as enzyme inactivation). All-*trans* retinol and 11-*cis* retinol formation were quantitated using normal-phase HPLC analysis with comparison to standards, as described above, and the data were analyzed using SigmaPlot. Controls for recovery included samples containing known amounts of standard compounds [138].

Analysis of histology and retinal thickness

Anesthetized mice were perfused, and the eyes were enucleated, post-fixed for at least 1 h in 4% paraformaldehyde or 2% paraformaldehyde plus 2% glutaraldehyde, and embedded in JB-4 plastic. Sections (5 µm) were stained with Lee's stain and imaged on a Nikon Eclipse E800 microscope with Nikon DMX1200 digital camera using the manufacturer's data acquisition software. Measurements of retinal outer nuclear layer

(ONL) thickness on sections parallel to the vertical meridian of the eye were plotted versus distance from the optic nerve head for animals of various ages [220].

Analysis of transcript abundance by quantitative real-time PCR

Total RNA was isolated from mouse retinas (~2–3 months old) using the RNeasy mini kit (Qiagen), and quality and quantity were assessed using an Agilent Bioanalyzer 2100. First strand cDNAs were generated using SuperScript II (Invitrogen) and oligo(dT) (Invitrogen). Sequences present in the 3′-untranslated regions of transcripts of interest were amplified using AmpliTaq Gold (Applied Biosystems) and SYBR Green I (Molecular Probes) with a Rotor-Gene3000 thermocycler (Corbett Research) as follows: 95 °C for 10 min, 95 °C for 25 s, 57 °C for 25 s, and 72 °C for 30 s, with steps 2–4 repeated 35 times. Samples in triplicate were each amplified in triplicate and normalized to the values for *Hprt* transcripts. Primers (sense, antisense) were as follows: *Rdh12*, 5′-GGCCAATCTGCTCTTCACTC-3′, 5′-ACTTTCCACTCAGGGGCTCTA-3′; *Rdh11*, 5′-CCACAGCAAACTAGCCAACA-3′, 5′-CCAACTGGCAATCACTGAAA-3; *Rdh8*, 5′-GATGTGGCCCAGGTCATT-3′, 5′-GACCAAGGTTGAGGAGGTGA-3′; *Hprt*, 5′-GCAAGCTTGCTGGTGAAAGGA-3′, 5′-CCTGAAGTACTCATTATAGTCAAGGG-3′.

Microarray analysis of expression

Total retinal RNA from *Rdh12*−/− and wild-type mice (~2 months old) was isolated as described above and converted into biotinylated, fragmented, and cleaned cRNA using Affymetrix reagents. Mouse genome arrays (Affymetrix 430_2.0) were hybridized with fragmented cRNA and processed as described (34). The arrays were optically read with a Hewlett-Packard GeneArray scanner, and CHP/.CEL files were

generated using the Affymetrix microarray suite of programs. The quality of the GeneChip hybridizations was excellent according to Affymetrix criteria. Normalization and calculation of signal intensities were performed using the Robust Multi-Chip Average software package (R-Project). Ratios of average signal intensity (log 2) were calculated for probe sets between pairs of genotypes and converted to average fold change. Statistical validation was performed as described previously by assigning p-values and fold changes of gene responses in a two-step procedure based on the construction of false discovery rate confidence intervals [221-223]. Affymetrix GeneChip data for flow-sorted GFP+ photoreceptor cells from wild-type and *Nrl−/−* mice at various developmental ages were generated as described previously [205].

Results

Visual cycle retinoids in Rdh12-deficient mouse eyes

The first step in the recycling aspect of the visual cycle is the conversion of all-*trans* retinal released from bleached visual pigments to all-*trans* retinol that is returned to the RPE. In studies employing retinoid extraction and HPLC analysis, we showed previously that steady-state levels of visual cycle retinoids were similar in the eyes of Rdh12-deficient and wild-type mice heterozygous for the Rpe65-Leu450Met (L/M) polymorphism that impacts rates of chromophore synthesis [204]. We have now used these methods to evaluate retinoid processing during dark adaptation in Rdh12-deficient mice homozygous for the Rpe65-Leu450 (L/L) variant associated with high visual cycle throughput [132]. During recovery in the dark after full bleaching, our results show that

rates of all-*trans* retinal reduction and 11-*cis* retinal formation are not significantly different between *Rdh12−/−* and wild-type animals (Figure 4-1).

RDH activity in Rdh12-deficient mouse retinas

To determine the contribution of Rdh12 to the overall capacity of the mouse retina to reduce retinaldehyde substrates, we performed *in vitro* assays of retinal homogenates with exogenous all-*trans* retinal or 11-*cis* retinal as substrate. Retinas from *Rdh12−/−* and wild-type mice on three different genetic backgrounds were evaluated: Rpe65-L/L or Rpe65-M/M on 129Sv:C57BL/6 (pigmented) and Rpe65-L/L on BALB/c (albino). For wild-type pigmented and albino mice that were Rpe65-L/L, we found that robust retinal reductase activity was present in assays with saturating levels of all-*trans* retinal or 11-*cis* retinal (Figure 4-2A and C). Initial rates of all-*trans* retinol formation were 0.51 and 0.62 pmol min^{-1} μg $protein^{-1}$ in the pigmented and albino mice, respectively. Similarly, initial rates of 11-*cis* retinol formation were 0.70 and 0.60 pmol min^{-1} μg $protein^{-1}$. For *Rdh12−/−* mice, significantly lower retinal reductase activity was observed with both substrates (Figure 4-2A and C). Initial rates of all-*trans* retinol formation were 0.052 and 0.057 pmol min^{-1} μg $protein^{-1}$ in pigmented and albino mice, respectively, whereas 11-*cis* retinol formation was undetectable. Mice on the Rpe65-M/M background exhibited lower RDH activity than Rpe65-L/L mice; however, the relative decrease in RDH activity seen in *Rdh12−/−* mice was similar (Figure 4-2B and D).

RDH activity in Rdh11-deficient mouse retinas

In vitro assays of retinal homogenates from *Rdh11−/−* mice exhibited retinoid reductase activity that was significantly greater than of *Rdh12−/−* mice on the same genetic background (pigmented Rpe65-L/L) (Figure 4-3). At saturating substrate

concentrations, initial rates of all-*trans* retinol and 11-*cis* retinol formation in *Rdh11−/−* retinal homogenates were 0.57 and 0.99 pmol min−1 μg protein−1, respectively.

Rdh12 expression on various genetic backgrounds and during development

To determine whether *Rdh12* expression reflects differences in visual cycle efficiency attributable to the Rpe65-L450M polymorphism, we used quantitative real-time PCR to compare transcript levels in eyes from pigmented wild-type mice that were Rpe65-L/L or Rpe65-M/M. We found that *Rdh12* transcripts were ~4-fold lower in mice with the Rpe65-M/M polymorphism associated with low levels of 11-*cis* retinal synthesis, compared to mice with Rpe65-L/L, associated with high levels of 11-*cis* retinal synthesis (Figure 4-4A). In Nrl-deficient mice having an 'all-cone' retina, *Rdh12* transcript levels were approximately 10-fold lower than in wild-type mice (Rpe65-M/M) (Figure 4-4B). Changes of the same magnitude were not seen for *Rdh11*.

To evaluate *Rdh12* expression during development, data from microarray analysis of flow-sorted GFP-positive photoreceptor cells were obtained as described previously [205]. The photoreceptor cells were from dissociated retinas of transgenic mice expressing GFP under the control of the *Nrl* promoter on the wild-type (predominantly rod) or the *Nrl−/−* (all-cone) background (Rpe65-M/M). Plots of normalized signal intensity showed that *Rdh12* transcript levels markedly increased from embryonic day 16 to postnatal day 28 in wild-type mice and to a lesser extent in *Nrl−/−* mice (Figure 4-4C). In contrast, *Rdh11* transcript levels remained relatively unchanged in both wild-type and *Nrl−/−* mice.

Expression of RDH isoforms in wild-type and Rdh12-deficient mice

The absence of retinal pathology in Rdh12-deficient mice suggests, as one possibility, that one or more RDH isoform(s) with overlapping activity compensates for Rdh12 loss-of-function. To compare the expression of RDH isoforms in *Rdh12−/−* and wild-type mice (Rpe65-L450M) in total retinal RNA, relative transcript abundance was evaluated using Affymetrix microarray profiling. For each of the RDH isoforms reported to be present in photoreceptor cells and represented on gene chips (*Rdh11*, *Rdh13*, *Rdh14*, *Dhrs3*), we found no marked differences in expression between the *Rdh12−/−* and wild-type mice (Table 4-1) [54, 135]. This was also the case for *Rdh10* expressed in RPE and Müller cells, as well as other known RDH isoforms, including *Rdh1*, *Rdh7*, *Rdh9*, and *Rdh16* (data not shown) [147]. One exception was *Rdh5*, for which transcripts were apparently decreased ~1.7-fold in *Rdh12−/−* mice. The presence of *Rdh5* transcripts in our RNA preparations likely reflects the presence of contaminating RPE cells in our dissected retinal tissue, as Rdh5 is an RPE-specific enzyme involved in the conversion of 11-*cis* retinol to 11-*cis* retinal [70]. A second exception was Rdh8, which localizes to photoreceptor OS. Because *Rdh8* is not represented by probe sets on the Affymetrix gene chips, *Rdh8* expression was evaluated using quantitative real-time PCR analysis, which showed that transcripts were decreased ~3.1-fold in *Rdh12−/−* mice. The apparent down-regulation of Rdh5 and Rdh8 suggests that retinoid processing associated with visual cycle function is less robust in the absence of Rdh12. As no known RDH isoforms appear to be up-regulated in *Rdh12−/−* mice, our findings suggest that the activity provided by the enzyme levels normally present in mouse retina are sufficient to compensate for Rdh12 loss-of-function.

Effects of aging and oxidative stress in Rdh12-deficient mice

To assess potential changes in retinal histology at advanced ages, we performed morphometric analysis of retina/RPE/choroid sections from Rdh12-deficient and wild-type mice reared in normal laboratory lighting. We found no evidence of increased retinal pathology or decreased ONL thickness in *Rdh12−/−* mice at 20 months old that were pigmented and Rpe65-L/L or Rpe65-M/M (Figure 4-5A and B). We also evaluated the retinas of albino *Rdh12−/−* mice on the BALB/c background, which imparts increased light sensitivity due in part to the presence of the Rpe65-L450 polymorphism [131]. Again, no increased retinal pathology or decreased ONL thickness was seen in Rdh12-deficient mice crossed onto the BALB/c background for six generations (Figure 4-5C).

To determine whether increased oxidative stress exacerbates the retinal phenotype of Rdh12-deficient mice, we crossed mice carrying a null allele of the superoxide dismutase 2 gene (*Sod2*) with *Rdh12−/−* animals. Although the homozygous null *Sod2−/−* genotype is lethal, *Sod2+/−* mice are viable and exhibit increased levels of reactive oxygen species associated with increased oxidative damage to proteins, DNA, and membranes [224, 225]. Mice with the *Rdh12−/−*;*Sod2+/−* (Rpe65-M/M) genotype were obtained by breeding and were evaluated by morphometric analysis. Retina sections from *Rdh12−/−*;*Sod2+/−* mice at 9 months old showed no evidence of increased retinal pathology or decreased ONL thickness relative to age-matched *Sod2+/−* mice that were wild-type for Rdh12 (Figure 4-5D). In addition, the RDH activity of retinal lysates assayed *in vitro* was equivalent in *Rdh12−/−*;*Sod2+/−* and *Rdh12−/−* animals on the Rpe65-M/M background (Figure 4-6).

Discussion

Our study establishes that Rdh12 loss-of-function markedly impacts the overall capacity of the mouse retina to reduce retinaldehyde substrates, even though *in vivo* rates of all-*trans* retinal reduction during recovery from bleaching are not significantly affected. The decrease in the ability of the Rdh12-deficient retina to reduce all-*trans* retinal and profound loss of activity toward 11-*cis* retinal suggest that Rdh12 makes a unique contribution to the capacity for retinoid processing in the photoreceptor cells. These findings are consistent with the assumption that defects in retinoid metabolism contribute to the disease phenotype resulting from *RDH12* mutations in patients. Together with previous studies, our results suggest that the supply of all-*trans* retinol needed for chromophore synthesis is not limited by RDH activity in the photoreceptors and that this need may be met by delivery from the circulation and stores of retinyl esters in the RPE. It follows that increased rates of regeneration attributed to IRBP may result from a potential role in reducing photoreceptor levels of all-*trans* retinol, rather than from delivery of all-*trans* retinol to the RPE [56, 73, 74, 204, 217, 226].

Previous studies of the retinal phenotype of Rdh12-deficient mice did not detect marked changes in retinoid processing or visual cycle function [204, 217]. In one study, delayed recovery of the electroretinogram (ERG) a-wave after bleaching was observed as well as increased levels of 11-*cis* retinal, but no decrease in all-*trans* retinal reductase activity was detected *in vitro* [217]. Subsequent studies of *Rdh12-Rdh8* double knockout mice showed that Rdh12 loss-of-function significantly decreased the all-*trans* retinal reductase activity of Rdh8-deficient mouse retinas [227]. In contrast, our studies show that retina homogenates from mice deficient in Rdh12 alone have significantly reduced

capacity for reduction of both *trans*- and *cis* retinaldehydes on all genetic backgrounds tested, but do not exhibit delayed dark adaptation or increased levels of retinaldehydes *in vivo* (this chapter and [204]). In addition, the decrease of retinal reductase activity in Rdh12-deficient mice is greater than that observed for Rdh11-deficient mice. We also found that wild-type mice with the Rpe65-M/M polymorphism exhibit lower levels of retinal reductase activity than mice with the Rpe65-L/L polymorphism, associated with higher visual cycle activity [131, 132]. In collaboration with the laboratory of Dr. Janet Sparrow at Columbia University, HPLC analysis of *N*-retinylidene-*N*-retinylethanolamine (A2E) and A2E isomers, the major fluorophores of lipofuscin granules associated with age-related macular degeneration present in posterior eyecups was performed. We observed that Rdh12-deficient mice exhibit elevated A2E levels regardless of background and that these levels increase with aging Additionally, levels of A2E were lower in *Rdh12*−/− mice on the Rpe65-M/M background than in Rpe65-L/L animals, in agreement with earlier studies [217] (Figure 4-7). Thus, a key finding of our study is that Rdh12 activity appears to correlate with visual cycle activity, with loss-of-function resulting in a shift in the equilibrium toward products that exit the visual cycle. As Rdh12 deficiency does not result in elevated levels of total retinaldehydes, such increases are likely to occur focally, transiently, or both. Although differing in mechanistic detail and degree of severity, the resulting accumulation of A2Es may reflect a situation akin to that due to mutations in *ABCA4*, which delay the removal of all-*trans* retinal from the disc membranes [49].

Retinoic acid synthesis involves the oxidation of retinaldehydes in a reaction typically catalyzed by members of the family of aldehyde dehydrogenase enzymes

(reviewed in [228]). Collaboration with Dr. Maureen Kane and the lab of Dr. Joseph Napoli at the University of California, Berkeley was established to assay levels of retinoic acid in retinal homogenates from dark-adapted mice using HPLC-coupled tandem mass spectrometry. We found that retinoic acid levels were decreased in *Rdh12−/−* mice relative to the wild-type (Figure 4-8A). In addition, significant decreases in total retinol content of retinas from *Rdh12−/−* mice were detected (Figure 4-8B). These findings suggest that Rdh12 deficiency in the retina produces a shift in retinoid homeostasis resulting in decreased retinoid content. This result was unexpected, as a previous study of recombinant RDH12 activity *in vitro* found increased levels of retinoic acid in transfected cells expressing loss-of-function mutants relative to cells expressing the wild-type protein [229]. This study suggests that RDH12 reduction of retinaldehydes is needed to protect against the potentially damaging effects of high levels of retinoic acid. However, our data do not support the view that RDH12 acts exclusively as a reductase *in vivo* to decrease levels of retinoic acid, as *in vivo* levels of both retinoic acid and total retinol were decreased in *Rdh12−/−* mice. The decrease in retinoic acid levels due to Rdh12 deficiency points to a complex mechanism involved in regulating retinoic acid biosynthesis, and suggests that RDH12 may play a role in this mechanism in the retina, either as a reductase or a dehydrogenase depending on its metabolic environment. Our findings further suggest that some aspects of the disease phenotype associated with human *RDH12* mutations may be a consequence of impaired retinoic acid production and/or bioavailability.

The broad substrate specificity of RDH12 has prompted suggestions that it functions in a number of various aspects of retinal cell biology. *In vitro* assays of

recombinant RDH12 activity have shown it can reduce certain lipid photo-oxidation products including the C9-aldehydes nonanal and 4-hydroxynonenal, as well as certain steroids including dihydrotestosterone, albeit with lower affinity and catalytic efficiency compared to all-*trans* retinal [136, 216]. In our initial analysis of the phenotype of Rdh12-deficient mice, we found no increase in oxidative products measured as thiobarbituric acid-reactive substances (TBARs) in the retina (Chapter 3 and [204]). We have now studied the retinal phenotype of Rdh12-deficient mice that were heterozygous for a null allele of manganese superoxide dismutase 2 (*Sod2*+/−). Mice heterozygous for Sod2 loss-of-function were used as model to test for effects of increased oxidative stress, as reduction of this enzyme activity results in increased mitochondrial oxidative damage and susceptibility to apoptotic cell death, whereas the *Sod2*−/− genotype is lethal and severe Sod2 deficiency alone results in profound retinal degeneration [224, 225, 230-232]. Our results show no evidence of increased retinal cell death in *Rdh12*−/−;*Sod2*+/− mice, as measurements of ONL thickness and retinoid reductase activity were similar to those of *Rdh12*−/− mice on the wild-type background. Previous studies also reported increased apoptotic cell death in retinas of Rdh12-deficient mice exposed to high intensity illumination [217]. However, we detected no increase in age-related pathology in *Rdh12*−/− mice, including animals on the albino BALB/c background that were reared in normal laboratory lighting. Thus, while our findings do not rule out the possibility that RDH12 may play a role in protecting against oxidative stress and light-damage, they do not support the view that this is an exclusive function.

Efforts to identify the RDH enzymes essential for visual cycle function have been confounded by the fact that photoreceptor cells express a number of isoforms which

exhibit the necessary specificity *in vitro* [54, 55, 135]. As no known RDH isoforms appear to be up-regulated in *Rdh12−/−* mice, our findings suggest that the activity provided by the basal levels of RDH activity present in mouse retina are sufficient to compensate for Rdh12 loss-of-function. Elegant studies of retinoid processing in retina slices and isolated photoreceptor cells have shown that all-*trans* retinol formation localizes to the OS during recovery from bleaching [233, 234]. Of the RDH isoforms known to be expressed in retina, only RDH8 has been localized to the OS [55, 227]. However, Rdh8-deficient mice exhibit only mild perturbations in retinoid processing in the form of decreased rates of dark adaptation, and no accompanying pathology [56]. Rates of dark adaptation are slightly decreased in *Rdh12-Rdh8* double knockout mice and OS are shorter, but significant levels of chromophore synthesis persist [227]. These findings are consistent with recent measurements of *in vivo* rates of all-*trans* retinol synthesis suggesting that the rate-limiting step in the production of the 11-*cis* retinal chromophore is the release of all-*trans* retinal from opsin [226]. Thus, the primary role of RDH enzymes present in the photoreceptors may be to reduce potentially toxic levels of retinaldehydes in various cellular compartments. It seems possible that RDH8, which recognizes *trans*- but not *cis*-retinaldehydes, is important for the rapid reduction of all-*trans* retinal in the vicinity of the rhodopsin signaling complex, whereas the contribution of RDH12, with its broader substrate specificity and localization near the metabolic source of NADPH, becomes more important under conditions of continuous illumination. As RDH12 is restricted to IS in both human and mouse retina and there is no evidence of light-induced translocation, this implies that all-*trans* retinal can move between outer and

IS compartments, perhaps associated with retinoid-binding proteins or with opsin found in the IS plasma membrane.

In summary, our analysis of the retinal phenotype of Rdh12-deficient mice supports the view that defects in retinoid metabolism are a contributing factor to disease resulting from RDH12 loss-of-function mutations in patients, providing new insights into the visual cycle mechanism and localization of retinoid processing reactions.

Outside contributions: Ritu Khanna analyzed microarray data from flow sorted GFP+ photoreceptors during development that was obtained from work performed in [205]. Kecia Feathers performed qRT-PCR and histological analysis of the mouse retinas. Matt Brooks performed the microarray analysis of the *Rdh12–/–* mouse.

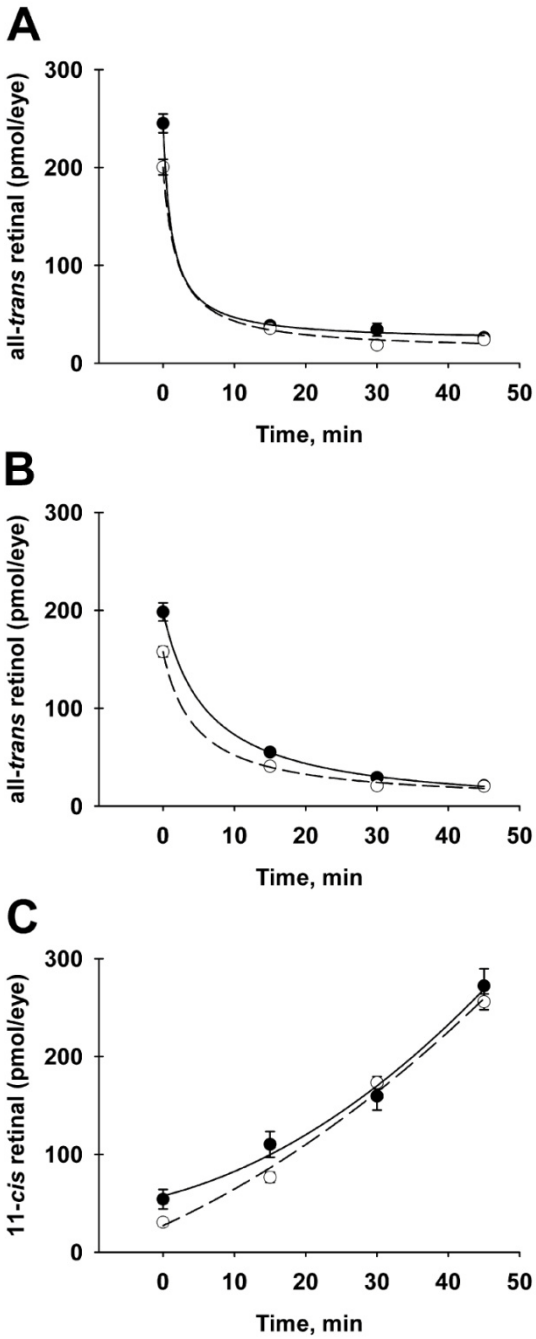

Figure 4-1. All-*trans* retinal, 11-*cis* retinal, and all-*trans* retinol levels during recovery from bleaching. *Rdh12*−/− and wild-type mice were exposed to bleaching light (5000 lux, 15 min) and recovered in the dark for the times shown. Retinoids extracted from whole eyes in organic solvents were quantitated using normal-phase HPLC analysis. A, all-*trans* retinal; B, all-*trans* retinol; C, 11-*cis* retinal. Experimental values are plotted as mean ± S.E. (n = 3). ○, *Rdh12*−/− mice; ●, wild-type mice.

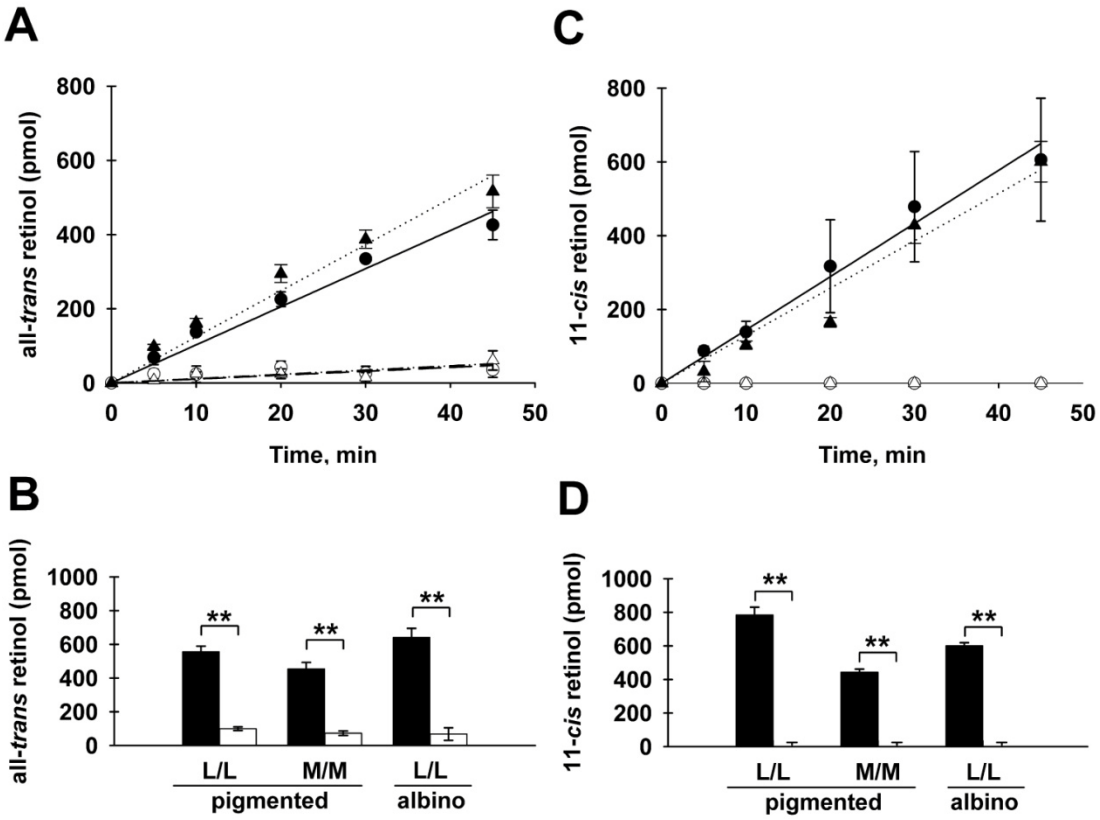

Figure 4-2. Effects of Rdh12 deficiency on *in vitro* retinoid reductase activity. Retinal homogenates were prepared from *Rdh12−/−* and wild-type mice that were homozygous for Rpe65-Leu450 (pigmented L/L) or Rpe65-Met450 (pigmented M/M) on the 129Sv:C57BL/6 background or for Rpe65-Leu450 (albino L/L) on the BALB/c background. The homogenates were incubated with exogenous retinaldehyde substrates (all-*trans* retinal or 11-*cis* retinal) and NADPH for various times, and retinol formation was quantitated by HPLC analysis of organic solvent extracts. Formation of all-*trans* retinol (A and B) and 11-*cis* retinol (C and D) in retinal lysates from *Rdh12−/−* and wild-type mice is shown. A and C, time course (0–45 min). ○, *Rdh12−/−* (pigmented L/L); ▵, *Rdh12−/−* (albino L/L); ●, wild-type (pigmented L/L); ▲, wild-type (albino L/L). B and D, single point assays (60 min), except 11-*cis* retinol albino L/L (45 min). Open bars, *Rdh12−/−* mice; solid bars, wild-type mice. Assays were performed in triplicate and plotted as mean ± S.D. ($n > 3$). **, $p < 0.01$.

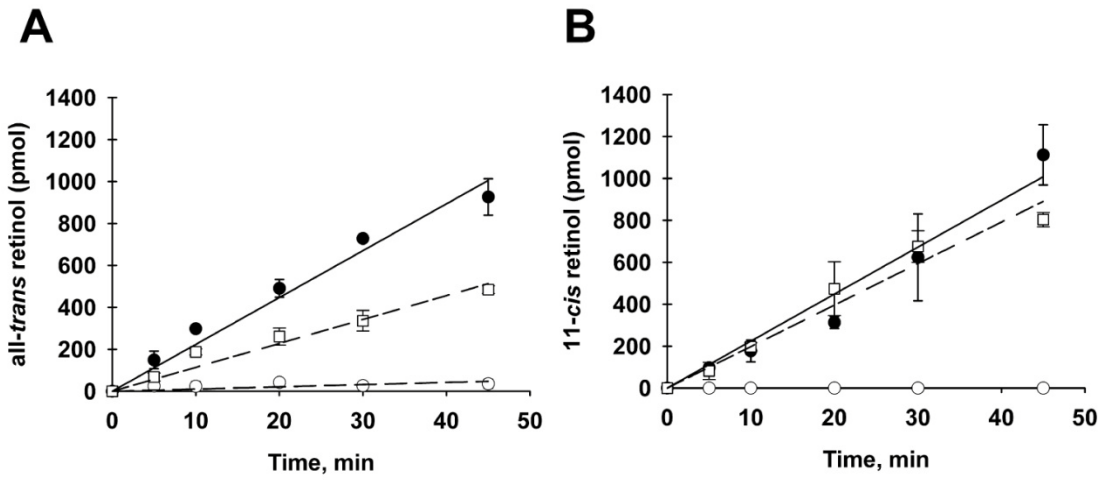

Figure 4-3. Effects of Rdh11 deficiency on *in vitro* retinoid reductase activity. Retinal homogenates from *Rdh11*−/− and wild-type mice (pigmented Rpe65-L/L) were assayed for RDH activity with exogenous retinoid substrates and NADPH for the times shown, and retinol formation was quantitated by HPLC analysis of organic solvent extracts and normalized to Rdh12 content. Assays were performed in triplicate and plotted as mean ± S.D. (n = 3). Data from *Rdh11*−/− mice (□) are shown alongside those from *Rdh12*−/− mice (○) and wild-type mice (●).

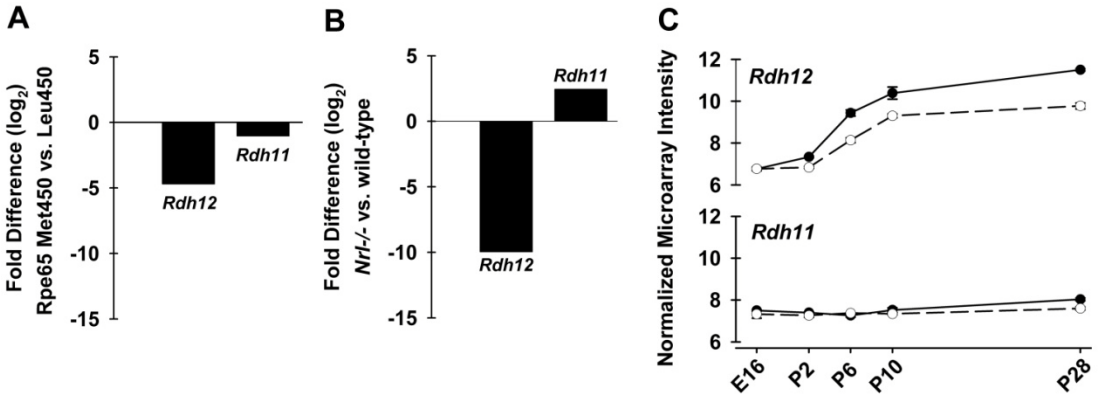

Figure 4-4. Comparative analysis of *Rdh11* and *Rdh12* expression in mouse retina. Quantitative real-time PCR was used to amplify RDH transcripts from retina total RNA, and cycle threshold data were normalized to *Hprt* and plotted as -fold difference. *A*, transcript levels in wild-type mice on the Rpe65-Met450 background compared with levels in wild-type mice on the Rpe65-Leu450 background (pigmented 110 days old; n = 3). *B*, RDH transcript levels in *Nrl*−/− mice compared with levels in wild-type mouse (pigmented Rpe65-M/M, 50 days old; n = 3). *C*, expression during retinal development in *Nrl*−/− and wild-type mice. Normalized microarray intensity data for flow-sorted GFP+ photoreceptors isolated and analyzed as described in [205] is shown for following ages: embryonic day 16 (*E16*) and postnatal (*P*) days 2, 6, 10, and 28 (n = 4 for each time point). ○, *Nrl*−/−; ●, wild-type.

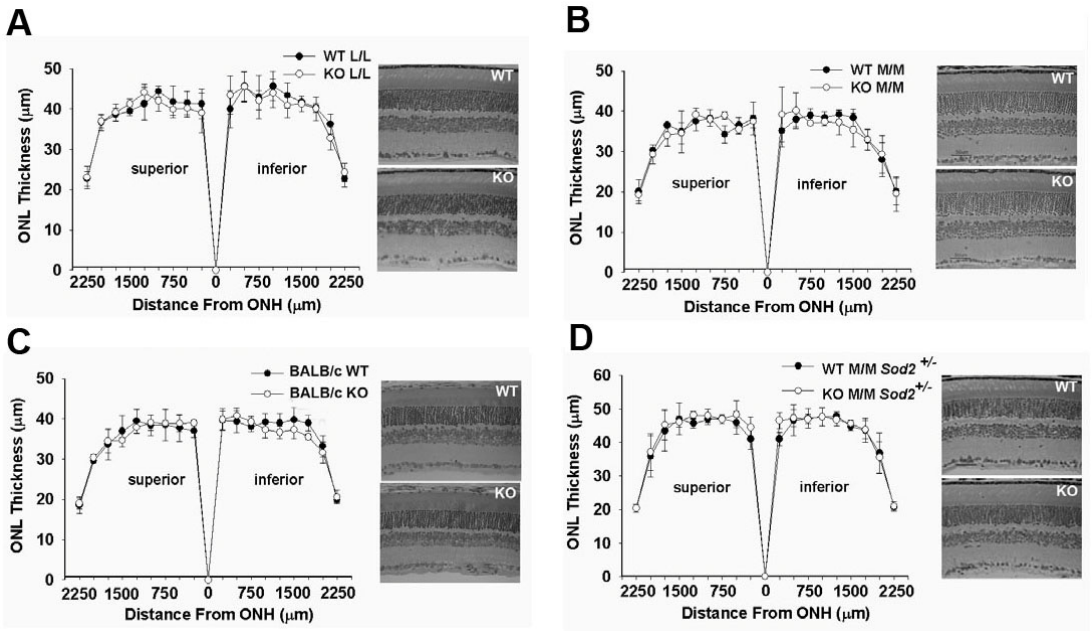

Figure 4-5. Retinal histology and ONL thickness in *Rdh12*−/− and wild-type mice at advanced age and on various genetic backgrounds. Anesthetized mice were perfused, and the eyes were enucleated, post-fixed for at least 1 h in 4% paraformaldehyde or 2% paraformaldehyde plus 2% glutaraldehyde, and embedded in JB-4 plastic [220]. Measurements of ONL thickness were obtained from plastic sections (5 μm) of Lee's stained retina parallel to the vertical meridian of the eye and plotted vs. distance from the optic nerve head ± std. dev. (n=3). Phase contrast micrographs show representative Lee's stained retina/RPE/choroid sections (7 μm) from central retina. (A) *Rdh12–/–* and wild-type (pigmented L/L; ~20 mo old). (B) *Rdh12–/–* and wild-type (pigmented M/M; ~20 mo old). (C) *Rdh12–/–* and wild-type (albino L/L, ~6 mo old). (D) *Rdh12–/–* and wild-type mice heterozygous for the *Sod2* gene (pigmented M/M; ~9 mo old). *Rdh12–/–*, ○; wild-type, ●.

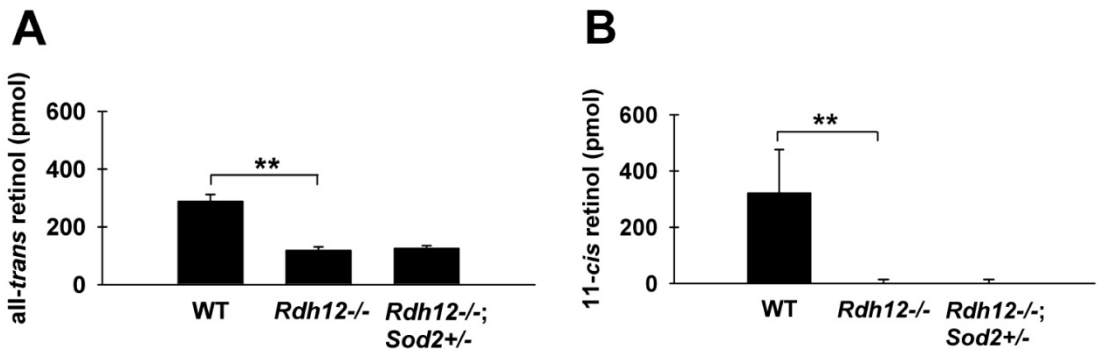

Figure 4-6. Effects of increased oxidative stress on *in vitro* retinoid reductase activity. Retinal homogenates were prepared from wild-type, *Rdh12−/−*, and *Rdh12−/−*;*Sod2+/–* mice that were homozygous for Rpe65-Met450 (pigmented M/M) on the 129Sv:C57BL/6 background. The homogenates were incubated with exogenous retinaldehyde substrates (all-*trans* retinal or 11-*cis* retinal) and NADPH for 60 min, and retinol formation was quantitated by HPLC analysis of organic solvent extracts. Formation of all-*trans* retinol (A) and 11-*cis* retinol (B) in retinal lysates is shown. Assays were performed in triplicate and plotted as mean ± S.D. ($n > 3$). **, $p < 0.01$.

Table 4-1. Microarray analysis of RDH isoforms expressed in mouse retina.

Gene I.D.	Probe Set	*Rdh12–/–* vs. WT
		-Fold change
Rdh12	1424256_at	-129.99
Rdh11	1418760_at	1.29
Rdh10	1426968_a_at	-1.38
Rdh13	1433799_at	1.15
Rdh14	1417438_at	1.05
Dhrs3	1448390_a_at	-1.06
Rdh5	1418808_at	-1.68
Rdh8[a]	N.A.	-3.15

[a] Values obtained by qRT-PCR analysis.

Rdh12−/− and wild-type mice (WT) were heterozygous for Rpe65-L450M. Data shown are the average *chp/cel* intensity of four replicates. For genes with multiple probes sets, the values shown correspond to those with the highest intensity signals.

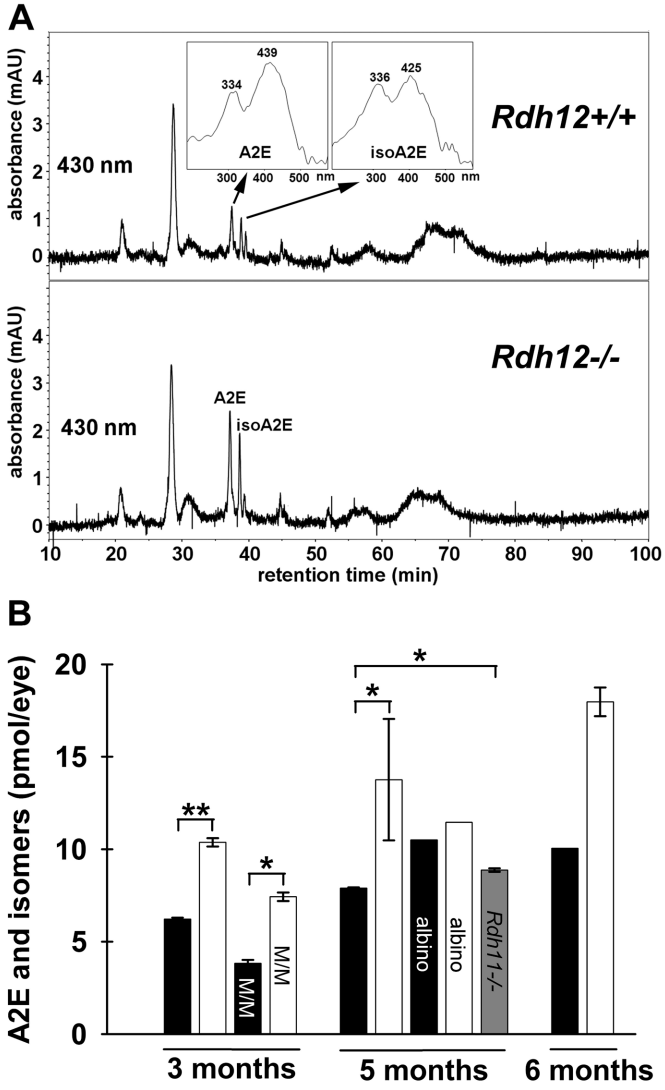

Figure 4-7. A2E levels in *Rdh12−/−* and wild-type mice. Mouse posterior eyecups of *Rdh12−/−* and wild-type mice were extracted using organic solvent, and A2E levels (the sum of A2E and isoA2E) were quantitated using HPLC with comparison to standards. *A*, representative reverse-phase HPLC chromatograms obtained by monitoring at 430 nm. *B*, A2E levels in posterior eyecups at the ages indicated. Mice were C57BL/6 and homozygous for Rpe65-Leu450 (pigmented) unless noted, with *M/M* designating data from mice homozygous for Rpe65-Met450 and *albino* indicating mice that were BALB/c. □, *Rdh12−/−*; ■, wild-type; ▨, *Rdh11−/−*. Assays were plotted as mean ± S.E. for $n > 3$. *, $p < 0.05$; **, $p < 0.01$.

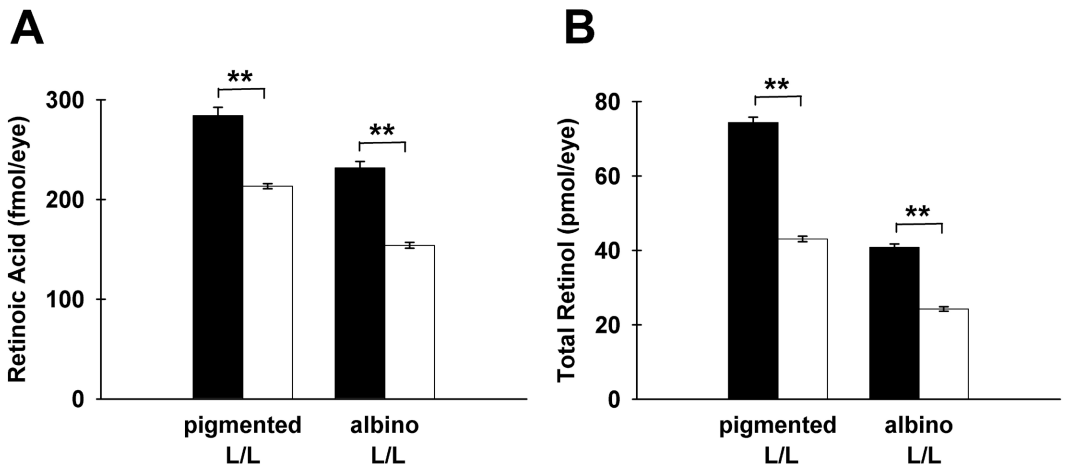

Figure 4-8. Retinoic acid and total retinol content in *Rdh12−/−* and wild-type mice. Isolated retinas from dark-adapted mice were extracted with organic solvent under neutral and acidic conditions to obtain total retinol and retinoic acid-containing extracts, respectively, that were subjected to reverse-phase HPLC. *A*, retinoic acid was quantitated by coupled tandem mass spectrometry analysis. *B*, total retinol was quantitated using UV-visible absorbance. Assays were plotted as mean ± S.E. for $n = 3$. □, *Rdh12−/−*; ■, wild-type. **, $p < 0.01$.

CHAPTER 5

DISCUSSION AND FUTURE DIRECTIONS

This dissertation presents studies that further our understanding of RPE65 structure and function and the role of RDH12 in retinoid processing within the retina. This work has led to the conclusion that RPE65 is localized solely to the RPE and not the retina in a number of rod- and cone-dominant species, limiting the likelihood of involvement in a cone-associated visual cycle. In addition, while RDH12 was not found to be rate limiting in the visual response, RDH12-deficiency results in a decreased capacity of the retina for the reduction of retinaldehydes. These findings give us better comprehension of the role that each enzyme plays in photoreceptor physiology, as well as in the pathogenesis associated with loss-of-function mutations in inherited retinal degeneration.

RPE65

When I began my studies in 2004, *RPE65* had been characterized by our group as a disease gene responsible for a severe form of retinal dystrophy. For the first time, this established a critical role for defects in RPE function in this class of diseases. Our group as well as many others began characterizing RPE65 function and its role in pathogenesis and the visual cycle, with the ultimate goal of formulating targeted therapies to compensate for RPE65 dysfunction. At the time, the role of RPE65 as the isomerase of the visual cycle was unknown, but RPE65 was known to be required for the synthesis of

the chromophore of the visual pigments, 11-*cis* retinal. Early studies suggested that RPE65 functions as a retinyl ester binding protein which interacts with other visual cycle proteins to present ester substrates to an unidentified retinoid isomerase. RPE65 was also proposed to function in cone photoreceptors in an alternative chromophore regenerating-pathway independent of the RPE. This proposal was based on reported expression of *RPE65* transcripts in salamander cones and RPE65 protein in mammalian cones, but not in rod photoreceptors [94, 95]. These findings stood in contrast to others that addressed this issue in mice, showing RPE65 expression only in the RPE.

Our goal in early studies was to identify RPE65 surface epitopes, assess protein interactions, and evaluate RPE65 expression in eyes from rod- and cone-dominant species using a monoclonal antibody approach. The antibody mAb 8B11, elicited using RPE membranes as immunogen, was generated before my arrival in the lab. The corresponding antigenic determinant, KVNPETLETI, is highly conserved - making this antibody an effective tool for studies of RPE65 from a number of species. It is interesting to note that, in previous studies by others to develop RPE65 antibodies by immunization with synthetic peptides, the most effective antibody obtained was elicited by peptide 150-NFITKVNPETLETIK-164 that contains the epitope recognized by mAb 8B11 (50). Antibodies recognizing this antigenic epitope were disseminated or replicated by the scientific community, and one such polyclonal antibody generated against a synthetic peptide corresponding to this epitope was utilized in the study showing RPE65 expression to mammalian cones.

To further pursue studies of RPE65 surface epitopes, protein interactions and localization within the retina, I set out to generate a second anti-RPE65 antibody (Chapter

2). This monoclonal antibody recognized a predicted antigenic sequence in RPE65 that was not recognized by the ubiquitous antibodies currently employed by the field. This antibody, mAb 1F9, recognized the epitope 312-FHHINTYEDNGFLIV-326. While mAb 1F9 lacked the high affinity and extensive cross-species reactivity of mAb 8B11, both antibodies: 1) co-eluted RPE65 with RDH5 and no other visual cycle proteins (in agreement with previous studies); 2) localized to surface-exposed regions in the structural models generated via *ab initio* and comparative methods; and 3) displayed immunoreactivity only within the RPE and not the retina of the various rod- and cone-dominant species tested. This allowed us to conclude that the primary site of RPE65 function is the RPE-based visual cycle. While recent evidence points to very low levels of RPE65 expression in retina as assayed by qRT-PCR, it does not address potential contamination of retina samples with RPE cells due to their close biophysical association [235]. Our identification of two distinct RPE65 surface epitopes represented an initial step toward developing a structural understanding of this important disease gene product. A better understanding of the isomerization mechanism of retinyl esters by RPE65 will be critical to the design of future therapeutic measures, and only recently has the crystal structure of RPE65 been resolved [236].

RDH12

Prior to my tenure in the laboratory, studies conducted by our group identified mutations in *RDH12* associated with severe, early-onset autosomal recessive retinal dystrophy. As one of the major interests of our group is the mechanism of the regeneration of the 11-*cis* retinal chromophore of the visual pigments vis-à-vis the visual cycle, this finding was particularly significant. RDHs perform critical oxidation-

reduction reactions in a number of pathways, including the visual cycle. Early studies had shown that RDH5, which oxidizes 11-*cis* retinol to 11-*cis* retinal in the RPE, is also a disease gene linked to retinal dystrophy. As the critical enzymes involved in major steps of the visual cycle were becoming better understood, it was still unclear which enzyme(s) was(were) responsible for the reduction of all-*trans* retinal, released following activation of rhodopsin and the cone opsins, to all-*trans* retinol that is returned to the RPE. RDH12 was found to be expressed in the photoreceptor cells by *in situ* hybridization, and displayed *in vitro* reductase activity toward retinaldehydes. The *RDH12*-associated disease phenotype being distinct yet similar to that associated with other visual cycle genes, it was proposed that RDH12 might serve as the all-*trans* retinal reductase in the visual cycle.

The work in Chapter 3 details the experiments undertaken to further understanding of the role of RDH12 within the context of the visual cycle. A collaboration was begun with Dr. Christian Hübner of the Institut für Humangenetik (Hamburg, Germany) to develop an *Rdh12–/–* mouse, such that aspects of retinal histology, visual cycle function and visual response could be assayed *in vivo*. My first priority was to examine the localization profile of RDH12 in the retina. The subcellular localization of the RDH12 protein would help us to understand what role it might play in photoreceptor physiology, with a localization to the OS being a strong indicator of involvement in the visual cycle. My approach to this end was the generation of an anti-RDH12 monoclonal antibody, given no such antibody existed at the time. This antibody, mAb 2C9, displayed immunoreactivity towards human RDH12 but not mouse Rdh12. Our German collaborators generated two independent polyclonal antibodies against the

mouse ortholog, and one of these (rAb CSP) recognized the mouse epitope corresponding to the human epitope recognized by mAb 2C9. Using these antibodies, I determined that RDH12 protein localizes to the photoreceptor IS and ONL in both human and mouse. In addition, Rdh12 was not found to exhibit light-induced translocation between the IS and OS, as seen with other photoreceptor proteins such as transducin and arrestin [40-43]. The finding that the localization profile of RDH12 is similar in both humans and mice suggests that it plays a similar role in retinal physiology in both species. However, the localization of RDH12 to the inner segments places it away from the site of phototransduction, complicating the view of RDH12 as the primary all-*trans* retinal dehydrogenase of the visual cycle.

Our further analysis of the phenotype of the *Rdh12–/–* mouse revealed grossly normal histology, retinoid content, and visual response as measured by ERG. We thus concluded that RDH12 does not limit visual cycle function, a finding which was in agreement with other studies of an independently generated Rdh12-deficient mouse [204]. It is not uncommon for mouse models to fail to show the human disease phenotype unless subjected to appropriate stress conditions or placed on a permissive genetic background [209]. While the *Rdh12–/–* mouse did not provide an immediate murine model of the human condition, it did allow us to study other aspects of RDH12 function in retinal physiology and pathology.

In order to further characterize the role of Rdh12 deficiency in the murine model, I crossbred Rdh12 deficient mice onto backgrounds of increased light susceptibility (albino BALB/c, homozygous for the Rpe65-Leu450 (L/L) variant associated with high visual cycle throughput) and increased oxidative stress (*Sod2+/–*) and utilized these mice

in assays of various aspects of retinoid processing [132, 231]. In L/L mice, I observed that *in vivo* rates of all-*trans* retinal reduction and 11-*cis* retinal regeneration during recovery from bleaching were not affected by Rdh12 deficiency. This led to a more in-depth study into the reductive capacity of the mouse retinas *in vitro*, in which I observed a decrease in the overall ability of *Rdh12–/–* retinas to reduce both *cis*- and *trans*-retinaldehyde substrates. The decrease in reductive capacity towards visual cycle retinoids was found regardless of genetic background. This is consistent with the viewpoint that *RDH12* deficiency results in an alteration of retinoid metabolism within the retina, which may play a role in pathogenesis.

In addition, wild-type mice with the Rpe65-M/M polymorphism exhibit lower levels of retinal reductase activity than mice with the Rpe65-L/L polymorphism associated with higher visual cycle activity. A collaborative effort between our lab and that of Dr. Janet Sparrow of Columbia University found that Rdh12-deficient mice exhibit elevated A2E levels in mouse eyecups that increase with aging. This appears to correlate Rdh12 activity and visual cycle activity, with loss-of-function resulting in a shift in the equilibrium toward products that exit the visual cycle. However, *in vitro* retinal reductase activity was not observed to change in *Rdh12–/–* mice crossbred on the *Sod2*+/– background, and we observed no changes in retinal histology for these animals or those on the light-susceptible albino background. While this does not rule out the possibility that RDH12 functions in protecting against oxidative stress and light-damage, it does not appear to be its exclusive function.

Subsequent *in vitro* studies by others showed that RDH12 also acts upon C9 aldehydes resulting from lipid photo-oxidation, as well as certain steroid substrates [136,

139, 140, 216]. Additionally, a study of recombinant RDH12 activity found increased levels of retinoic acid in transfected cells expressing loss-of-function mutants relative to cells expressing the wild-type protein [229]. This suggested that RDH12 may contribute to additional pathways important for photoreceptor function. In an attempt to understand the potential role of RDH12 in the context of other retinal retinoid processing pathways, a collaboration with the laboratory of Dr. Joseph Napoli of the University of California, Berkeley was established to assess the levels of retinoic acid in the retina. The aforementioned study suggested that reduction of retinaldehydes by RDH12 is required to protect against the potentially damaging effects of high levels of retinoic acid which can lead to apoptosis in many types of cells [237-239]. However, our studies showed that retinoic acid levels are decreased in the retinas of Rdh12-deficient mice. While this does not support the view that RDH12 plays an exclusive role as a reductase *in vivo* to decrease levels of retinoic acid, it does suggest that the RDH12 deficiency alters certain aspects of retinoid metabolism in the retina.

One critically important aspect of the work in Chapter 4 is that whereby we attempted to better understand the role of RDH in retinal physiology within the context of other RDH isoforms. Efforts to identify the RDH enzymes essential for visual cycle function have been confounded by the fact that photoreceptor cells express a number of isoforms which exhibit the necessary specificity *in vitro* [54, 55, 135]. Studies of mice deficient in Rdh5, Rdh11, and Rdh8 resulted only in mild phenotypes, suggesting redundancy in RDH function relative to the visual cycle mechanism. We did not observe upregulation of any of the other RDH isoforms in the *Rdh12–/–* mice using microarray analysis. While this does not identify a particular RDH isoform that compensates for

Rdh12-deficiency, it doesn't rule out the possibility that normal levels of RDH expression in the mouse retina are sufficient for unperturbed visual cycle function and visual response.

When taken in aggregate, our studies support the view that the primary role of RDH enzymes present in the photoreceptors may be to reduce potentially toxic levels of retinaldehydes in various cellular compartments. RDH8, which recognizes *trans*- but not *cis*-retinaldehydes, may serve to rapidly reduce all-*trans* retinal in the vicinity of the rhodopsin signaling complex in the OS. RDH12, with its specificity for both all-*trans* and 11-*cis* retinaldhydes and localization near the metabolic source of NADPH, may be more important towards protecting the IS and the remainder of the inner retina under conditions of continuous illumination. Given the similar localization of RDH12 to the IS in both human and mouse retina and that no evidence of light-induced translocation exists, it can be inferred that all-*trans* retinal can move between OS and IS compartments, perhaps associated with retinoid-binding proteins or with opsin found in the inner segment plasma membrane (Figure 5-1).

Future Directions

The ultimate goals of research in the field of retinal dystrophy are to provide molecular diagnostics and novel treatments. Accomplishing these goals will require efforts combining the strengths of genetics, molecular biology, biological chemistry and vision science. Effective treatment regimes are only possible when a thorough knowledge of the normal function of the disease proteins and their context in retinal physiology has been ascertained. The encouraging results of Phase 1 gene therapy trials for the *RPE65*

gene provide a basis to expand this treatment to other retinal disorders. However, overexpression and mislocalization of therapeutic constructs can have detrimental effects in the course of therapy. Knowledge of disease mechanisms will be necessary to enable accurate analysis of the effects caused by variation in gene expression. Approaches such as microarray analysis and proteomics provide promising possibilities for determining the retinal pathways involved in retinal dystrophy.

The failure of the Rdh12-deficient mouse model to replicate the phenotype of human disease may reflect differences between human and mouse relative to expression and/or catalytic activity of a second RDH isoform that maintains activity levels above a critical threshold in mouse, but not in human, retinas. If so, RDH11 is a likely candidate for providing this activity, as it is expressed in the photoreceptor inner segment, and no other RDH isoforms appear to be significantly up-regulated in Rdh12-deficient mice. In addition, the genes encoding RDH11 and RDH12 are highly related evolutionarily and are located in head-to-head orientation on the same chromosome in human and mouse. The generation of a mouse lacking both of these isoforms would be extremely advantageous in determining if Rdh11 compensates for lack of Rdh12 function in the mouse. Unfortunately, an *Rdh12/Rdh11* double knockout mouse cannot be obtained by breeding due to the fact that the two genes are located within 8 kb of one another on mouse chromosome 12, too close for the two genes to spontaneously recombine. Thus, an important future goal will be to produce a double knockout mouse using genetic engineering. If Rdh11 can in fact compensate for Rdh12 deficiency in the mouse, one would expect to find a mouse phenotype more consistent with that found in human RDH12 loss-of-function patients. This phenotype could range from small yet significant

decreases in all-*trans* retinal clearance as measured by HPLC to extreme cases of retinal cell death as measured by histology.

Another factor that could explain differences between the human and mouse phenotype is species differences in the intrinsic catalytic activities of RDH12. While previous studies have evaluated the catalytic efficiency of recombinant human RDH12 towards retinaldehyde and C-9 aldehyde substrates, no direct comparison to mouse Rdh12 activity has been published [136]. My latest work in lab has been the design and creation of baculoviral vectors encoding the human and mouse forms of RDH12 and RDH11 for expression in and purification from insect cells. The decision to use an insect cell-based purification system was based on its suitability for expression of membrane associated proteins, the retention of posttranslational modifications that might be critical to RDH activity, and increased protein yield as compared to transfection of mammalian cells. Preliminary work has yielded high titer baculoviral vectors, and early small scale purifications of RDH11 and RDH12 have been successful. Once purified, it will be important to evaluate the kinetics of these proteins toward various retinaldehydes and other short-chain aldehydes, such as 4-hydroxynonenal [240]. A hypothetical result that might explain differences in the mouse and human phenotype would be a higher catalytic efficiency of human RDH12 than mouse Rdh12 for the reduction of all-*trans* retinal.

The encouraging results of early *RPE65* gene therapy trials make this one of the more promising methods of potential treatments for *RDH12* patients. In order to develop such gene replacement therapies, it will be necessary to gain a better understanding of the structure and function of the *RDH12* promoter. Just as promoter studies have been critical for targeting the *RPE65* constructs currently being used in human gene therapy

trials, identification of the specific promoter elements of *RDH12* will allow specific cell targeting and high level expression of potential gene therapeutics. Misexpression of RDH12 to the wrong retinal cells could have drastic effects on both retinoid and visual processing. For example, RDH12 misexpression in the RPE rather than the photoreceptor IS could potentially cause decreases in 11-*cis* retinal, the result of which might be akin to night blindness found in users of pharmaceuticals known to be RPE65 antagonists (e.g. 13-*cis* retinoic acid) [241, 242]. Additionally, comparative analysis of the specific elements that regulate gene expression in human and mouse will aid in understanding the different outcomes resulting from RDH12 loss-of-function in each species. Early findings by our lab suggest that the genes encoding RDH11 and RDH12 each have a single transcription start-site in human and mouse retina, and that promoter activity is present in the genomic region located directly upstream of the initiation codon. Identification of the key regulatory elements of the RDH12 promoter will help to ensure that gene replacement strategies lead to proper levels of expression in the appropriate cells.

In conclusion, the studies presented in this dissertation provide significant insights into the role of RPE65 and RDH12 in the physiology of the RPE/retina and visual cycle mechanism. Our localization of RPE65 to the RPE excludes a proposed direct role of RPE65 in a cone pathway of 11-*cis* retinal regeneration. We also reached a better understanding of RPE65 structure and verified its interaction with RDH5. We found that RDH12 protein expression was localized to the photoreceptor inner segments, and is not essential for visual cycle throughput. However, retinas of *Rdh12–/–* mice display a

decreased reductive capacity towards retinaldehydes. In addition, transcript levels of *Rdh12* correlate with visual cycle activity. Thus our results suggest that RDH12 may act on all-*trans* retinal that gains access to the inner segments in constant illumination, possibly by means of carrier proteins, and that a critical function of RDH12 is the reduction of retinaldehydes that exceed the reductive capacity of the photoreceptor outer segment. The grossly normal phenotype of the *Rdh12–/–* mouse may be a result of compensatory mechanisms (possibly involving other members of the RDH family) that are species-specific, or due to species-specific difference in the activity of RDH12.

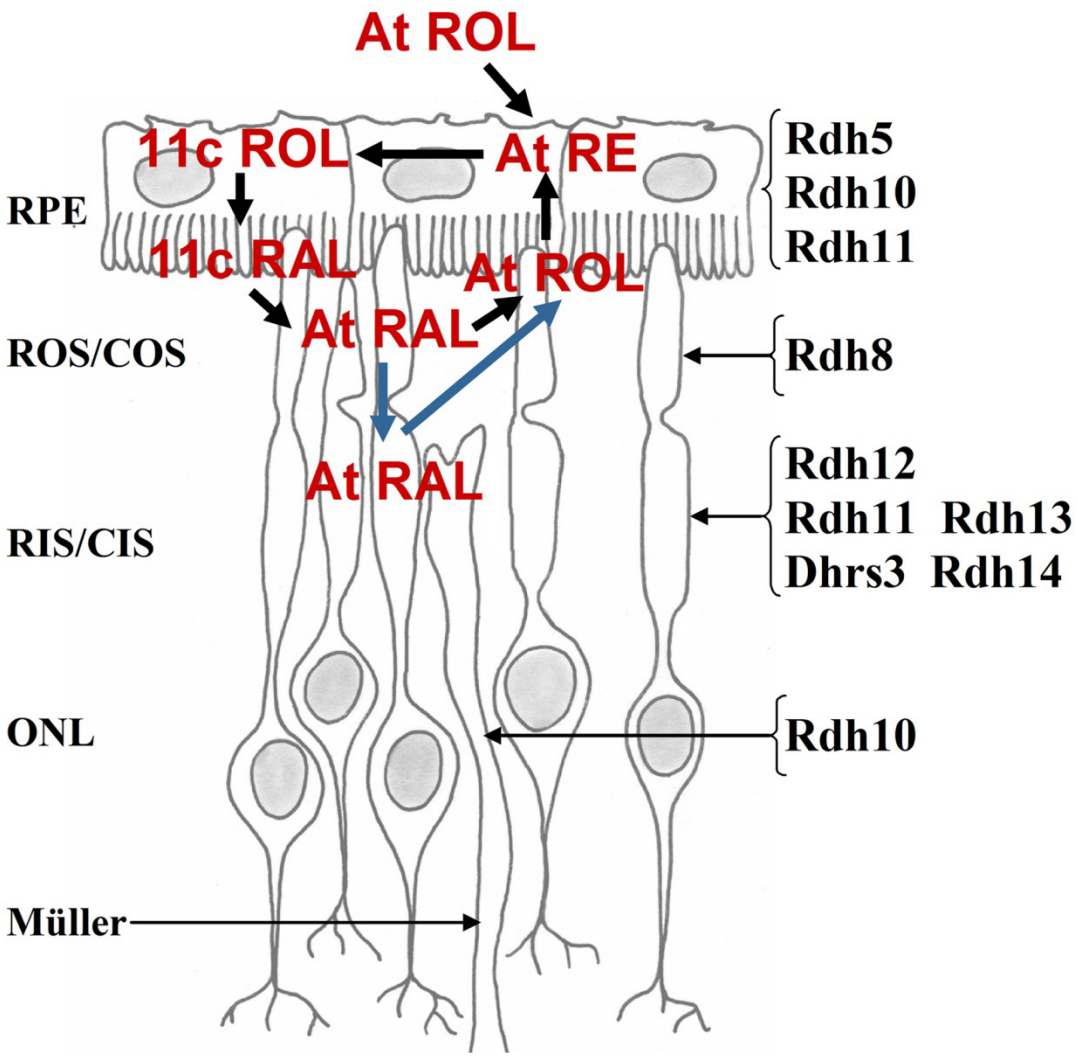

Figure 5-1. Schematic of RDH isoforms and retinoids present in the outer retina and RPE. Photoreceptor cells express a number of isoforms which exhibit the necessary specificity *in vitro*. Studies of retinoid processing in retina slices and isolated photoreceptor cells have shown that all-*trans*-retinol formation localizes to the outer segments during recovery from bleaching. The primary role of RDH isoforms present in the photoreceptors may be to reduce potentially toxic levels of retinaldehydes in various cellular compartments. It seems possible that RDH8 is important for the rapid reduction of all-*trans*-retinal in the vicinity of the rhodopsin signaling complex, whereas the contribution of RDH12, with its broader substrate specificity and localization near the metabolic source of NADPH, becomes more important under conditions of continuous illumination. As RDH12 is restricted to inner segments in both human and mouse retinas and we found no evidence of light-induced translocation, this implies that all-*trans*-retinal can move between outer and inner segment compartments, perhaps associated with retinoid-binding proteins or with opsin found in the inner segment plasma membrane. atROL, all-*trans* retinol; atRAL, all-*trans* retinal; atRE, all-*trans* retinyl esters; 11cROL, 11-*cis* retinol; 11cRAL, 11-*cis* retinal.

BIBLIOGRAPHY

1. Lamb, T.D. and E.N. Pugh, Jr., *Dark adaptation and the retinoid cycle of vision.* Prog Retin Eye Res, 2004. **23**(3): p. 307-80.
2. Kukura, P., D.W. McCamant, S. Yoon, D.B. Wandschneider, and R.A. Mathies, *Structural observation of the primary isomerization in vision with femtosecond-stimulated Raman.* Science, 2005. **310**(5750): p. 1006-9.
3. Rizzolo, L.J. and Z.Q. Li, *Diffusible, retinal factors stimulate the barrier properties of junctional complexes in the retinal pigment epithelium.* J Cell Sci, 1993. **106 (Pt 3)**: p. 859-67.
4. Rizzolo, L.J., *The distribution of Na+,K(+)-ATPase in the retinal pigmented epithelium from chicken embryo is polarized in vivo but not in primary cell culture.* Exp Eye Res, 1990. **51**(4): p. 435-46.
5. Flood, M.T., P. Gouras, and H. Kjeldbye, *Growth characteristics and ultrastructure of human retinal pigment epithelium in vitro.* Invest Ophthalmol Vis Sci, 1980. **19**(11): p. 1309-20.
6. Sakuragawa, M. and T. Kuwabara, *The pigment epithelium of the monkey. Topographic study by scanning and transmission electron microscopy.* Arch Ophthalmol, 1976. **94**(2): p. 285-92.
7. Rizzolo, L.J., *Polarity and the development of the outer blood-retinal barrier.* Histol Histopathol, 1997. **12**(4): p. 1057-67.
8. Bok, D., *The retinal pigment epithelium: a versatile partner in vision.* J Cell Sci Suppl, 1993. **17**: p. 189-95.
9. Clark, V.M., *The cell biology of the retinal pigment epithelium.* The Retina, Part II, 1986: p. 129-168.
10. Strauss, O., *The retinal pigment epithelium in visual function.* Physiol Rev, 2005. **85**(3): p. 845-81.
11. Chuang, J.Z., Y. Zhao, and C.H. Sung, *SARA-regulated vesicular targeting underlies formation of the light-sensing organelle in mammalian rods.* Cell, 2007. **130**(3): p. 535-47.
12. Morgan, J.L., T. Schubert, and R.O. Wong, *Developmental patterning of glutamatergic synapses onto retinal ganglion cells.* Neural Dev, 2008. **3**: p. 8.
13. Swain, P.K., D. Hicks, A.J. Mears, I.J. Apel, J.E. Smith, S.K. John, A. Hendrickson, A.H. Milam, and A. Swaroop, *Multiple phosphorylated isoforms of NRL are expressed in rod photoreceptors.* J Biol Chem, 2001. **276**(39): p. 36824-30.
14. Rehemtulla, A., R. Warwar, R. Kumar, X. Ji, D.J. Zack, and A. Swaroop, *The basic motif-leucine zipper transcription factor Nrl can positively regulate rhodopsin gene expression.* Proc Natl Acad Sci U S A, 1996. **93**(1): p. 191-5.

15. Pittler, S.J., Y. Zhang, S. Chen, A.J. Mears, D.J. Zack, Z. Ren, P.K. Swain, S. Yao, A. Swaroop, and J.B. White, *Functional analysis of the rod photoreceptor cGMP phosphodiesterase alpha-subunit gene promoter: Nrl and Crx are required for full transcriptional activity.* J Biol Chem, 2004. **279**(19): p. 19800-7.
16. Lerner, L.E., Y.E. Gribanova, M. Ji, B.E. Knox, and D.B. Farber, *Nrl and Sp nuclear proteins mediate transcription of rod-specific cGMP-phosphodiesterase beta-subunit gene: involvement of multiple response elements.* J Biol Chem, 2001. **276**(37): p. 34999-5007.
17. Mears, A.J., M. Kondo, P.K. Swain, Y. Takada, R.A. Bush, T.L. Saunders, P.A. Sieving, and A. Swaroop, *Nrl is required for rod photoreceptor development.* Nat Genet, 2001. **29**(4): p. 447-52.
18. Wald, G., *Molecular basis of visual excitation.* Science, 1968. **162**(850): p. 230-9.
19. Hargrave, P.A., *Rhodopsin structure, function, and topography the Friedenwald lecture.* Invest Ophthalmol Vis Sci, 2001. **42**(1): p. 3-9.
20. Saari, J.C., ed. *Metabolism of Retinoids*. The Retinoids: Biology, Chemistry, and Medicine, ed. M.B. Sporn, Roberts, A. B. & Goodman, D. S. 1994, Raven Press: New York. 351-385.
21. Stryer, L., *Cyclic GMP cascade of vision.* Annu Rev Neurosci, 1986. **9**: p. 87-119.
22. Kaupp, U.B., W. Hanke, R. Simmoteit, and H. Luhring, *Electrical and biochemical properties of the cGMP-gated cation channel from rod photoreceptors.* Cold Spring Harb Symp Quant Biol, 1988. **53**(Pt 1): p. 407-15.
23. Baylor, D., *How photons start vision.* Proc Natl Acad Sci U S A, 1996. **93**(2): p. 560-5.
24. Kuhn, H. and U. Wilden, *Deactivation of photoactivated rhodopsin by rhodopsin-kinase and arrestin.* J Recept Res, 1987. **7**(1-4): p. 283-98.
25. Dizhoor, A.M., S. Ray, S. Kumar, G. Niemi, M. Spencer, D. Brolley, K.A. Walsh, P.P. Philipov, J.B. Hurley, and L. Stryer, *Recoverin: a calcium sensitive activator of retinal rod guanylate cyclase.* Science, 1991. **251**(4996): p. 915-8.
26. Bennett, N. and A. Sitaramayya, *Inactivation of photoexcited rhodopsin in retinal rods: the roles of rhodopsin kinase and 48-kDa protein (arrestin).* Biochemistry, 1988. **27**(5): p. 1710-5.
27. Wilden, U. and H. Kuhn, *Light-dependent phosphorylation of rhodopsin: number of phosphorylation sites.* Biochemistry, 1982. **21**(12): p. 3014-22.
28. He, W., C.W. Cowan, and T.G. Wensel, *RGS9, a GTPase accelerator for phototransduction.* Neuron, 1998. **20**(1): p. 95-102.
29. Hurley, J.B., *Molecular properties of the cGMP cascade of vertebrate photoreceptors.* Annu Rev Physiol, 1987. **49**: p. 793-812.
30. Dizhoor, A.M. and J.B. Hurley, *Regulation of photoreceptor membrane guanylyl cyclases by guanylyl cyclase activator proteins.* Methods, 1999. **19**(4): p. 521-31.
31. Koch, K.W., T. Duda, and R.K. Sharma, *Photoreceptor specific guanylate cyclases in vertebrate phototransduction.* Mol Cell Biochem, 2002. **230**(1-2): p. 97-106.
32. Burns, M.E. and V.Y. Arshavsky, *Beyond counting photons: trials and trends in vertebrate visual transduction.* Neuron, 2005. **48**(3): p. 387-401.
33. Whelan, J.P. and J.F. McGinnis, *Light-dependent subcellular movement of photoreceptor proteins.* J Neurosci Res, 1988. **20**(2): p. 263-70.

34. Strissel, K.J., P.V. Lishko, L.H. Trieu, M.J. Kennedy, J.B. Hurley, and V.Y. Arshavsky, *Recoverin undergoes light-dependent intracellular translocation in rod photoreceptors.* J Biol Chem, 2005. **280**(32): p. 29250-5.
35. Brann, M.R. and L.V. Cohen, *Diurnal expression of transducin mRNA and translocation of transducin in rods of rat retina.* Science, 1987. **235**(4788): p. 585-7.
36. Sokolov, M., A.L. Lyubarsky, K.J. Strissel, A.B. Savchenko, V.I. Govardovskii, E.N. Pugh, Jr., and V.Y. Arshavsky, *Massive light-driven translocation of transducin between the two major compartments of rod cells: a novel mechanism of light adaptation.* Neuron, 2002. **34**(1): p. 95-106.
37. Philp, N.J., W. Chang, and K. Long, *Light-stimulated protein movement in rod photoreceptor cells of the rat retina.* FEBS Lett, 1987. **225**(1-2): p. 127-32.
38. Calvert, P.D., K.J. Strissel, W.E. Schiesser, E.N. Pugh, Jr., and V.Y. Arshavsky, *Light-driven translocation of signaling proteins in vertebrate photoreceptors.* Trends Cell Biol, 2006. **16**(11): p. 560-8.
39. Rosenzweig, D.H., K.S. Nair, J. Wei, Q. Wang, G. Garwin, J.C. Saari, C.K. Chen, A.V. Smrcka, A. Swaroop, J. Lem, J.B. Hurley, and V.Z. Slepak, *Subunit dissociation and diffusion determine the subcellular localization of rod and cone transducins.* J Neurosci, 2007. **27**(20): p. 5484-94.
40. Zhang, H., N. Cuenca, T. Ivanova, J. Church-Kopish, J.M. Frederick, P.R. MacLeish, and W. Baehr, *Identification and light-dependent translocation of a cone-specific antigen, cone arrestin, recognized by monoclonal antibody 7G6.* Invest Ophthalmol Vis Sci, 2003. **44**(7): p. 2858-67.
41. Chen, J., M. Wu, S.A. Sezate, and J.F. McGinnis, *Light threshold-controlled cone alpha-transducin translocation.* Invest Ophthalmol Vis Sci, 2007. **48**(7): p. 3350-5.
42. Zhu, X., A. Li, B. Brown, E.R. Weiss, S. Osawa, and C.M. Craft, *Mouse cone arrestin expression pattern: light induced translocation in cone photoreceptors.* Mol Vis, 2002. **8**: p. 462-71.
43. Mirshahi, M., B. Thillaye, M. Tarraf, Y. de Kozak, and J.P. Faure, *Light-induced changes in S-antigen (arrestin) localization in retinal photoreceptors: differences between rods and cones and defective process in RCS rat retinal dystrophy.* Eur J Cell Biol, 1994. **63**(1): p. 61-7.
44. Fain, G.L., *Why photoreceptors die (and why they don't).* Bioessays, 2006. **28**(4): p. 344-54.
45. Fulton, B.S. and R.R. Rando, *Biosynthesis of 11-cis-retinoids and retinyl esters by bovine pigment epithelium membranes.* Biochemistry, 1987. **26**(24): p. 7938-45.
46. Ahn, J., J.T. Wong, and R.S. Molday, *The effect of lipid environment and retinoids on the ATPase activity of ABCR, the photoreceptor ABC transporter responsible for Stargardt macular dystrophy.* J Biol Chem, 2000. **275**(27): p. 20399-405.
47. Liu, J., Y. Itagaki, S. Ben-Shabat, K. Nakanishi, and J.R. Sparrow, *The biosynthesis of A2E, a fluorophore of aging retina, involves the formation of the precursor, A2-PE, in the photoreceptor outer segment membrane.* J Biol Chem, 2000. **275**(38): p. 29354-60.

48. Sun, H., R.S. Molday, and J. Nathans, *Retinal stimulates ATP hydrolysis by purified and reconstituted ABCR, the photoreceptor-specific ATP-binding cassette transporter responsible for Stargardt disease.* J Biol Chem, 1999. **274**(12): p. 8269-81.
49. Weng, J., N.L. Mata, S.M. Azarian, R.T. Tzekov, D.G. Birch, and G.H. Travis, *Insights into the function of Rim protein in photoreceptors and etiology of Stargardt's disease from the phenotype in abcr knockout mice.* Cell, 1999. **98**(1): p. 13-23.
50. Radu, R.A., Q. Yuan, J. Hu, J.H. Peng, M. Lloyd, S. Nusinowitz, D. Bok, and G.H. Travis, *Accelerated accumulation of lipofuscin pigments in the RPE of a mouse model for ABCA4-mediated retinal dystrophies following Vitamin A supplementation.* Invest Ophthalmol Vis Sci, 2008. **49**(9): p. 3821-9.
51. Maeda, A., T. Maeda, M. Golczak, and K. Palczewski, *Retinopathy in mice induced by disrupted all-trans-retinal clearance.* J Biol Chem, 2008. **283**(39): p. 26684-93.
52. Higgins, C.F. and K.J. Linton, *The ATP switch model for ABC transporters.* Nat Struct Mol Biol, 2004. **11**(10): p. 918-26.
53. Beharry, S., M. Zhong, and R.S. Molday, *N-retinylidene-phosphatidylethanolamine is the preferred retinoid substrate for the photoreceptor-specific ABC transporter ABCA4 (ABCR).* J Biol Chem, 2004. **279**(52): p. 53972-9.
54. Haeseleer, F., J. Huang, L. Lebioda, J.C. Saari, and K. Palczewski, *Molecular characterization of a novel short-chain dehydrogenase/reductase that reduces all-trans-retinal.* J Biol Chem, 1998. **273**(34): p. 21790-9.
55. Rattner, A., P.M. Smallwood, and J. Nathans, *Identification and characterization of all-trans-retinol dehydrogenase from photoreceptor outer segments, the visual cycle enzyme that reduces all-trans-retinal to all-trans-retinol.* J Biol Chem, 2000. **275**(15): p. 11034-43.
56. Maeda, A., T. Maeda, Y. Imanishi, V. Kuksa, A. Alekseev, J.D. Bronson, H. Zhang, L. Zhu, W. Sun, D.A. Saperstein, F. Rieke, W. Baehr, and K. Palczewski, *Role of photoreceptor-specific retinol dehydrogenase in the retinoid cycle in vivo.* J Biol Chem, 2005. **280**(19): p. 18822-32.
57. Parker, R.O., J. Fan, J.M. Nickerson, G.I. Liou, and R.K. Crouch, *Normal cone function requires the interphotoreceptor retinoid binding protein.* J Neurosci, 2009. **29**(14): p. 4616-21.
58. Pfeffer, B.A., V.M. Clark, J.G. Flannery, and D. Bok, *Membrane receptors for retinol-binding protein in cultured human retinal pigment epithelium.* Invest Ophthalmol Vis Sci, 1986. **27**(7): p. 1031-40.
59. Quadro, L., W.S. Blaner, D.J. Salchow, S. Vogel, R. Piantedosi, P. Gouras, S. Freeman, M.P. Cosma, V. Colantuoni, and M.E. Gottesman, *Impaired retinal function and vitamin A availability in mice lacking retinol-binding protein.* Embo J, 1999. **18**(17): p. 4633-44.
60. Vogel, S., R. Piantedosi, S.M. O'Byrne, Y. Kako, L. Quadro, M.E. Gottesman, I.J. Goldberg, and W.S. Blaner, *Retinol-binding protein-deficient mice: biochemical basis for impaired vision.* Biochemistry, 2002. **41**(51): p. 15360-8.

61. Saari, J.C., L. Bredberg, and G.G. Garwin, *Identification of the endogenous retinoids associated with three cellular retinoid-binding proteins from bovine retina and retinal pigment epithelium.* J Biol Chem, 1982. **257**(22): p. 13329-33.
62. Barry, R.J., F.J. Canada, and R.R. Rando, *Solubilization and partial purification of retinyl ester synthetase and retinoid isomerase from bovine ocular pigment epithelium.* J Biol Chem, 1989. **264**(16): p. 9231-8.
63. Saari, J.C. and D.L. Bredberg, *Lecithin:retinol acyltransferase in retinal pigment epithelial microsomes.* J Biol Chem, 1989. **264**(15): p. 8636-40.
64. Saari, J.C., *Biochemistry of visual pigment regeneration: the Friedenwald lecture.* Invest Ophthalmol Vis Sci, 2000. **41**(2): p. 337-48.
65. Trehan, A., F.J. Canada, and R.R. Rando, *Inhibitors of retinyl ester formation also prevent the biosynthesis of 11-cis-retinol.* Biochemistry, 1990. **29**(2): p. 309-12.
66. Gollapalli, D.R., P. Maiti, and R.R. Rando, *RPE65 operates in the vertebrate visual cycle by stereospecifically binding all-trans-retinyl esters.* Biochemistry, 2003. **42**(40): p. 11824-30.
67. Redmond, T.M., S. Yu, E. Lee, D. Bok, D. Hamasaki, N. Chen, P. Goletz, J.X. Ma, R.K. Crouch, and K. Pfeifer, *Rpe65 is necessary for production of 11-cis-vitamin A in the retinal visual cycle.* Nat Genet, 1998. **20**(4): p. 344-51.
68. Jin, M., S. Li, W.N. Moghrabi, H. Sun, and G.H. Travis, *Rpe65 is the retinoid isomerase in bovine retinal pigment epithelium.* Cell, 2005. **122**(3): p. 449-59.
69. Moiseyev, G., Y. Chen, Y. Takahashi, B.X. Wu, and J.X. Ma, *RPE65 is the isomerohydrolase in the retinoid visual cycle.* Proc Natl Acad Sci U S A, 2005. **102**(35): p. 12413-8.
70. Simon, A., U. Hellman, C. Wernstedt, and U. Eriksson, *The retinal pigment epithelial-specific 11-cis retinol dehydrogenase belongs to the family of short chain alcohol dehydrogenases.* J Biol Chem, 1995. **270**(3): p. 1107-12.
71. Driessen, C.A., B.P. Janssen, H.J. Winkens, A.H. van Vugt, T.L. de Leeuw, and J.J. Janssen, *Cloning and expression of a cDNA encoding bovine retinal pigment epithelial 11-cis retinol dehydrogenase.* Invest Ophthalmol Vis Sci, 1995. **36**(10): p. 1988-96.
72. Saari, J.C., M. Nawrot, B.N. Kennedy, G.G. Garwin, J.B. Hurley, J. Huang, D.E. Possin, and J.W. Crabb, *Visual cycle impairment in cellular retinaldehyde binding protein (CRALBP) knockout mice results in delayed dark adaptation.* Neuron, 2001. **29**(3): p. 739-48.
73. Kim, T.S., A. Maeda, T. Maeda, C. Heinlein, N. Kedishvili, K. Palczewski, and P.S. Nelson, *Delayed dark adaptation in 11-cis-retinol dehydrogenase-deficient mice: a role of RDH11 in visual processes in vivo.* J Biol Chem, 2005. **280**(10): p. 8694-704.
74. Kasus-Jacobi, A., J. Ou, D.G. Birch, K.G. Locke, J.M. Shelton, J.A. Richardson, A.J. Murphy, D.M. Valenzuela, G.D. Yancopoulos, and A.O. Edwards, *Functional characterization of mouse RDH11 as a retinol dehydrogenase involved in dark adaptation in vivo.* J Biol Chem, 2005. **280**(21): p. 20413-20.
75. Yamamoto, H., A. Simon, U. Eriksson, E. Harris, E.L. Berson, and T.P. Dryja, *Mutations in the gene encoding 11-cis retinol dehydrogenase cause delayed dark adaptation and fundus albipunctatus.* Nat Genet, 1999. **22**(2): p. 188-91.

76. Saari, J.C., D.L. Bredberg, and D.F. Farrell, *Retinol esterification in bovine retinal pigment epithelium: reversibility of lecithin:retinol acyltransferase.* Biochem J, 1993. **291 (Pt 3)**: p. 697-700.
77. Mata, N.L. and A.T. Tsin, *Distribution of 11-cis LRAT, 11-cis RD and 11-cis REH in bovine retinal pigment epithelium membranes.* Biochim Biophys Acta, 1998. **1394**(1): p. 16-22.
78. Lai, Y.L., B. Wiggert, Y.P. Liu, and G.J. Chader, *Interphotoreceptor retinol-binding proteins: possible transport vehicles between compartments of the retina.* Nature, 1982. **298**(5877): p. 848-9.
79. Liou, G.I., C.D. Bridges, S.L. Fong, R.A. Alvarez, and F. Gonzalez-Fernandez, *Vitamin A transport between retina and pigment epithelium--an interstitial protein carrying endogenous retinol (interstitial retinol- binding protein).* Vision Res, 1982. **22**(12): p. 1457-67.
80. Palczewski, K., J.P. Van Hooser, G.G. Garwin, J. Chen, G.I. Liou, and J.C. Saari, *Kinetics of visual pigment regeneration in excised mouse eyes and in mice with a targeted disruption of the gene encoding interphotoreceptor retinoid-binding protein or arrestin.* Biochemistry, 1999. **38**(37): p. 12012-9.
81. Ripps, H., N.S. Peachey, X. Xu, S.E. Nozell, S.B. Smith, and G.I. Liou, *The rhodopsin cycle is preserved in IRBP "knockout" mice despite abnormalities in retinal structure and function.* Vis Neurosci, 2000. **17**(1): p. 97-105.
82. Ho, M.T., J.B. Massey, H.J. Pownall, R.E. Anderson, and J.G. Hollyfield, *Mechanism of vitamin A movement between rod outer segments, interphotoreceptor retinoid-binding protein, and liposomes.* J Biol Chem, 1989. **264**(2): p. 928-35.
83. Jiang, M., S. Pandey, and H.K. Fong, *An opsin homologue in the retina and pigment epithelium.* Invest Ophthalmol Vis Sci, 1993. **34**(13): p. 3669-78.
84. Shen, D., M. Jiang, W. Hao, L. Tao, M. Salazar, and H.K. Fong, *A human opsin-related gene that encodes a retinaldehyde-binding protein.* Biochemistry, 1994. **33**(44): p. 13117-25.
85. Pandey, S., J.C. Blanks, C. Spee, M. Jiang, and H.K. Fong, *Cytoplasmic retinal localization of an evolutionary homolog of the visual pigments.* Exp Eye Res, 1994. **58**(5): p. 605-13.
86. Hao, W. and H.K. Fong, *The endogenous chromophore of retinal G protein-coupled receptor opsin from the pigment epithelium.* J Biol Chem, 1999. **274**(10): p. 6085-90.
87. Chen, P., W. Hao, L. Rife, X.P. Wang, D. Shen, J. Chen, T. Ogden, G.B. Van Boemel, L. Wu, M. Yang, and H.K. Fong, *A photic visual cycle of rhodopsin regeneration is dependent on Rgr.* Nat Genet, 2001. **28**(3): p. 256-60.
88. Maeda, T., J.P. Van Hooser, C.A. Driessen, S. Filipek, J.J. Janssen, and K. Palczewski, *Evaluation of the role of the retinal G protein-coupled receptor (RGR) in the vertebrate retina in vivo.* J Neurochem, 2003. **85**(4): p. 944-56.
89. Wenzel, A., V. Oberhauser, E.N. Pugh, Jr., T.D. Lamb, C. Grimm, M. Samardzija, E. Fahl, M.W. Seeliger, C.E. Reme, and J. von Lintig, *The retinal G protein-coupled receptor (RGR) enhances isomerohydrolase activity independent of light.* J Biol Chem, 2005. **280**(33): p. 29874-84.

90. Chen, P., T.D. Lee, and H.K. Fong, *Interaction of 11-cis-retinol dehydrogenase with the chromophore of retinal g protein-coupled receptor opsin.* J Biol Chem, 2001. **276**(24): p. 21098-104.
91. Yang, M. and H.K. Fong, *Synthesis of the all-trans-retinal chromophore of retinal G protein-coupled receptor opsin in cultured pigment epithelial cells.* J Biol Chem, 2002. **277**(5): p. 3318-24.
92. Jones, G.J., A. Fein, E.F. MacNichol, Jr., and M.C. Cornwall, *Visual pigment bleaching in isolated salamander retinal cones. Microspectrophotometry and light adaptation.* J Gen Physiol, 1993. **102**(3): p. 483-502.
93. Blanks, J.C. and L.V. Johnson, *Specific binding of peanut lectin to a class of retinal photoreceptor cells. A species comparison.* Invest Ophthalmol Vis Sci, 1984. **25**(5): p. 546-57.
94. Znoiko, S.L., R.K. Crouch, G. Moiseyev, and J.X. Ma, *Identification of the RPE65 protein in mammalian cone photoreceptors.* Invest Ophthalmol Vis Sci, 2002. **43**(5): p. 1604-9.
95. Ma, J., L. Xu, D.K. Othersen, T.M. Redmond, and R.K. Crouch, *Cloning and localization of RPE65 mRNA in salamander cone photoreceptor cells1.* Biochim Biophys Acta, 1998. **1443**(1-2): p. 255-61.
96. Trevino, S.G., E.T. Villazana-Espinoza, A. Muniz, and A.T. Tsin, *Retinoid cycles in the cone-dominated chicken retina.* J Exp Biol, 2005. **208**(Pt 21): p. 4151-7.
97. Villazana-Espinoza, E.T., A.L. Hatch, and A.T. Tsin, *Effect of light exposure on the accumulation and depletion of retinyl ester in the chicken retina.* Exp Eye Res, 2006. **83**(4): p. 871-6.
98. Das, S.R., N. Bhardwaj, H. Kjeldbye, and P. Gouras, *Muller cells of chicken retina synthesize 11-cis-retinol.* Biochem J, 1992. **285 (Pt 3)**: p. 907-13.
99. Muniz, A., E.T. Villazana-Espinoza, B. Thackeray, and A.T. Tsin, *11-cis-Acyl-CoA:retinol O-acyltransferase activity in the primary culture of chicken Muller cells.* Biochemistry, 2006. **45**(40): p. 12265-73.
100. Mata, N.L., R.A. Radu, R.C. Clemmons, and G.H. Travis, *Isomerization and oxidation of vitamin a in cone-dominant retinas: a novel pathway for visual-pigment regeneration in daylight.* Neuron, 2002. **36**(1): p. 69-80.
101. Jang, G.F., J.P. Van Hooser, V. Kuksa, J.K. McBee, Y.G. He, J.J. Janssen, C.A. Driessen, and K. Palczewski, *Characterization of a dehydrogenase activity responsible for oxidation of 11-cis-retinol in the retinal pigment epithelium of mice with a disrupted RDH5 gene. A model for the human hereditary disease fundus albipunctatus.* J Biol Chem, 2001. **276**(35): p. 32456-65.
102. Koenekoop, R.K., *An overview of Leber congenital amaurosis: a model to understand human retinal development.* Surv Ophthalmol, 2004. **49**(4): p. 379-98.
103. den Hollander, A.I., R. Roepman, R.K. Koenekoop, and F.P. Cremers, *Leber congenital amaurosis: genes, proteins and disease mechanisms.* Prog Retin Eye Res, 2008. **27**(4): p. 391-419.
104. Morimura, H., G.A. Fishman, S.A. Grover, A.B. Fulton, E.L. Berson, and T.P. Dryja, *Mutations in the RPE65 gene in patients with autosomal recessive retinitis pigmentosa or leber congenital amaurosis.* Proc Natl Acad Sci U S A, 1998. **95**(6): p. 3088-93.

105. Thompson, D.A., Y. Li, C.L. McHenry, T.J. Carlson, X. Ding, P.A. Sieving, E. Apfelstedt-Sylla, and A. Gal, *Mutations in the gene encoding lecithin retinol acyltransferase are associated with early-onset severe retinal dystrophy.* Nat Genet, 2001. **28**(2): p. 123-4.
106. Janecke, A.R., D.A. Thompson, G. Utermann, C. Becker, C.A. Hubner, E. Schmid, C.L. McHenry, A.R. Nair, F. Ruschendorf, J. Heckenlively, B. Wissinger, P. Nurnberg, and A. Gal, *Mutations in RDH12 encoding a photoreceptor cell retinol dehydrogenase cause childhood-onset severe retinal dystrophy.* Nat Genet, 2004. **36**(8): p. 850-4.
107. Nicoletti, A., D.J. Wong, K. Kawase, L.H. Gibson, T.L. Yang-Feng, J.E. Richards, and D.A. Thompson, *Molecular characterization of the human gene encoding an abundant 61 kDa protein specific to the retinal pigment epithelium.* Hum Mol Genet, 1995. **4**(4): p. 641-9.
108. Hamel, C.P., N.A. Jenkins, D.J. Gilbert, N.G. Copeland, and T.M. Redmond, *The gene for the retinal pigment epithelium-specific protein RPE65 is localized to human 1p31 and mouse 3.* Genomics, 1994. **20**(3): p. 509-12.
109. Hamel, C.P., E. Tsilou, B.A. Pfeffer, J.J. Hooks, B. Detrick, and T.M. Redmond, *Molecular cloning and expression of RPE65, a novel retinal pigment epithelium-specific microsomal protein that is post-transcriptionally regulated in vitro.* J Biol Chem, 1993. **268**(21): p. 15751-7.
110. Hamel, C.P., E. Tsilou, E. Harris, B.A. Pfeffer, J.J. Hooks, B. Detrick, and T.M. Redmond, *A developmentally regulated microsomal protein specific for the pigment epithelium of the vertebrate retina.* J Neurosci Res, 1993. **34**(4): p. 414-25.
111. Manes, G., R. Leducq, J. Kucharczak, A. Pages, C.F. Schmitt-Bernard, and C.P. Hamel, *Rat messenger RNA for the retinal pigment epithelium-specific protein RPE65 gradually accumulates in two weeks from late embryonic days.* FEBS Lett, 1998. **423**(2): p. 133-7.
112. Gu, S.M., D.A. Thompson, C.R. Srikumari, B. Lorenz, U. Finckh, A. Nicoletti, K.R. Murthy, M. Rathmann, G. Kumaramanickavel, M.J. Denton, and A. Gal, *Mutations in RPE65 cause autosomal recessive childhood-onset severe retinal dystrophy.* Nat Genet, 1997. **17**(2): p. 194-7.
113. Marlhens, F., C. Bareil, J.M. Griffoin, E. Zrenner, P. Amalric, C. Eliaou, S.Y. Liu, E. Harris, T.M. Redmond, B. Arnaud, M. Claustres, and C.P. Hamel, *Mutations in RPE65 cause Leber's congenital amaurosis.* Nat Genet, 1997. **17**(2): p. 139-41.
114. Veske, A., S.E. Nilsson, K. Narfstrom, and A. Gal, *Retinal dystrophy of Swedish briard/briard-beagle dogs is due to a 4-bp deletion in RPE65.* Genomics, 1999. **57**(1): p. 57-61.
115. Crouch, R.K., G. Moiseyev, P. Gloletz, G. Bealle, T.M. Redmond, and J.X. Ma, *RPE65 is essential but not sufficient for production of 11-cis retinal.* Invest. Ophthalmol. Vis. Sci., 2001. **42**(ARVO Abstract 3525): p. S655.
116. Grimm, C., A. Wenzel, F. Hafezi, S. Yu, T.M. Redmond, and C.E. Reme, *Protection of Rpe65-deficient mice identifies rhodopsin as a mediator of light-induced retinal degeneration.* Nat Genet, 2000. **25**(1): p. 63-6.

117. Woodruff, M.L., E.V. Olshevskaya, A.B. Savchenko, I.V. Peshenko, R. Barrett, R.A. Bush, P.A. Sieving, G.L. Fain, and A.M. Dizhoor, *Constitutive excitation by Gly90Asp rhodopsin rescues rods from degeneration caused by elevated production of cGMP in the dark.* J Neurosci, 2007. **27**(33): p. 8805-15.
118. Mata, N.L., W.N. Moghrabi, J.S. Lee, T.V. Bui, R.A. Radu, J. Horwitz, and G.H. Travis, *Rpe65 is a retinyl ester binding protein that presents insoluble substrate to the isomerase in retinal pigment epithelial cells.* J Biol Chem, 2004. **279**(1): p. 635-43.
119. Gollapalli, D.R. and R.R. Rando, *All-trans-retinyl esters are the substrates for isomerization in the vertebrate visual cycle.* Biochemistry, 2003. **42**(19): p. 5809-18.
120. Redmond, T.M., E. Poliakov, S. Yu, J.Y. Tsai, Z. Lu, and S. Gentleman, *Mutation of key residues of RPE65 abolishes its enzymatic role as isomerohydrolase in the visual cycle.* Proc Natl Acad Sci U S A, 2005. **102**(38): p. 13658-63.
121. Moiseyev, G., Y. Takahashi, Y. Chen, S. Gentleman, T.M. Redmond, R.K. Crouch, and J.X. Ma, *RPE65 Is an Iron(II)-dependent Isomerohydrolase in the Retinoid Visual Cycle.* J Biol Chem, 2006. **281**(5): p. 2835-40.
122. Jin, M., Q. Yuan, S. Li, and G.H. Travis, *Role of LRAT on the retinoid isomerase activity and membrane association of Rpe65.* J Biol Chem, 2007. **282**(29): p. 20915-24.
123. Boulton, M., F. Docchio, P. Dayhaw-Barker, R. Ramponi, and R. Cubeddu, *Age-related changes in the morphology, absorption and fluorescence of melanosomes and lipofuscin granules of the retinal pigment epithelium.* Vision Res, 1990. **30**(9): p. 1291-303.
124. Saari, J.C., G.G. Garwin, J.P. Van Hooser, and K. Palczewski, *Reduction of all-trans-retinal limits regeneration of visual pigment in mice.* Vision Res, 1998. **38**(10): p. 1325-33.
125. Parish, C.A., M. Hashimoto, K. Nakanishi, J. Dillon, and J. Sparrow, *Isolation and one-step preparation of A2E and iso-A2E, fluorophores from human retinal pigment epithelium.* Proc Natl Acad Sci U S A, 1998. **95**(25): p. 14609-13.
126. Eagle, R.C., Jr., A.C. Lucier, V.B. Bernardino, Jr., and M. Yanoff, *Retinal pigment epithelial abnormalities in fundus flavimaculatus: a light and electron microscopic study.* Ophthalmology, 1980. **87**(12): p. 1189-200.
127. Radu, R.A., Y. Han, T.V. Bui, S. Nusinowitz, D. Bok, J. Lichter, K. Widder, G.H. Travis, and N.L. Mata, *Reductions in serum vitamin A arrest accumulation of toxic retinal fluorophores: a potential therapy for treatment of lipofuscin-based retinal diseases.* Invest Ophthalmol Vis Sci, 2005. **46**(12): p. 4393-401.
128. Holz, F.G., C. Bellmann, M. Margaritidis, F. Schutt, T.P. Otto, and H.E. Volcker, *Patterns of increased in vivo fundus autofluorescence in the junctional zone of geographic atrophy of the retinal pigment epithelium associated with age-related macular degeneration.* Graefes Arch Clin Exp Ophthalmol, 1999. **237**(2): p. 145-52.
129. Schmitz-Valckenberg, S., S. Bultmann, J. Dreyhaupt, A. Bindewald, F.G. Holz, and K. Rohrschneider, *Fundus autofluorescence and fundus perimetry in the junctional zone of geographic atrophy in patients with age-related macular degeneration.* Invest Ophthalmol Vis Sci, 2004. **45**(12): p. 4470-6.

130. Scholl, H.P., C. Bellmann, S.S. Dandekar, A.C. Bird, and F.W. Fitzke, *Photopic and scotopic fine matrix mapping of retinal areas of increased fundus autofluorescence in patients with age-related maculopathy.* Invest Ophthalmol Vis Sci, 2004. **45**(2): p. 574-83.
131. Danciger, M., M.T. Matthes, D. Yasamura, N.B. Akhmedov, T. Rickabaugh, S. Gentleman, T.M. Redmond, M.M. La Vail, and D.B. Farber, *A QTL on distal chromosome 3 that influences the severity of light- induced damage to mouse photoreceptors.* Mamm Genome, 2000. **11**(6): p. 422-7.
132. Wenzel, A., C.E. Reme, T.P. Williams, F. Hafezi, and C. Grimm, *The Rpe65 Leu450Met variation increases retinal resistance against light-induced degeneration by slowing rhodopsin regeneration.* J Neurosci, 2001. **21**(1): p. 53-8.
133. Redmond, T.M., C.H. Weber, E. Poliakov, S. Yu, and S. Gentleman, *Effect of Leu/Met variation at residue 450 on isomerase activity and protein expression of RPE65 and its modulation by variation at other residues.* Mol Vis, 2007. **13**: p. 1813-21.
134. Kim, S.R., N. Fishkin, J. Kong, K. Nakanishi, R. Allikmets, and J.R. Sparrow, *Rpe65 Leu450Met variant is associated with reduced levels of the retinal pigment epithelium lipofuscin fluorophores A2E and iso-A2E.* Proc Natl Acad Sci U S A, 2004. **101**(32): p. 11668-72.
135. Haeseleer, F., G.F. Jang, Y. Imanishi, C.A. Driessen, M. Matsumura, P.S. Nelson, and K. Palczewski, *Dual-substrate specificity short chain retinol dehydrogenases from the vertebrate retina.* J Biol Chem, 2002. **277**(47): p. 45537-46.
136. Belyaeva, O.V., O.V. Korkina, A.V. Stetsenko, T. Kim, P.S. Nelson, and N.Y. Kedishvili, *Biochemical properties of purified human retinol dehydrogenase 12 (RDH12): catalytic efficiency toward retinoids and C9 aldehydes and effects of cellular retinol-binding protein type I (CRBPI) and cellular retinaldehyde-binding protein (CRALBP) on the oxidation and reduction of retinoids.* Biochemistry, 2005. **44**(18): p. 7035-47.
137. Perrault, I., S. Hanein, S. Gerber, F. Barbet, D. Ducroq, H. Dollfus, C. Hamel, J.L. Dufier, A. Munnich, J. Kaplan, and J.M. Rozet, *Retinal dehydrogenase 12 (RDH12) mutations in leber congenital amaurosis.* Am J Hum Genet, 2004. **75**(4): p. 639-46.
138. Thompson, D.A., A.R. Janecke, J. Lange, K.L. Feathers, C.A. Hubner, C.L. McHenry, D.W. Stockton, G. Rammesmayer, J.R. Lupski, G. Antinolo, C. Ayuso, M. Baiget, P. Gouras, J.R. Heckenlively, A. den Hollander, S.G. Jacobson, R.A. Lewis, P.A. Sieving, B. Wissinger, S. Yzer, E. Zrenner, G. Utermann, and A. Gal, *Retinal degeneration associated with RDH12 mutations results from decreased 11-cis retinal synthesis due to disruption of the visual cycle.* Hum Mol Genet, 2005. **14**(24): p. 3865-75.
139. Lee, S.A., O.V. Belyaeva, and N.Y. Kedishvili, *Effect of lipid peroxidation products on the activity of human retinol dehydrogenase 12 (RDH12) and retinoid metabolism.* Biochim Biophys Acta, 2008. **1782**(6): p. 421-5.
140. Wicker, L.D. and A. Kasus-Jacobi, *Regulation of retinol dehydrogenase RDH12 by light and 4-hydroxynonenal-induced stress.* ARVO Abstract, 2008: p. #4397.

141. Wang, J., X. Chai, U. Eriksson, and J.L. Napoli, *Activity of human 11-cis-retinol dehydrogenase (Rdh5) with steroids and retinoids and expression of its mRNA in extra-ocular human tissue.* Biochem J, 1999. **338**(Pt 1): p. 23-7.
142. Driessen, C.A., H.J. Winkens, K. Hoffmann, L.D. Kuhlmann, B.P. Janssen, A.H. Van Vugt, J.P. Van Hooser, B.E. Wieringa, A.F. Deutman, K. Palczewski, K. Ruether, and J.J. Janssen, *Disruption of the 11-cis-retinol dehydrogenase gene leads to accumulation of cis-retinols and cis-retinyl esters.* Mol Cell Biol, 2000. **20**(12): p. 4275-87.
143. Shang, E., K. Lai, A.I. Packer, J. Paik, W.S. Blaner, M. de Morais Vieira, P. Gouras, and D.J. Wolgemuth, *Targeted disruption of the mouse cis-retinol dehydrogenase gene: visual and nonvisual functions.* J Lipid Res, 2002. **43**(4): p. 590-7.
144. Lin, B., J.T. White, C. Ferguson, S. Wang, R. Vessella, R. Bumgarner, L.D. True, L. Hood, and P.S. Nelson, *Prostate short-chain dehydrogenase reductase 1 (PSDR1): a new member of the short-chain steroid dehydrogenase/reductase family highly expressed in normal and neoplastic prostate epithelium.* Cancer Res, 2001. **61**(4): p. 1611-8.
145. Belyaeva, O.V., A.V. Stetsenko, P. Nelson, and N.Y. Kedishvili, *Properties of short-chain dehydrogenase/reductase RalR1: characterization of purified enzyme, its orientation in the microsomal membrane, and distribution in human tissues and cell lines.* Biochemistry, 2003. **42**(50): p. 14838-45.
146. Moore, S., C. Pritchard, B. Lin, C. Ferguson, and P.S. Nelson, *Isolation and characterization of the murine prostate short-chain dehydrogenase/reductase 1 (Psdr1) gene, a new member of the short-chain steroid dehydrogenase/reductase family.* Gene, 2002. **293**(1-2): p. 149-60.
147. Wu, B.X., Y. Chen, J. Fan, B. Rohrer, R.K. Crouch, and J.X. Ma, *Cloning and characterization of a novel all-trans retinol short-chain dehydrogenase/reductase from the RPE.* Invest Ophthalmol Vis Sci, 2002. **43**(11): p. 3365-72.
148. Wu, B.X., G. Moiseyev, Y. Chen, B. Rohrer, R.K. Crouch, and J.X. Ma, *Identification of RDH10, an All-trans Retinol Dehydrogenase, in Retinal Muller Cells.* Invest Ophthalmol Vis Sci, 2004. **45**(11): p. 3857-62.
149. Sandell, L.L., B.W. Sanderson, G. Moiseyev, T. Johnson, A. Mushegian, K. Young, J.P. Rey, J.X. Ma, K. Staehling-Hampton, and P.A. Trainor, *RDH10 is essential for synthesis of embryonic retinoic acid and is required for limb, craniofacial, and organ development.* Genes Dev, 2007. **21**(9): p. 1113-24.
150. Belyaeva, O.V., O.V. Korkina, A.V. Stetsenko, and N.Y. Kedishvili, *Human retinol dehydrogenase 13 (RDH13) is a mitochondrial short-chain dehydrogenase/reductase with a retinaldehyde reductase activity.* Febs J, 2007. **275**(1): p. 138-47.
151. Graw, J., *The genetic and molecular basis of congenital eye defects.* Nat Rev Genet, 2003. **4**(11): p. 876-88.
152. Dyer, M.A. and C.L. Cepko, *Regulating proliferation during retinal development.* Nat Rev Neurosci, 2001. **2**(5): p. 333-42.
153. Purves, D., ed. *Neuroscience*. 4th ed. 2008, Sinauer Associates.
154. Thompson, D.A. and A. Gal, *Genetic defects in vitamin A metabolism of the retinal pigment epithelium.* Dev Ophthalmol, 2003. **37**: p. 141-54.

155. Van Hooser, J.P., T.S. Aleman, Y.G. He, A.V. Cideciyan, V. Kuksa, S.J. Pittler, E.M. Stone, S.G. Jacobson, and K. Palczewski, *Rapid restoration of visual pigment and function with oral retinoid in a mouse model of childhood blindness.* Proc Natl Acad Sci U S A, 2000. **97**(15): p. 8623-8.
156. Acland, G.M., G.D. Aguirre, J. Ray, Q. Zhang, T.S. Aleman, A.V. Cideciyan, S.E. Pearce-Kelling, V. Anand, Y. Zeng, A.M. Maguire, S.G. Jacobson, W.W. Hauswirth, and J. Bennett, *Gene therapy restores vision in a canine model of childhood blindness.* Nat Genet, 2001. **28**(1): p. 92-5.
157. Narfstrom, K., M.L. Katz, R. Bragadottir, M. Seeliger, A. Boulanger, T.M. Redmond, L. Caro, C.M. Lai, and P.E. Rakoczy, *Functional and structural recovery of the retina after gene therapy in the RPE65 null mutation dog.* Invest Ophthalmol Vis Sci, 2003. **44**(4): p. 1663-72.
158. Acland, G.M., G.D. Aguirre, J. Bennett, T.S. Aleman, A.V. Cideciyan, J. Bennicelli, N.S. Dejneka, S.E. Pearce-Kelling, A.M. Maguire, K. Palczewski, W.W. Hauswirth, and S.G. Jacobson, *Long-term restoration of rod and cone vision by single dose rAAV-mediated gene transfer to the retina in a canine model of childhood blindness.* Mol Ther, 2005. **12**(6): p. 1072-82.
159. Maguire, A.M., F. Simonelli, E.A. Pierce, E.N. Pugh, Jr., F. Mingozzi, J. Bennicelli, S. Banfi, K.A. Marshall, F. Testa, E.M. Surace, S. Rossi, A. Lyubarsky, V.R. Arruda, B. Konkle, E. Stone, J. Sun, J. Jacobs, L. Dell'Osso, R. Hertle, J.X. Ma, T.M. Redmond, X. Zhu, B. Hauck, O. Zelenaia, K.S. Shindler, M.G. Maguire, J.F. Wright, N.J. Volpe, J.W. McDonnell, A. Auricchio, K.A. High, and J. Bennett, *Safety and efficacy of gene transfer for Leber's congenital amaurosis.* N Engl J Med, 2008. **358**(21): p. 2240-8.
160. Bainbridge, J.W., A.J. Smith, S.S. Barker, S. Robbie, R. Henderson, K. Balaggan, A. Viswanathan, G.E. Holder, A. Stockman, N. Tyler, S. Petersen-Jones, S.S. Bhattacharya, A.J. Thrasher, F.W. Fitzke, B.J. Carter, G.S. Rubin, A.T. Moore, and R.R. Ali, *Effect of gene therapy on visual function in Leber's congenital amaurosis.* N Engl J Med, 2008. **358**(21): p. 2231-9.
161. Cideciyan, A.V., W.W. Hauswirth, T.S. Aleman, S. Kaushal, S.B. Schwartz, S.L. Boye, E.A. Windsor, T.J. Conlon, A. Sumaroka, J.J. Pang, A.J. Roman, B.J. Byrne, and S.G. Jacobson, *Human RPE65 gene therapy for Leber congenital amaurosis: persistence of early visual improvements and safety at 1 year.* Hum Gene Ther, 2009. **20**(9): p. 999-1004.
162. Maguire, A.M., K.A. High, A. Auricchio, J.F. Wright, E.A. Pierce, F. Testa, F. Mingozzi, J.L. Bennicelli, G.S. Ying, S. Rossi, A. Fulton, K.A. Marshall, S. Banfi, D.C. Chung, J.I. Morgan, B. Hauck, O. Zelenaia, X. Zhu, L. Raffini, F. Coppieters, E. De Baere, K.S. Shindler, N.J. Volpe, E.M. Surace, C. Acerra, A. Lyubarsky, T.M. Redmond, E. Stone, J. Sun, J.W. McDonnell, B.P. Leroy, F. Simonelli, and J.B. Gauderman, *Age-dependent effects of RPE65 gene therapy for Leber's congenital amaurosis: a phase 1 dose-escalation trial.* Lancet, 2009.
163. Deigner, P.S., W.C. Law, F.J. Canada, and R.R. Rando, *Membranes as the energy source in the endergonic transformation of vitamin A to 11-cis-retinol.* Science, 1989. **244**(4907): p. 968-71.

164. Gollapalli, D.R., P. Maiti, and R.R. Rando, *RPE65 Operates in the Vertebrate Visual Cycle by Stereospecifically Binding All-trans-Retinyl Esters.* Biochemistry, 2004. **43**(22): p. 7226.
165. Xue, L., D.R. Gollapalli, P. Maiti, W.J. Jahng, and R.R. Rando, *A palmitoylation switch mechanism in the regulation of the visual cycle.* Cell, 2004. **117**(6): p. 761-71.
166. Woodruff, M.L., Z. Wang, H.Y. Chung, T.M. Redmond, G.L. Fain, and J. Lem, *Spontaneous activity of opsin apoprotein is a cause of Leber congenital amaurosis.* Nat Genet, 2003. **35**(2): p. 158-64.
167. Woodruff, M.L., A.Z. Wang, G.L. Fain, and J. Lem, *Constitutive activation and photoreceptor degeneration in Rpe65 knockout mice.* Invest Ophthalmol Vis Sci, 2003. **ARVO Abstract**: p. 3553.
168. Rohrer, B., Z. Ablonczy, S. Znoiko, M. Redmond, J.X. Ma, and R. Crouch, *Does constitutive phosphorylation protect against photoreceptor degeneration in Rpe65-/- mice?* Adv Exp Med Biol, 2003. **533**: p. 221-7.
169. Porto, F.B., I. Perrault, D. Hicks, J.M. Rozet, N. Hanoteau, S. Hanein, J. Kaplan, and J.A. Sahel, *Prenatal human ocular degeneration occurs in Leber's congenital amaurosis (LCA2).* J Gene Med, 2002. **4**(4): p. 390-6.
170. Valeria Canto Soler, M., J.E. Gallo, R.A. Dodds, and A.M. Suburo, *A mouse model of proliferative vitreoretinopathy induced by dispase.* Exp Eye Res, 2002. **75**(5): p. 491-504.
171. Tan, E., X.Q. Ding, A. Saadi, N. Agarwal, M.I. Naash, and M.R. Al-Ubaidi, *Expression of cone-photoreceptor-specific antigens in a cell line derived from retinal tumors in transgenic mice.* Invest Ophthalmol Vis Sci, 2004. **45**(3): p. 764-8.
172. West, K.A., L. Yan, M. Miyagi, J.S. Crabb, A.D. Marmorstein, L. Marmorstein, and J.W. Crabb, *Proteome survey of proliferating and differentiating rat RPE-J cells.* Exp Eye Res, 2001. **73**(4): p. 479-91.
173. Heller, J. and P. Jones, *Purification of bovine retinal pigment epithelial cells by dissociation in calcium free buffers and centrifugation in Ficoll density gradients followed by "recovery" in tissue culture.* Exp Eye Res, 1980. **30**(5): p. 481-7.
174. Mircheff, A.K., S.S. Miller, D.B. Farber, M.E. Bradley, W.T. O'Day, and D. Bok, *Isolation and provisional identification of plasma membrane populations from cultured human retinal pigment epithelium.* Invest Ophthalmol Vis Sci, 1990. **31**(5): p. 863-78.
175. Hemati, N., K.L. Feathers, J.D. Chrispell, D.M. Reed, T.J. Carlson, and D.A. Thompson, *RPE65 surface epitopes, protein interactions, and expression in rod- and cone-dominant species.* Mol Vis, 2005. **11**: p. 1151-65.
176. Claflin, J.L., S. Hudak, and A. Maddalena, *Anti-phosphocholine hybridoma antibodies. I. Direct evidence for three distinct families of antibodies in the murine response.* J Exp Med, 1981. **153**(2): p. 352-64.
177. Gefter, M.L., D.H. Margulies, and M.D. Scharff, *A simple method for polyethylene glycol-promoted hybridization of mouse myeloma cells.* Somatic Cell Genet, 1977. **3**(2): p. 231-6.
178. Kearney, J.F., A. Radbruch, B. Liesegang, and K. Rajewsky, *A new mouse myeloma cell line that has lost immunoglobulin expression but permits the*

construction of antibody-secreting hybrid cell lines. J Immunol, 1979. **123**(4): p. 1548-50.
179. Birk, H.W. and H. Koepsell, *Reaction of monoclonal antibodies with plasma membrane proteins after binding on nitrocellulose: renaturation of antigenic sites and reduction of nonspecific antibody binding.* Anal Biochem, 1987. **164**(1): p. 12-22.
180. Harlow, E., Lane, D., *Antibodies: A Laboratory Manual*. 1988, Cold Spring Harbor, NY: Cold Spring Harbor Laboratory Press.
181. Bok, D., A. Ruiz, O. Yaron, W.J. Jahng, A. Ray, L. Xue, and R.R. Rando, *Purification and characterization of a transmembrane domain-deleted form of lecithin retinol acyltransferase.* Biochemistry, 2003. **42**(20): p. 6090-8.
182. Bystroff, C. and Y. Shao, *Fully automated ab initio protein structure prediction using I-SITES, HMMSTR and ROSETTA.* Bioinformatics, 2002. **18 Suppl 1**: p. S54-61.
183. Bystroff, C., V. Thorsson, and D. Baker, *HMMSTR: a hidden Markov model for local sequence-structure correlations in proteins.* J Mol Biol, 2000. **301**(1): p. 173-90.
184. Simons, K.T., R. Bonneau, I. Ruczinski, and D. Baker, *Ab initio protein structure prediction of CASP III targets using ROSETTA.* Proteins, 1999. **Suppl 3**: p. 171-6.
185. Kloer, D.P., S. Ruch, S. Al-Babili, P. Beyer, and G.E. Schulz, *The structure of a retinal-forming carotenoid oxygenase.* Science, 2005. **308**(5719): p. 267-9.
186. Schwede, T., J. Kopp, N. Guex, and M.C. Peitsch, *SWISS-MODEL: An automated protein homology-modeling server.* Nucleic Acids Res, 2003. **31**(13): p. 3381-5.
187. Strettoi, E., A.J. Mears, and A. Swaroop, *Recruitment of the rod pathway by cones in the absence of rods.* J Neurosci, 2004. **24**(34): p. 7576-82.
188. Daniele, L.L., C. Lillo, A.L. Lyubarsky, S.S. Nikonov, N. Philp, A.J. Mears, A. Swaroop, D.S. Williams, and E.N. Pugh, Jr., *Cone-like morphological, molecular, and electrophysiological features of the photoreceptors of the Nrl knockout mouse.* Invest Ophthalmol Vis Sci, 2005. **46**(6): p. 2156-67.
189. Nikonov, S.S., L.L. Daniele, X. Zhu, C.M. Craft, A. Swaroop, and E.N. Pugh, Jr., *Photoreceptors of Nrl -/- mice coexpress functional S- and M-cone opsins having distinct inactivation mechanisms.* J Gen Physiol, 2005. **125**(3): p. 287-304.
190. Redmond, T.M. and C.P. Hamel, *Genetic analysis of RPE65: from human disease to mouse model.* Methods Enzymol, 2000. **316**: p. 705-24.
191. Wilhelm, M. and R. Gabriel, *Functional anatomy of the photoreceptor and second-order cell mosaics in the retina of Xenopus laevis.* Cell Tissue Res, 1999. **297**(1): p. 35-46.
192. Meyer, D.B. and H.C. May, Jr., *The topographical distribution of rods and cones in the adult chicken retina.* Exp Eye Res, 1973. **17**(4): p. 347-55.
193. Wenzel, A., C. Grimm, M.W. Seeliger, G. Jaissle, F. Hafezi, R. Kretschmer, E. Zrenner, and C.E. Reme, *Prevention of photoreceptor apoptosis by activation of the glucocorticoid receptor.* Invest Ophthalmol Vis Sci, 2001. **42**(7): p. 1653-9.
194. Salvador-Silva, M., S. Ghosh, R. Bertazolli-Filho, J.H. Boatright, J.M. Nickerson, G.G. Garwin, J.C. Saari, and M. Coca-Prados, *Retinoid processing proteins in the ocular ciliary epithelium.* Mol Vis, 2005. **11**: p. 356-65.

195. Jang, G.F., J.K. McBee, A.M. Alekseev, F. Haeseleer, and K. Palczewski, *Stereoisomeric specificity of the retinoid cycle in the vertebrate retina.* J Biol Chem, 2000. **275**(36): p. 28128-38.
196. Haeseleer, F. and K. Palczewski, *Short-chain dehydrogenases/reductases in retina.* Methods Enzymol, 2000. **316**: p. 372-83.
197. Callaway, J.K., P.M. Beart, and B. Jarrott, *A reliable procedure for comparison of antioxidants in rat brain homogenates.* J Pharmacol Toxicol Methods, 1998. **39**(3): p. 155-62.
198. Bligh, E.G. and W.J. Dyer, *A rapid method of total lipid extraction and purification.* Can J Biochem Physiol, 1959. **37**(8): p. 911-7.
199. Garwin, G.G. and J.C. Saari, *High-performance liquid chromatography analysis of visual cycle retinoids.* Methods Enzymol, 2000. **316**: p. 313-24.
200. Poss, K.D. and S. Tonegawa, *Reduced stress defense in heme oxygenase 1-deficient cells.* Proc Natl Acad Sci U S A, 1997. **94**(20): p. 10925-30.
201. Rohrer, B., H.R. Lohr, P. Humphries, T.M. Redmond, M.W. Seeliger, and R.K. Crouch, *Cone opsin mislocalization in Rpe65-/- mice: a defect that can be corrected by 11-cis retinal.* Invest Ophthalmol Vis Sci, 2005. **46**(10): p. 3876-82.
202. Fan, J., M.L. Woodruff, M.C. Cilluffo, R.K. Crouch, and G.L. Fain, *Opsin activation of transduction in the rods of dark-reared Rpe65 knockout mice.* J Physiol, 2005. **568**(Pt 1): p. 83-95.
203. Znoiko, S.L., B. Rohrer, K. Lu, H.R. Lohr, R.K. Crouch, and J.X. Ma, *Downregulation of cone-specific gene expression and degeneration of cone photoreceptors in the Rpe65-/- mouse at early ages.* Invest Ophthalmol Vis Sci, 2005. **46**(4): p. 1473-9.
204. Kurth, I., D.A. *Thompson, K. Ruther, K.L. Feathers, J.D. Chrispell, J. Schroth, C.L. McHenry, M. Schweizer, S. Skosyrski, A. Gal, and C.A. *Hubner, *Targeted disruption of the murine retinal dehydrogenase gene Rdh12 does not limit visual cycle function.* Mol Cell Biol, 2007. **27**(4): p. 1370-9 *corresponding authors.
205. Akimoto, M., H. Cheng, D. Zhu, J.A. Brzezinski, R. Khanna, E. Filippova, E.C. Oh, Y. Jing, J.L. Linares, M. Brooks, S. Zareparsi, A.J. Mears, A. Hero, T. Glaser, and A. Swaroop, *Targeting of GFP to newborn rods by Nrl promoter and temporal expression profiling of flow-sorted photoreceptors.* Proc Natl Acad Sci U S A, 2006. **103**(10): p. 3890-5.
206. Chrispell, J.D., Feathers, K.L., Brooks, M.J., Khanna, R., Mears, A.J., Swaroop, A., Thompson, D.A., *RDH12 Expression Relative to Other Short Chain Dehydrogenase/Reductase Isoforms Present in the Retina.* ARVO Abstract, 2007.
207. Thompson, D.A., P. Gyurus, L.L. Fleischer, E.L. Bingham, C.L. McHenry, E. Apfelstedt-Sylla, E. Zrenner, B. Lorenz, J.E. Richards, S.G. Jacobson, P.A. Sieving, and A. Gal, *Genetics and phenotypes of RPE65 mutations in inherited retinal degeneration.* Invest Ophthalmol Vis Sci, 2000. **41**(13): p. 4293-9.
208. Wrigstad, A., K. Narfstrom, and S.E. Nilsson, *Slowly progressive changes of the retina and retinal pigment epithelium in Briard dogs with hereditary retinal dystrophy. A morphological study.* Doc Ophthalmol, 1994. **87**(4): p. 337-54.
209. Argmann, C.A., P. Chambon, and J. Auwerx, *Mouse phenogenomics: the fast track to "systems metabolism".* Cell Metab, 2005. **2**(6): p. 349-60.

210. Sun, W., C. Gerth, A. Maeda, D.T. Lodowski, L. Van Der Kraak, D.A. Saperstein, E. Heon, and K. Palczewski, *Novel RDH12 mutations associated with Leber congenital amaurosis and cone-rod dystrophy: biochemical and clinical evaluations.* Vision Res, 2007. **47**(15): p. 2055-66.
211. Schuster, A., A.R. Janecke, R. Wilke, E. Schmid, D.A. Thompson, G. Utermann, B. Wissinger, E. Zrenner, and A. Gal, *The phenotype of early-onset retinal degeneration in persons with RDH12 mutations.* Invest Ophthalmol Vis Sci, 2007. **48**(4): p. 1824-31.
212. Jacobson, S.G., A.V. Cideciyan, T.S. Aleman, A. Sumaroka, S.B. Schwartz, E.A. Windsor, A.J. Roman, E. Heon, E.M. Stone, and D.A. Thompson, *RDH12 and RPE65, visual cycle genes causing leber congenital amaurosis, differ in disease expression.* Invest Ophthalmol Vis Sci, 2007. **48**(1): p. 332-8.
213. Liden, M. and U. Eriksson, *Understanding retinol metabolism: structure and function of retinol dehydrogenases.* J Biol Chem, 2006. **281**(19): p. 13001-4.
214. Napoli, J.L., *17beta-Hydroxysteroid dehydrogenase type 9 and other short-chain dehydrogenases/reductases that catalyze retinoid, 17beta- and 3alpha-hydroxysteroid metabolism.* Mol Cell Endocrinol, 2001. **171**(1-2): p. 103-9.
215. Thompson, D.A. and A. Gal, *Vitamin A metabolism in the retinal pigment epithelium: genes, mutations, and diseases.* Prog Retin Eye Res, 2003. **22**(5): p. 683-703.
216. Keller, B. and J. Adamski, *RDH12, a retinol dehydrogenase causing Leber's congenital amaurosis, is also involved in steroid metabolism.* J Steroid Biochem Mol Biol, 2007. **104**(3-5): p. 190-4.
217. Maeda, A., T. Maeda, Y. Imanishi, W. Sun, B. Jastrzebska, D.A. Hatala, H.J. Winkens, K.P. Hofmann, J.J. Janssen, W. Baehr, C.A. Driessen, and K. Palczewski, *Retinol dehydrogenase (RDH12) protects photoreceptors from light-induced degeneration in mice.* J Biol Chem, 2006. **281**(49): p. 37697-704.
218. Landers, G.M., *High-performance liquid chromatography of retinoid isomers.* Methods Enzymol, 1990. **189**: p. 70-80.
219. Peterson, G.L., *A simplification of the protein assay method of Lowry et al. which is more generally applicable.* Anal Biochem, 1977. **83**(2): p. 346-56.
220. LaVail, M.M., Matthes, M.T., Yasumura, D., Faktorovich, E.G., and Steinberg, R.H., *Histological method to assess photoreceptor light damage and protection by survival factors*. Degenerative Retinal Diseases, ed. J.G.H.a.R.E.A. M.M. LaVail. 1997, New York: Plenum Press.
221. Reiner, A., D. Yekutieli, and Y. Benjamini, *Identifying differentially expressed genes using false discovery rate controlling procedures.* Bioinformatics, 2003. **19**(3): p. 368-75.
222. Benjamini, Y. and D. Yekutieli, *Quantitative trait Loci analysis using the false discovery rate.* Genetics, 2005. **171**(2): p. 783-90.
223. Yoshida, S., A.J. Mears, J.S. Friedman, T. Carter, S. He, E. Oh, Y. Jing, R. Farjo, G. Fleury, C. Barlow, A.O. Hero, and A. Swaroop, *Expression profiling of the developing and mature Nrl-/- mouse retina: identification of retinal disease candidates and transcriptional regulatory targets of Nrl.* Hum Mol Genet, 2004. **13**(14): p. 1487-503.

224. Lebovitz, R.M., H. Zhang, H. Vogel, J. Cartwright, Jr., L. Dionne, N. Lu, S. Huang, and M.M. Matzuk, *Neurodegeneration, myocardial injury, and perinatal death in mitochondrial superoxide dismutase-deficient mice.* Proc Natl Acad Sci U S A, 1996. **93**(18): p. 9782-7.
225. Li, Y., T.T. Huang, E.J. Carlson, S. Melov, P.C. Ursell, J.L. Olson, L.J. Noble, M.P. Yoshimura, C. Berger, P.H. Chan, D.C. Wallace, and C.J. Epstein, *Dilated cardiomyopathy and neonatal lethality in mutant mice lacking manganese superoxide dismutase.* Nat Genet, 1995. **11**(4): p. 376-81.
226. Wu, Q., L.R. Blakeley, M.C. Cornwall, R.K. Crouch, B.N. Wiggert, and Y. Koutalos, *Interphotoreceptor retinoid-binding protein is the physiologically relevant carrier that removes retinol from rod photoreceptor outer segments.* Biochemistry, 2007. **46**(29): p. 8669-79.
227. Maeda, A., T. Maeda, W. Sun, H. Zhang, W. Baehr, and K. Palczewski, *Redundant and unique roles of retinol dehydrogenases in the mouse retina.* Proc Natl Acad Sci U S A, 2007. **104**(49): p. 19565-70.
228. Napoli, J.L., *Interactions of retinoid binding proteins and enzymes in retinoid metabolism.* Biochim Biophys Acta, 1999. **1440**(2-3): p. 139-62.
229. Lee, S.A., O.V. Belyaeva, I.K. Popov, and N.Y. Kedishvili, *Overproduction of bioactive retinoic acid in cells expressing disease-associated mutants of retinol dehydrogenase 12.* J Biol Chem, 2007. **282**(49): p. 35621-8.
230. Sandbach, J.M., P.E. Coscun, H.E. Grossniklaus, J.E. Kokoszka, N.J. Newman, and D.C. Wallace, *Ocular pathology in mitochondrial superoxide dismutase (Sod2)-deficient mice.* Invest Ophthalmol Vis Sci, 2001. **42**(10): p. 2173-8.
231. Williams, M.D., H. Van Remmen, C.C. Conrad, T.T. Huang, C.J. Epstein, and A. Richardson, *Increased oxidative damage is correlated to altered mitochondrial function in heterozygous manganese superoxide dismutase knockout mice.* J Biol Chem, 1998. **273**(43): p. 28510-5.
232. Justilien, V., J.J. Pang, K. Renganathan, X. Zhan, J.W. Crabb, S.R. Kim, J.R. Sparrow, W.W. Hauswirth, and A.S. Lewin, *SOD2 knockdown mouse model of early AMD.* Invest Ophthalmol Vis Sci, 2007. **48**(10): p. 4407-20.
233. Tsina, E., C. Chen, Y. Koutalos, P. Ala-Laurila, M. Tsacopoulos, B. Wiggert, R.K. Crouch, and M.C. Cornwall, *Physiological and microfluorometric studies of reduction and clearance of retinal in bleached rod photoreceptors.* J Gen Physiol, 2004. **124**(4): p. 429-43.
234. Chen, C., E. Tsina, M.C. Cornwall, R.K. Crouch, S. Vijayaraghavan, and Y. Koutalos, *Reduction of all-trans retinal to all-trans retinol in the outer segments of frog and mouse rod photoreceptors.* Biophys J, 2005. **88**(3): p. 2278-87.
235. Muniz, A., B.S. Betts, A.R. Trevino, K. Buddavarapu, R. Roman, J.X. Ma, and A.T. Tsin, *Evidence for two retinoid cycles in the cone-dominated chicken eye.* Biochemistry, 2009. **48**(29): p. 6854-63.
236. Kiser, P.D., M. Golczak, D.T. Lodowski, M.R. Chance, and K. Palczewski, *Crystal structure of native RPE65, the retinoid isomerase of the visual cycle.* Proc Natl Acad Sci U S A, 2009. **106**(41): p. 17325-30.
237. Soderpalm, A.K., D.A. Fox, J.O. Karlsson, and T. van Veen, *Retinoic acid produces rod photoreceptor selective apoptosis in developing mammalian retina.* Invest Ophthalmol Vis Sci, 2000. **41**(3): p. 937-47.

238. Birnbach, C.D., M. Jarvelainen, D.E. Possin, and A.H. Milam, *Histopathology and immunocytochemistry of the neurosensory retina in fundus flavimaculatus.* Ophthalmology, 1994. **101**(7): p. 1211-9.
239. Smith, S.B., N. Bora, D. McCool, G. Kutty, P. Wong, R.K. Kutty, and B. Wiggert, *Photoreceptor cells in the vitiligo mouse die by apoptosis. TRPM-2/clusterin expression is increased in the neural retina and in the retinal pigment epithelium.* Invest Ophthalmol Vis Sci, 1995. **36**(11): p. 2193-201.
240. Marchette, L.D., D.A. Thompson, M. Kravtsova, T.N. Ngansop, M.N. Mandal, and A. Kasus-Jacobi, *Retinol dehydrogenase 12 detoxifies 4-hydroxynonenal in photoreceptor cells.* Free Radic Biol Med, 2009.
241. Gollapalli, D.R. and R.R. Rando, *The specific binding of retinoic acid to RPE65 and approaches to the treatment of macular degeneration.* Proc Natl Acad Sci U S A, 2004. **101**(27): p. 10030-5.
242. Maiti, P., J. Kong, S.R. Kim, J.R. Sparrow, R. Allikmets, and R.R. Rando, *Small molecule RPE65 antagonists limit the visual cycle and prevent lipofuscin formation.* Biochemistry, 2006. **45**(3): p. 852-60.